

Universität  
Rostock



Traditio et Innovatio

# Influence of Fc $\gamma$ receptor distribution on mannose receptor mediated phagocytosis

Dissertation

zur

Erlangung des akademischen Grades

*doctor rerum naturalium* (Dr. rer. nat.)

der Mathematisch-Naturwissenschaftlichen Fakultät

der Universität Rostock

vorgelegt von

*Syed Furquan Ahmad*

aus Lucknow, India

Rostock, September 2010

**Gutachter:**

PD Dr. Sergei A. Kuznetsov  
University of Rostock, Germany

Prof. Peter Hinterdorfer  
University of Linz, Austria

Datum des Wissenschaftlichen Kolloquium: 29.11.2010

**Table of contents**

<b>Abstract</b>	<b>1</b>
<b>1 Introduction</b>	<b>2</b>
1.1 Phagocytosis	
1.1.1 Phagocytic receptors	3
1.1.2 Fc Receptors	4
1.1.3 Mannose receptor	10
1.2 Phagocytic signaling	11
1.3 Nano-scale imaging using atomic force microscopy (AFM)	14
1.3.1 Principle of AFM	15
1.3.2 Simultaneous Topography and RECOgnition imaging (TREC)	17
1.4 Latex beads system as a tool to study the crosstalk and landscape of receptors on macrophages surface	19
1.5 Aims of the study	20
<b>2 Material and Methods</b>	<b>21</b>
2.1 Cultivation of J774A.1 macrophage cells and bacteria	21
2.1.1 Used material, reagents and instruments	21
2.1.2 Cultivation of macrophage cells	21
2.1.3 Cultivation of bacteria	22
2.2 Preparation and coupling of latex beads to ligands	23
2.2.1 Used material and reagents	23
2.2.2 Coupling of latex beads to avidin	24
2.2.3 Coupling of latex beads to IgG Fc fragment	24
2.2.4 Coupling of latex beads to mannan	25
2.3 Confocal Microscopy	25
2.3.1. Fixation and labelling of cells	25
2.3.2 Procedure for analyzing phagocytic uptake rates	26
2.3.3 Immunofluorescence	27
2.3.4 Phagocytic assay using Fc-coated latex beads for AFM studies	27
2.3.5 Confocal microscopy for uptake rates and colocalization	28
2.4 Atomic force microscopy	29
2.4.1 Functionalization of tip with Fc fragment via PEG-linker	29
2.4.2 Molecular recognition force spectroscopy	30
2.4.3 Topographical and recognition imaging (TREC)	30
2.5 Electron microscopy	31
2.5.1 Scanning Electron Microscopy	31
2.5.2 Transmission electron microscopy	31
2.5.3 Analysis and derivation of the equation	32

<b>3 Results</b>	<b>34</b>
3.1 Determination of the nano-landscape of Fc $\gamma$ Rs by Atomic force microscopy	34
3.1.1 Binding activity of Fc $\gamma$ Rs on macrophage surface	34
3.1.2 Topographical landscape of J774.A1 cells	37
3.1.3 Nano-mapping of Fc $\gamma$ Rs using TREC	40
3.2 Immunofluorescent and immune-electron microscopic studies of mannose receptor and Fc $\gamma$ receptors on the macrophages	42
3.3 Investigation of binding and internalization of latex beads coupled to different ligands in mouse macrophages	46
3.3.1. Determination of the rate of phagocytic particle binding and internalization using differently coated latex beads	46
3.3.2 Binding and internalization analysis of Fc beads and mannan beads simultaneously used in a mixture	49
3.3.3 Use of mixed beads in different ratios and beads of smaller size to find out the distance between MR and Fc $\gamma$ Rs	51
3.4 Interaction between <i>Mycobacterium smegmatis</i> and J774 macrophages in presence of 1 $\mu$ Fc beads	52
3.5 Effect of kinase inhibitors on Fc and mannose receptor mediated phagocytosis	54
<b>4. Discussion</b>	<b>58</b>
4.1 Fc $\gamma$ Rs are homogeneously distributed on macrophage surface as nano-domains of various size	58
4.2 Latex beads system offers a powerful tool to study the receptors distribution on the cell surface	61
4.3 Mannose receptors are present in lesser number than Fc $\gamma$ Rs and majority of them are located very near to Fc $\gamma$ RI	65
4.4 Fc beads inhibit the phagocytosis of <i>mycobaterium smegmatis</i>	67
4.5 Kinases are required for the initial steps of mannose receptor mediated phagocytosis of latex beads	67
<b>References</b>	<b>69</b>
<b>Acknowledgements</b>	<b>79</b>
<b>Curriculum vitae</b>	<b>80</b>
<b>Declaration</b>	<b>82</b>

# *Abstract*

Macrophages have been referred to as professional phagocytes and are very efficient at recognizing and internalizing foreign particles. The multiplicity of phagocytosis promoting receptors, surface organization and interaction with different ligands influence the signaling events during phagocytosis. Previous work in my lab showed that latex beads coated with different ligands, like Fc fragment or mannose, can be successfully used in studies on receptor-specific phagocytosis and supported the notion of the existence of a specific receptor-ligand 'signature' during the whole process of phagocytosis<sup>1</sup>.

For this study I used latex beads conjugated to specific ligands as a tool to analyze the response of a phagocyte when two different beads coated with a single ligand are applied simultaneously to these cells and thus to explore the landscape of their cognate receptors. The recognition maps obtained by the simultaneous topography and recognition (TREC) imaging revealed that Fc $\gamma$  receptors are distributed in prominent micro-domains of various sizes out of which about ~4 % were large clusters (> 200 nm), which were surrounded by ~ 50 % of small (4-30 nm) and the rest by middle size (50, 150 nm) domains<sup>2</sup>. The fluorescent and electron microscopy provided further evidence that these clusters are located within very close proximity of mannose receptors (MR). This pattern of distribution of Fc $\gamma$ R and MRs led to inhibition of the MR mediated attachment and internalization of 1 $\mu$ m mannan beads in presence of 1 $\mu$ m Fc beads. Furthermore, MR mediated phagocytosis of *mycobacterium smegmatis* was also found to be inhibited of in presence of 1 $\mu$ m Fc beads.

Taking together, the data presented in this thesis provide evidences of cross-talk between opsonin-dependent (Fc $\gamma$ R mediated) and opsonin-independent (MR mediated) phagocytosis and that distribution of Fc $\gamma$ R influences MR mediated phagocytosis.

---

<sup>1</sup> Hoffmann, E., S.Marion, B.B.Mishra, M.John, R.Kratzke, Ahmad S.F., D.Holzer, P.K.Anand, D.G.Weiss, G.Griffiths, and S.A.Kuznetsov. 2010. Initial receptor-ligand interactions modulate gene expression and phagosomal properties during both early and late stages of phagocytosis. *Eur. J. Cell Biol.* 89:693-704

<sup>2</sup> Ahmad, S.F., L.A.Chtcheglova, B.Mayer, S.A.Kuznetsov, and P.Hinterdorfer. 2010. Nanosensing of Fc $\gamma$  receptors on macrophages. *Anal. Bioanal. Chem.*(in press)

# *Introduction*

## 1.1 Phagocytosis

Phagocytosis is an actin-dependent mechanism by which cells (phagocytes) ingest large particles that are usually greater than  $0.5\mu\text{m}$  in diameter (Aderem and Underhill, 1999). Phagocytosis is phylogenetically conserved in mammals and has evolved into a remarkably intricate process. Elie Metchnikoff was the first to describe it in the late nineteenth century and he was awarded the Nobel Prize in Physiology or Medicine in 1908 for his discovery. One hundred years later, Metchnikoff's cellular theory of immunity still significant, but we are now aware that the phagocytic process is much more complex than originally envisioned and we are only just beginning to decipher its various mechanistic and molecular workings. Phagocytosis is essential for host defense against invading pathogens and the clearance of apoptotic cells, thereby playing a central role in tissue homeostasis. In addition, internalization and degradation of pathogenic microbes by professional phagocytes trigger activation of the innate and adaptive immune response after antigen presentation at the surface of the phagocytic cell. The phagocytic process is initiated by the recognition of specific ligands present on the surface of the phagocytosed particle. These interactions between receptor and ligand trigger a specific signaling pathway that activates actin cytoskeleton and membrane remodeling, leading to particle uptake. The organelle with the enclosed particle, termed phagosome, then fuses transiently and sequentially with the endosomal and lysosomal machinery to eventually degrade the phagosome content (Aderem and Underhill, 1999). While lower organisms use phagocytosis primarily for the acquisition of nutrients, phagocytosis in Metazoa occurs primarily in specialized phagocytic cells such as macrophages and neutrophils, and it has evolved into an extraordinarily complex process underlying a variety of critical biological phenomena. Thus, phagocytosis by macrophages is critical for the uptake and degradation of infectious agents and senescent cells, and it participates in development, tissue remodeling, the immune response, and inflammation. Monocytes/macrophages and neutrophils have been referred to as professional phagocytes and are very efficient at internalizing particles. On the other hand, most cells have some phagocytic capacity. For example, thyroid and bladder epithelial cells phagocytose erythrocytes *in vivo*, and numerous cell types have been induced to phagocytose particles in culture. A group of cells termed paraprofessional phagocytes by Rabinovitch also have intermediate phagocytic ability (Allen and Aderem, 1996b; Rabinovitch, 1995). These include retinal epithelial cells that internalize the effete ends of retinal rods (Rabinovitch, 1995). The major difference with respect to phagocytic capacity and efficiency of professional and



nonprofessional phagocytes can probably be ascribed to the presence of an array of dedicated phagocytic receptors that increase particle range and phagocytic rate. Transfection of fibroblasts and epithelial cells with cDNAs encoding Fc receptors (FcRs) dramatically increases the phagocytic rate (Indik et al., 1995) and this system has been used to dissect signaling pathways leading to particle internalization. After the recognition of ligands on the surface of a particle by phagocytic receptors, signaling events occur leading to phagocytic cup formation and uptake of the particle (Garcia-Garcia and Rosales, 2002). The remodeling of the plasma membrane during phagocytic cup formation, in particular the initial extension of pseudopodia that grow and enclose the particle, requires the localized and rapid assembly of actin filaments (F-actin) at the site of ingestion (Allison et al., 1971). However, it is clear that many other differences between professional and nonprofessional phagocytes exist that lead to the enhancement of both rate and efficiency of particle internalization. The study of phagocytosis requires insight into the mechanisms of signal transduction, actin-based motility, membrane trafficking, and infectious disease. Macrophages and other phagocytic cells such as neutrophils certainly use similar mechanisms, but important differences exist that may be important to the role each cell type plays in the immune response.

### **1.1.1 Phagocytic receptors**

During microbial contact, many parallel signaling pathways are simultaneously activated that together define the phagocyte response and regulate internalization (figure 1). Many different receptors recognize microbes, and phagocytosis is usually mediated simultaneously by multiple receptors. Different microbe-recognition receptors induce different signaling pathways, and these signals interact cooperatively (and sometimes destructively) to mediate ultimate responses to particles. Microbe recognition is coupled (either directly through phagocytic receptors or indirectly through co-receptors) to inflammatory responses that in turn affect the efficiency of particle internalization by the phagocyte or neighboring phagocytes. Many pathogenic microbes actively attempt to regulate the mechanisms of phagocytosis to evade destruction. Phagocytosis also is required for normal clearance of apoptotic cells, a process in which many of the same levels of complexity apply. Phagocytes express a broad spectrum of receptors that participate in microbe or particle recognition and internalization (Table 1). Some of these receptors are capable of transmitting intracellular signals that trigger phagocytosis, while other receptors appear primarily to participate in binding or to increase the efficiency of

internalization. The most reliable method for establishing the phagocytic capacity of a specific receptor is to express it in a non-phagocytic cell and demonstrate that it confers on the cell the ability to internalize specific target particles. While this method has been used to analyze phagocytosis through receptors such as Fc-receptors, complement receptor 3, and the mannose receptor, in many cases the ability of a receptor to function (or not) in this type of assay has not been assessed. Detail descriptions of Fc and mannose receptor implicated in phagocytosis is described.

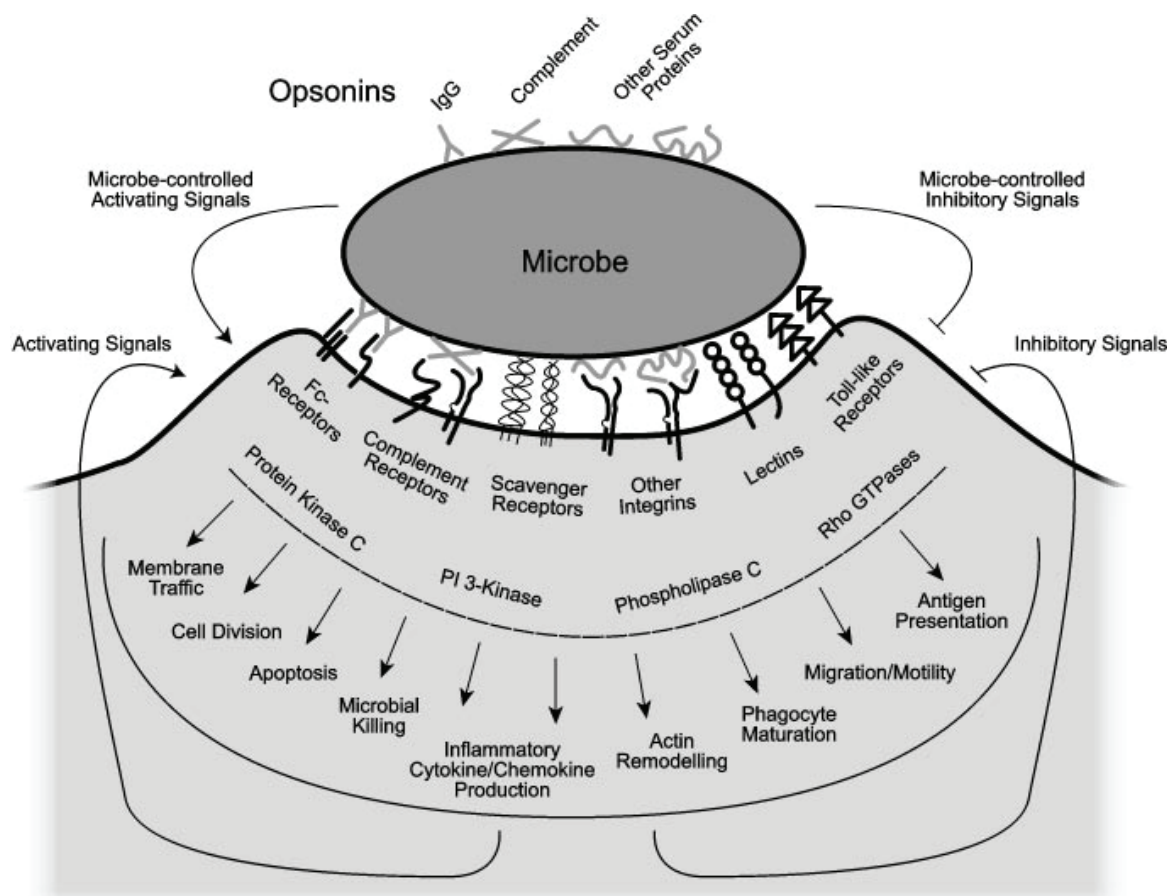


**Figure 1:** Receptor and signaling interactions during phagocytosis of microbes. Multiple receptors simultaneously recognize microbes both through direct binding and by binding to opsonins on the microbe surface. Receptor engagement induces many intracellular signals, and several molecules are utilized in many pathways. Signaling during phagocytosis may subsequently serve to activate or inhibit further phagocytosis and microbe-induced responses. Many pathogenic microbes actively regulate phagocyte responses. (Adapted from Underhill and Ozinsky 2002)

### 1.1.2 Fc Receptors

Our current understanding of the signalling pathways leading to phagocytosis in macrophages comes from studies of receptors binding to the Fc region of immunoglobulin (Ig), the so-called Fc receptors (FcR). Receptors for IgG (FcγR), IgE (FcεR) and IgA (FcαR) have been described (Janeway, Jr. and Medzhitov, 2002). Interaction of FcRs with

their immunoglobulin ligands triggers a wide series of leukocyte responses including phagocytosis, respiratory burst, antibody-dependent cell-mediated cytotoxicity, release of pro-inflammatory mediators and production of cytokines (Sanchez-Mejorada and Rosales, 1998). Fc $\alpha$ R is expressed in neutrophils, monocytes and macrophages. The three classes of Fc $\gamma$ Rs (FcRI, FcRII, FcRIII) are expressed differentially in many cell types of the immune system (Ravetch and Kinet, 1991b; Ravetch, 1994).

The most distinctive property of Fc $\gamma$ RI is its relatively high affinity for ligand; it is the only IgG FcR for which the binding of monomeric ligand can be measured directly. Fc $\gamma$ RI receptor is present on monocytes and macrophages (Perussia et al., 1983a; Looney et al., 1986), in human neutrophils it is inducible by gamma interferon (IFN- $\gamma$ ) (Perussia et al., 1983b). On monocytes and various monocyte lines, expression can be enhanced as much as 20-fold by IFN- $\gamma$  (Guyre et al., 1983a). Human monocytes have a few tens of thousands Fc $\gamma$ RI (Anderson and Abraham, 1980; Fries et al., 1982; Guyre et al., 1983b; Kurlander and Batker, 1982; Maluish et al., 1988; Perussia et al., 1983b) while murine' macrophages have many more (Unkeless and Eisen, 1975; Unkeless, 1977). Fc $\gamma$ Rs are integral membrane proteins constituted of glycosylated extracellular Ig-like domains, a short transmembrane domain and a cytoplasmic domain (figure 2). Fc $\gamma$ RI is a high affinity receptor ( $K_d \sim 10^{-8}$  M) capable of binding monomeric IgG. Human Fc $\gamma$ RII is also coded by three different genes (A,B,C) and is a low affinity receptor ( $K_d \sim 10^{-7}$  M) capable of binding only multimeric IgG. Fc $\gamma$ RIII is coded by two genes (A and B) and is also a low affinity receptor ( $K_d \sim 10^{-6}$  M) (Ravetch and Kinet, 1991b; Ravetch, 1994). The high affinity of Fc $\gamma$  receptors is attributed to three immunoglobulin like domains (EC1, EC2 and EC3) in their extracellular ligand binding region, whereas low affinity Fc $\gamma$  receptors, Fc $\gamma$ RII and Fc $\gamma$ RIII, have been characterized by the presence of two Ig-like domains (EC1 and EC2) in their extracellular region. The outer two domains (EC1 and EC2) of Fc $\gamma$ RI illustrate considerable homology to the respective domains of Fc $\gamma$ RII and Fc $\gamma$ RIII but the third domain (EC3) appears unique and may confer upon Fc $\gamma$ RI the ability to bind monomeric IgG and necessary for high affinity IgG binding (Ravetch and Kinet, 1991b; Ravetch, 1994; Ravetch and Kinet, 1991a). These related Fc $\gamma$ R proteins result from gene duplication and alternative splicing. This general scheme is true for the rodent Fc $\gamma$ Rs as well. In mammals, four different classes of Fc $\gamma$  receptors have been defined: Fc $\gamma$ RI (CD64), Fc $\gamma$ RII (CD32), Fc $\gamma$ RIII (CD16), and Fc $\gamma$ RIV (Nimmerjahn et al., 2005; Nimmerjahn and Ravetch, 2006).

Functionally two general classes of Fc $\gamma$ R are now recognized—the activation receptors, characterized by the presence of a cytoplasmic ITAM sequence associated with the receptor, and the inhibitory receptor, characterized by the presence of an ITIM sequence (figure 2) (Bolland et al., 1998;Daeron, 1997b;Ravetch and Kinet, 1991b;Hulett and Hogarth, 1994b;Ravetch and Kinet, 1991b). These two classes of receptors function in concert and are usually found coexpressed on the cell surface. Because activation and inhibitory receptors bind IgG with comparable affinity and specificity (Hulett and Hogarth, 1994a;Ravetch and Kinet, 1991b) co-engagement of both signaling pathways is thus the rule, setting thresholds for and ultimately determining the magnitude of effector cell responses. This appreciation of the balanced function of these receptors has been primarily developed through the analysis of mice deficient in either receptor or signaling pathway.

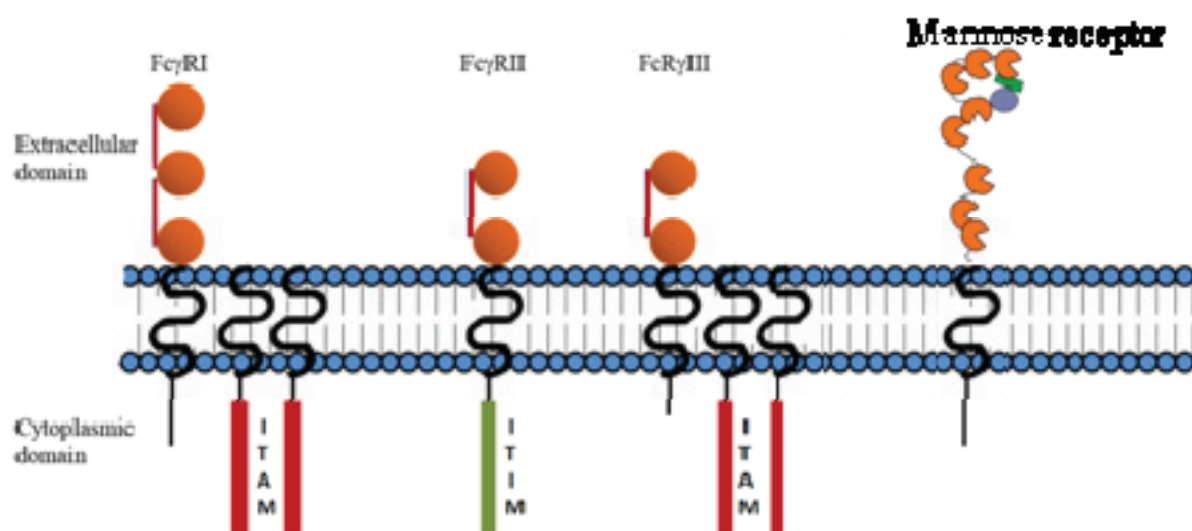


**Figure 2.** Schematic representation of Fc $\gamma$ R and MR. Each type of receptor possesses an extracellular, a transmembrane and a cytoplasmic domain. The extracellular portion of Fc $\gamma$ RI consists of three IgG-like domains, while Fc $\gamma$ RII and Fc $\gamma$ RIII have only two domains. In addition, Fc $\gamma$ RI and Fc $\gamma$ RIII associate with a common homodimeric  $\gamma$ -subunit, which contains immunoreceptor tyrosine-based activation motifs (ITAMs), whereas Fc $\gamma$ RII contains an immunoreceptor tyrosine-based inhibitory motif (ITIM) in its cytoplasmic domain. MR shows 'bent' conformation.

### Activating Fc $\gamma$ Rs and signaling

These molecules are characterized by the presence of an immunoreceptor tyrosine-based activation (ITAM) motifs either intrinsic to the receptor, as in the case of the human Fc $\gamma$ RIIA or mouse Fc $\gamma$ RIIB (Fc $\gamma$ RIIA receptors are not found in the mouse), or more commonly, as part of an associated subunit, the  $\gamma$  chain, as in Fc $\gamma$ RI and Fc $\gamma$ RIIIA,

receptors conserved between mouse and human (Daeron, 1997a;Hulett and Hogarth, 1994a;Ravetch and Kinet, 1991b). (A neutrophil specific decoy receptor, FcγRIIB, is additionally found in humans that binds IgG immune complexes without triggering activation.) Activation receptors bind IgG either with relatively high affinity ( $10^{-9}$ ) for the case of Fc RI or with low affinity ( $10^{-6}$ ), as is the case for FcγRII and FcγRIIA (17, 20). Cross-linking of the ligand binding extracellular domain results in tyrosine phosphorylation of the ITAM by members of the src kinase family, with subsequent recruitment of SH2 containing signaling molecules that bind the phosphorylated ITAM, most notably the syk kinase family of molecules. Depending on the particular cell type activated by the Fc receptor, different kinases are involved in these signaling pathways. For instance, FcγRIIA aggregation activates lck in NK cells, while FcγRIIA or FcγRIIA activate lyn and hck in monocytic and mast cells (Ghazizadeh et al., 1994;Salcedo et al., 1993). Likewise, syk is activated in mast cells and macrophages, whereas the related kinase ZAP70 is activated in NK cells (Agarwal et al., 1993;Crowley et al., 1997;Cone et al., 1993). Subsequent signaling pathways associated with cellular activation by FcγRs are similar to that observed for other ITAM-containing receptors such as the B cell receptors (BCR) and T cell receptors (TCR) (Kurosaki, 1999;Weiss and Littman, 1994). Early events include the activation of PI3-kinase, the enzymatic activity of which leads to production of PIP3 and recruitment of PH domain containing molecules, such as PLC and Tec kinases, through a PIP3-PH domain interaction(Falasca et al., 1998;Ferguson et al., 1995;Salim et al., 1996;Kawakami et al., 1996). Myeloid cells contain several Tec kinases, named Btk, Itk, and Emt (Kawakami et al., 1996), that can all be activated upon Fc receptor aggregation. The newly discovered adaptor molecules SLP-76 and BLNK link Syk activation with Btk and PLC responses in FcR-dependent macrophage activation (Bonilla et al., 2000). Ultimately, activation of PLC leads to generation of IP3, DAG, and sustained calcium mobilization. The significance of this activity for FcR function has been appreciated by the analysis of PLC 2-deficient mice, which are defective for FcγRIII-dependent NK cell function (Wang et al., 2000). Cellular phenotypes associated with FcR activation receptors include degranulation, phagocytosis, ADCC, transcription of cytokine genes, and release of inflammatory mediators (Anderson et al., 1990;Young et al., 1984;Titus et al., 1987). In general, these phenotypes are indicative of the central role of these receptors in mediating inflammatory responses to cytotoxic IgGs or IgG immune complexes. Activation FcγRs are found on most effector cells of the immune system, notably monocytes, macrophages, NK cells, mast cells, eosinophils, neutrophils, and

platelets, while absent from lymphoid cells. In general, activation and inhibitory Fc $\gamma$ Rs are coexpressed on the same cell, a physiologically important means of setting thresholds for activating stimuli, because the IgG ligand will coengage both receptors. The ratio of expression of these two opposing signaling systems will determine the cellular response. It is, therefore, not surprising that these receptors are modulated in their expression during the differentiation and development of effector cells and by cytokine activation of these cells (Ravetch and Kinetic, 1991b; Weinshank et al., 1988).

### **Inhibitory Fc $\gamma$ R and signaling**

In both mouse and human, a single gene for an inhibitory Fc $\gamma$ R, Fc $\gamma$ RIIB, encodes a single chain glycoprotein characterized by a ligand-binding extracellular domain highly homologous to its activation counterparts, but containing the distinctive immunoreceptor tyrosine-based inhibitory motif (ITIM) sequence in its cytoplasmic domain (figure 2). The inhibitory Fc $\gamma$ R binds IgG with low affinity ( $10^{-6}$ ), interacting with immune complexes only at physiological concentration of antibody (Hulett and Hogarth, 1994a; Ravetch and Kinetic, 1991b). The prototype six amino acid ITIM cytoplasmic sequence, I/V/L/SxYxxL/V, in which x denotes any amino acid, has been found in a growing number of receptors, most notably the NK inhibitory molecules that bind MHC class I (Bolland and Ravetch, 1999; Lanier, 1998; Long, 1999; Unkeless and Jin, 1997; Vivier and Daeron, 1997). The inhibitory activity of Fc $\gamma$ RIIB, embedded in the cytoplasmic domain of the single chain Fc $\gamma$ RIIB molecule, was defined as a 13 amino acid sequence AENTITYSLLKHP, shown to be both necessary and sufficient to mediate the inhibition of BCR-generated calcium mobilization and cellular proliferation (Amigorena et al., 1992; Muta et al., 1994). Significantly, phosphorylation of the tyrosine of this motif was shown to occur upon BCR coligation and was required for its inhibitory activity (Muta et al., 1994). This modification generated an SH2 recognition domain that is the binding site for the inhibitory signaling molecule SHIP that leads to the abrogation of ITAM activation signaling by hydrolyzing the membrane inositol phosphate PIP<sub>3</sub>, itself the product of receptor activation (Ono et al., 1996). In the absence of PIP<sub>3</sub>, binding proteins of the PH domain class (e.g. Btk and PLC) are released from the membrane and a sustained calcium signal is blocked by preventing influx of extracellular calcium through the capacitance-coupled channel (Bolland et al., 1998; Scharenberg et al., 1998). Fc $\gamma$ RIIB phosphorylation also leads to an arrest of B cell receptors (BCR) triggered proliferation by potentially perturbing the activation of MAP kinases and preventing the recruitment of the anti-

apoptotic protein kinase, Akt (Liu et al., 1999; Tamir et al., 2000; Yamanashi et al., 2000). In addition to its expression on B cells, where it is the only IgG Fc receptor, Fc RIIB is widely expressed on effector cells such as macrophages, neutrophils, and mast cells, missing only from T and NK cells (Hulett and Hogarth, 1994b; Ravetch and Kinetic, 1991b). Fc $\gamma$ RIIB displays three separable inhibitory activities, two of which are dependent on the ITIM motif and one independent of this motif. Coengagement of Fc $\gamma$ RIIB to an ITAM-containing receptor leads to tyrosine phosphorylation of the ITIM by the lyn kinase, recruitment of SHIP, and the inhibition of ITAM-triggered calcium mobilization and cellular proliferation (Daeron et al., 1995; Ono et al., 1996). However, inhibition of calcium mobilization and arrest of cellular proliferation, while both ITIM-dependent processes, are the result of different signaling pathways. Calcium inhibition requires the phosphatase activity of SHIP to hydrolyse PIP3 and the ensuing dissociation of PH domain containing proteins like Btk and PLC (Bolland et al., 1998; Ono et al., 1996; Scharenberg et al., 1998). The net effect is to block calcium influx and prevent sustained calcium signaling. Calcium-dependent processes such as degranulation, phagocytosis, ADCC, cytokine release and proinflammatory activation are all blocked. Arrest of proliferation in B cells is also dependent upon the ITIM pathway, through the activation of the adaptor protein dok and subsequent inactivation of MAP kinases (Tamir et al., 2000; Yamanashi et al., 2000). The role of SHIP in this process has not been fully delineated, although it can affect proliferation in several ways. SHIP, through its catalytic phosphatase domain, can prevent recruitment of the PH domain survival factor Akt by hydrolysis of PIP3 (Aman et al., 1998; Liu et al., 1999). SHIP also contains PTB domains that could act to recruit dok to the membrane and provide access to the lyn kinase that is involved in its activation. Dok-deficient B cells are unable to mediate Fc $\gamma$ RIIB triggered arrest of BCR-induced proliferation, while retaining their ability to inhibit a calcium influx, demonstrating the dissociation of these two ITIM-dependent pathways (Yamanashi et al., 2000). The third inhibitory activity displayed by Fc $\gamma$ RIIB is independent of the ITIM sequence and is displayed upon homo-aggregation of the receptor. Under these conditions of Fc $\gamma$ RIIB clustering, a proapoptotic signal is generated through the transmembrane sequence. This proapoptotic signal is blocked by recruitment of SHIP, which occurs upon coligation of Fc $\gamma$ RIIB to the BCR, due to the Btk requirement for this apoptotic pathway. This novel activity has been reported only in B cells and has been proposed to act as a means of maintaining peripheral tolerance for B cells that have undergone somatic hypermutation (Pearse et al., 1999).

### 1.1.3 Mannose receptor (MR)

The mannose receptor (MR) (CD206) is a type-I transmembrane protein that is characterized as a Group VI C-type lectin. It shares the same overall structure with three other receptors (phospholipase A2 receptor, ENDO 180 and DEC205) which together are known as the MR family (Allen and Aderem, 1996b; East and Isacke, 2002). Structurally, it consists of an extracellular region containing an amino terminal cysteine rich domain, a fibronectin type II repeat domain, eight CTLDs, a transmembrane region and a short cytoplasmic tail. A structural model has been proposed where at least two conformations of the MR exist – an extended form and a more compact “bent” form (Boskovic et al., 2006)(figure. 2). The MR has a single tyrosine residue in its cytoplasmic tail that occurs within a diaromatic amino acid sequence (Kruskal et al., 1992). (Lew et al., 1994; Linehan et al., 1999) Its expression was originally thought to be restricted to mammalian tissue macrophages but it is now known to be expressed on lymphatic and hepatic epithelium, kidney mesangial cells, tracheal smooth muscle cells and retinal pigment epithelium (Lew et al., 1994; Linehan et al., 1999; Shepherd et al., 1991). Expression has also been observed on human monocyte-derived DCs (Avrameas et al., 1996), (Engering et al., 1997; Sallusto et al., 1995). and on a subpopulation of murine DCs (McKenzie et al., 2007). The bulk of the MR is intracellular, located within the endocytic pathway, with only a small proportion present on the cell surface. Its expression is up-regulated by IL-4, IL-13 and IL-10, whereas IFN $\gamma$  has a down-regulatory effect (Martinez-Pomares et al., 2003; Harris et al., 1992; Stein and Gordon, 1991a). Surface expression is also influenced by proteolytic cleavage of the membrane-bound receptor by a metallo protease resulting in a functional soluble form of the receptor (Martinez-Pomares et al., 1998). The MR binds a broad array of microorganisms, including *Candida albicans*, *Pneumocystis carinii*, *Leishmania donovani*, *Mycobacterium tuberculosis*, and capsular polysaccharides of *Klebsiella pneumoniae* and *Streptococcus pneumonia* (Chakraborty et al., 2001; Ezekowitz et al., 1991; Marodi et al., 1991; O’Riordan et al., 1995; Schlesinger, 1993; Zamze et al., 2002). The receptor recognises mannose, fucose or N-acetylglucosamine sugar residues on the surfaces of these microorganisms (Taylor et al., 1992; Largent et al., 1984) and carbohydrate recognition is mediated by CTLDs 4–8 (Taylor et al., 1992). The MR has been implicated in the phagocytic uptake of pathogens, but there are limited examples actually demonstrating MR-dependent phagocytosis. The first suggestion that the MR was a phagocytic receptor was based on the mannan-inhibitable uptake of zymosan by mouse peritoneal macrophages (Sung et al., 1983). It has subsequently been shown that mannan



can be recognised by a number of receptors, including DC specific ICAM grabbing non-integrin (DC-SIGN), and studies that have attributed a phagocytic role to the MR based purely on experiments using mannan as a specific inhibitor of the MR are therefore not reliable. Others have reported that transfection of the nonphagocytic COS-1 cell line with the MR results in phagocytosis of *C. albicans* and *P. carinii* and that the cytoplasmic tail of the receptor is essential for this activity (Ezekowitz et al., 1990; Ezekowitz et al., 1991). A further study showed that MR-positive J774-E macrophages ingested three fold more *Francisella tularensis* than MR-negative J744-E cells. This study used receptor-blocking antibody in addition to soluble mannan as inhibitors (Schulert and Allen, 2006). In macrophages the MR is also thought to be involved in the non-opsonic phagocytosis of virulent *M. tuberculosis* (Schlesinger, 1993). MR recognition of mannose-capped lipoarabinomannan (ManLAM) on the mycobacterial cell wall initiates a specific phagocytic pathway resulting in limited phagosome–lysosome fusion (Kang et al., 2005) suggesting a mechanism of how the pathogen survives in the phagosome. The MR has also been implicated in the phagocytic uptake of apoptotic cells in Chronic Obstructive Pulmonary Disease (COPD) (Hodge et al., 2003). Alveolar macrophages from COPD patients express significantly less MR than alveolar macrophages from healthy controls. This link was more firmly established when the phagocytic ability of alveolar macrophages was shown to be significantly reduced by blocking the expression of the MR using a specific blocking antibody (Hodge et al., 2008). There has been some examination of the mechanism of MR-mediated phagocytosis. The cytoplasmic tail is required for uptake in MR-transfected cells, however, mutation of the single cytoplasmic tyrosine reduced, but did not abolish phagocytosis (Kruskal et al., 1992).

## 1.2 Phagocytic signaling

Phagocytosis is extremely complex, and no single model can fully account for the diverse structures and outcomes associated with particle internalization. This complexity is in part due to the diversity of receptors capable of stimulating phagocytosis, and in part due to the capacity of a variety of microbes to influence their fate as they are internalized. The fact that most particles are recognized by more than one receptor, and that these receptors are capable of cross-talk and synergy, further complicates our understanding. In addition, many phagocytic receptors have dual functions; often mediating both adhesion and particle internalization, and a complex relationship exists between these two related processes. Adhesion receptors and phagocytic receptors can both activate and inhibit each other's

function. For example, ligation of the fibronectin receptor at the substrate-adherent surface of a monocyte establishes preconditions within the cell that permit the otherwise inactive

**Table 1: Phagocytic receptors present on macrophages surface participates in phagocytosis of microbes**

Receptors	Ligands	Reference
Opsonin-dependent receptors		
Fc $\gamma$ RI (CD64)	Monomeric IgG	(Ravetch and Kinet, 1991b)
Fc $\gamma$ RII (CD32)	IgG immune complexes	(Ravetch and Kinet, 1991b)
Fc $\gamma$ RIII (CD16)	IgG immune complexes	(Ravetch and Kinet, 1991b)
CR1 (CD35)	Complement fragment C1q, C4b, C3b	(Aderem and Underhill, 1999)
CR3(CD11b/CD18)	Complement fragment iC3b	(Aderem and Underhill, 1999)
CR4(CD11c/CD18)	Complement fragment iC	(Aderem and Underhill, 1999)
Opsonin-independent receptors		
Mannose receptor (CD206)	Mannan	(Ezekowitz et al., 1990)
Dectin-1	$\beta$ 1,3-glucan	(Brown and Gordon, 2001)
Scavenger receptor CD14	Lipoteichoic acid, LPS LPS, peptidoglycan	(Krieger and Herz, 1994) (Devitt et al., 1998)
$\beta$ -glucan receptor	$\beta$ -glucan	(Czop and Kay, 1991)

complement receptor CR3 to mediate phagocytosis (Pommier et al., 1983; Wright et al., 1983). On the other hand, adherent cells often round up during phagocytosis, implying that there is competition for cytoskeletal and membrane components necessary for phagocytosis and adhesion. Many of the cytoskeletal components known to participate in adhesion are also enriched in the phagocytic cup. These include paxillin, talin, vinculin,  $\alpha$ -actinin, protein kinase C, MARCKS and MacMARCKS (Allen and Aderem, 1996b; Allen and Aderem, 1996a; Allen and Aderem, 1995). Despite the complexity associated with different phagocytic mechanisms, a number of shared features follow: Particle internalization is initiated by the interaction of specific receptors on the surface of the phagocyte with ligands on the surface of the particle. This leads to the polymerization of actin at the site of ingestion, and the internalization of the particle via an actin-based mechanism. After internalization actin is shed from the phagosome, and the phagosome matures by a series of fusion and fission events with components of the endocytic pathway, culminating in the formation of the mature phagolysosome. Since endosome-lysosome trafficking occurs primarily in association with microtubules, phagosome maturation requires the coordinated interaction of the actin and tubulin based cytoskeletons.

Phagocytic cells are involved in a number of biological processes, including the recognition and control of invading microbes. Innate pathogen recognition is mediated by a series of germline encoded pattern recognition receptors (PRRs) that are either soluble or membrane-bound. These PRRs recognise conserved microbial structures, such as bacterial lipopolysaccharide or fungal  $\beta$ -glucans, that are known as pathogen associated molecular patterns (PAMPs) (Janeway, Jr. and Medzhitov, 2002). Soluble PRRs include the collectins, ficolins, pentraxins and complement. These proteins coat or “opsonise” the infectious agent which can then be ingested via specific opsonic receptors. Some of these proteins can also regulate the surface expression of other phagocytic receptors and thereby exert an indirect influence on uptake. Membrane bound PRRs, such as mannose receptor, directly recognise microbes and mediate their uptake. The role of toll-like receptors (TLRs) in phagocytosis is a topic which is fervently debated in the literature. One side of this debate argues that signaling through surface TLRs, which are recruited to the phagosome upon uptake of microbial pathogens, is critical for phagosome maturation (Blander and Medzhitov, 2006a; Blander and Medzhitov, 2006b; Blander, 2007b; Blander, 2007a). The other side argues that phagosome maturation proceeds independently of TLR signalling (Yates and Russell, 2005). TLR signalling has also been shown to participate in autophagy (Xu et al., 2007) and a recent study reports that engagement of the autophagy pathway via TLR signalling enhances phagosome maturation (Sanjuan et al., 2007). This makes it tempting to assign a role for TLR signaling in the regulation of phagosome maturation, but further studies are first needed to clarify the current ambiguities. The Fc and complement receptor 3 (CR3) are involved in the uptake of opsonised pathogens and are the two best characterised phagocytic receptors in macrophages. Fc $\gamma$ Rs bind to immunoglobulin G (IgG)-opsonised particles, whereas CR3 binds complement-coated particles (Aderem and Underhill, 1999; Garcia-Garcia and Rosales, 2002; Swanson and Hoppe, 2004). The reorganisation of actin underlies uptake by both receptors but the mechanisms are distinct. It has long been known that during Fc $\gamma$ Rs-mediated phagocytosis, actin-rich pseudopodia extend circumferentially around the particle and draw it into the cell forming a tight-fitting “zippered” phagosome (Griffin, Jr. et al., 1975; Kaplan, 1977). In contrast, complement-opsonised particles appear to sink into the cell with little or no protrusions resulting in a more spacious phagosome (Griffin, Jr. et al., 1975; Kaplan, 1977). During Fc $\gamma$ R-phagocytosis, which is mediated by signalling through defined cytoplasmic immunoreceptor tyrosine-based activation (ITAM) motifs, PI-3 kinase, Rac and Cdc42 have been shown to have essential roles in actin reorganisation, membrane protrusion,

pseudopod extension and phagosome closure (Caron and Hall, 1998). On the other hand, Rho is required for CR3-mediated phagocytosis, whereas tyrosine kinases, Cdc42 and Rac are not critical (Caron and Hall, 1998). In addition, unlike Fc $\gamma$ R-mediated phagocytosis, induction of the respiratory burst and production of inflammatory mediators do not accompany CR3-mediated phagocytosis (Aderem et al., 1985; Stein and Gordon, 1991b; Yamamoto and Johnston, Jr., 1984). In contrast, relatively little is known about mechanisms underlying C-type lectin-mediated phagocytosis and indeed the precise role of certain C-type lectins in phagocytosis is still contentious. Thus the diversity of phagocytic mechanisms presents a challenge to elucidate the underlying principles of the process. Roles for many receptors and many signaling molecules have been described, and key signaling molecules are emerging as regulators of multiple phagocytic responses.

### **1.3 Nano-scale imaging using atomic force microscopy (AFM)**

In biological science, probing receptor–ligand interactions is essential to gain a detailed understanding of cellular events such as cell adhesion and to control cell responses (Gumbiner, 2005; Mrksich, 2002; Ratner and Bryant, 2004; Wehrle-Haller and Imhof, 2002). During the past decades, tremendous progress has been made in characterizing biomolecular forces, using techniques like the osmotic stress method the surface forces apparatus magnetic beads, optical tweezers and the biomembrane force probe (Ashkin et al., 1990; Leckband et al., 1992; LeNeveu et al., 1976; Merkel et al., 1999; Smith et al., 1992). Yet, these techniques do not offer lateral resolution and are generally not suited for mapping recognition sites on living cells or in physiological buffer solution. AFM has become a very powerful technique for achieving high resolution imaging of biological samples in the past decade after its invention by Binnig, Quate, and Gerber in 1996 (Binnig et al., 1986). Despite the vast body of available literature on the structure and function of receptor-ligand complexes, information about the molecular dynamics within the complexes during the association and dissociation process is usually lacking. Moreover, until recently, mapping the spatial distribution of individual binding sites on model or cellular surfaces was not accessible because of a lack of appropriate imaging techniques. Consequently, there is clearly a need to develop and exploit single molecule tools for sensing and mapping molecular recognition interactions on biosurfaces.

### 1.3.1 Principle of AFM

The advent of atomic force microscopy (AFM) has opened a wide range of novel possibilities for exploring biosurfaces, in terms of structure, properties and biomolecular interactions. While AFM imaging is used for generating three-dimensional topographic views of biological specimens at high resolution and under physiological conditions (Engel and Muller, 2000; Horber and Miles, 2003), single-molecule force spectroscopy allows researchers to measure biomolecular forces with piconewton sensitivity ( $10^{-12}$  N) (Clausen-Schaumann et al., 2000; Fisher et al., 2000). These nanoscale measurements provide new insight into the structure–function relationships of biosurfaces and contribute to the development of novel biotechnological and biomedical applications. The basic idea behind AFM is that three-dimensional images of surfaces can be obtained by sensing the force between a sample and a sharp tip mounted at the end of a soft cantilever, without using an incident beam as in classical microscopes. To this end, the specimen is mounted on a piezoelectric scanner, which allows three dimensional positioning with sub-nanometer accuracy while the force is monitored with piconewton sensitivity by measuring the deflection of the cantilever. The deflection, or vertical bending of the cantilever, is usually detected using a laser beam focused on the free end of the cantilever and reflected into a photodiode. AFM cantilevers and tips are typically made of silicon or silicon nitride using microfabrication techniques. Measuring molecular recognition forces by AFM requires recording force curves between the modified tip with the ligand of choice and sample surface. AFM force curves are obtained by monitoring, at a given (x, y) location, the cantilever deflection (d) as a function of the vertical displacement of the piezoelectric scanner (z). This yields a raw ‘voltage displacement’ curve, which can be converted into a ‘force-displacement’ curve using two conversions. First, the sensitivity of the AFM detector, that is, the slope of the retraction curve in the region where tip and sample are in contact, is used to convert the voltage into a cantilever deflection. It is important to note that the estimated sensitivity is only valid when the sample behaves like a hard, nondeformable material, which is often true for purified molecules attached on hard supports. For soft cells, however, the value obtained for the sensitivity may be incorrect owing to sample deformation by the tip. In this case, it is mandatory to assess the sensitivity of the detector on a hard support, before or after the force measurements on cells. Second, the cantilever deflection is converted into a force (F) using Hooke’s law:  $F = k \times d$ , where k is the cantilever spring constant. The force resolution of the AFM is in first approximation limited by the thermal noise of the cantilever that, in turn, is determined by

its spring constant. In addition, the resonance frequency, the quality factor, and the measurement bandwidth can also substantially contribute (Hinterdorfer and Dufrene, 2006). Therefore, for single-molecule force measurements, best results are generally obtained with cantilevers exhibiting small spring constants (that is, in the range of 0.01 to 0.10 N/m) and short lengths ( $<50\ \mu\text{m}$ ), because they exhibit lower force noise. Force–distance curves can be recorded either at single, well-defined locations of the  $(x, y)$  plane or at multiple locations to yield a so-called ‘force–volume image’ (Heinz and Hoh, 1999). In doing so, spatially resolved maps of sample properties and molecular interaction forces can be produced. For quantitative force measurements, researchers must calibrate the actual spring constants of the cantilevers, using geometric or thermal methods (Dupres et al., 2007). A typical force–distance curve is shown in figure 3. At large tip–sample separation distances, the interaction force is zero (A) and the cantilever is not deflected. As the tip approaches the surface, the cantilever may bend upward due to repulsive forces (B) until the tip jumps onto the sample surface. This approach portion of the curve can be used to measure surface forces, including van der Waals, electrostatic, solvation, hydration, and steric/bridging forces. In principle, moving the sample further causes a cantilever deflection of the same amount as the sample movement. In fact, different behaviors may occur in the contact region, depending on the sample stiffness. On a hard and non-deformable surface, a vertical line is recorded (C); while on a soft surface, sample indentation will occur, leading to a different shape ( $C_0$ ). Analyzing this behavior with appropriate theoretical models may provide direct information on the sample elasticity.

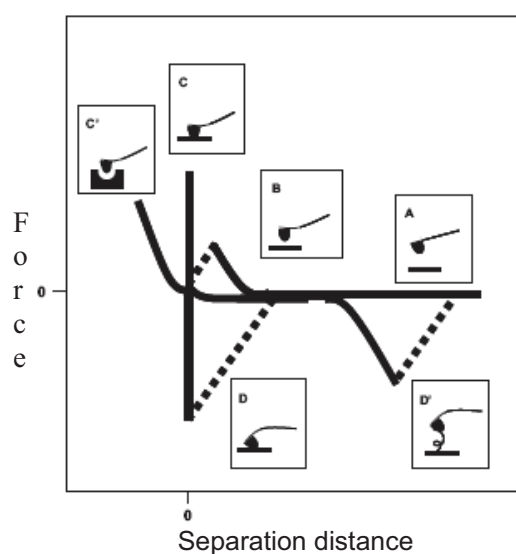


**Figure 3.** Principle of AFM force spectroscopy: the different portions of a force vs. distance curve (adapted from Dupres et al 2007)

Upon retracting the tip from the surface, the curve often shows a hysteresis referred to as the adhesion “pull-off” force (label D), which can be used to estimate the surface energy of solids or the binding forces between complementary biomolecules. In the presence of long, flexible molecules, an attractive force, referred to as an elongation force, may develop nonlinearly (label  $D_0$ )

### 1.3.2 Simultaneous Topography and RECOgnition imaging (TREC)

Since the beginnings of AFM measurement techniques have steadily evolved leading to a growing field of successful applications in biology. Although force spectroscopy (consisting in recording force vs. distance curves) represents an excellent method for studying one key issue in biological processes, molecular recognition, until recently it was impossible to record recognition maps at the same resolution and imaging speed as the conventional maps of topography, lateral force, phase, etc. The introduction of simultaneous Topography and RECOgnition (TREC) imaging (Hinterdorfer and Dufrene, 2006;Ebner et al., 2005;Dupres et al., 2007;Stroh et al., 2004b) provided a simple and fast Dynamic Force Microscopy (DFM) mode capable of simultaneously recording images of topography and specific recognition between the molecules at scanning tip and sample.

In dynamic recognition imaging, molecular recognition signals are detected during dynamic force microscopy imaging (Han et al., 1997;Hinterdorfer et al., 1996;Raab et al., 1999). AFM tips carrying ligands are oscillated at very small (5–10 nm) amplitudes while being scanned along the surface to which the cognate receptors are bound. Topography and recognition images are simultaneously obtained (by simultaneous topography and recognition (TREC) imaging) using an electronic circuit (PicoTrec; Molecular Imaging) (Stroh et al., 2004a;Stroh et al., 2004b). Maxima ( $U_{up}$ ) and minima ( $U_{down}$ ) of each sinusoidal cantilever deflection period are depicted and fed into the AFM controller, with  $U_{down}$  driving the feedback loop to record the height (that is, the topography) image and  $U_{up}$  providing the data for construction of the recognition image (figure. 4a). It is important to note that only for cantilevers with a low quality factor ( $\sim 1$  in liquid) driven at frequencies below resonance both types of information are independent. Using this approach, singly distributed avidin molecules were scanned with a biotinylated AFM tip (Ebner et al., 2005) yielding topography and recognition images at the same time (figure. 4b). The lateral positions of the avidin molecules obtained in the topography image were spatially well correlated with the recognition signals of the recognition image (figure. 4b). Dynamic recognition imaging offers the advantage that topography and recognition images can be recorded at the same speed as that used for conventional topographic imaging,

typically 1–5 minutes per image. Yet, this is still slower than the rate of most dynamic processes, meaning that developing AFM instruments with increased imaging rates is an important challenge. The biggest advantage of the TREC is that topography and recognition images can be recorded simultaneously. Imaging of biological specimen has therefore greatly benefited from the development of TREC. Soft samples are significantly less deformed and probes weakly adhered to surfaces are not easily displaced by the forces applied. In a recently demonstrated MACmode, AFM yields high-resolution topographical images of rigid protein membranes, surface-attached viruses and living cells. The magnetically coated cantilevers are oscillated by an alternating magnetic field. In addition to the low force applied, the oscillation amplitude is, in contrast to the deflection used for contact-mode AFM, insensitive to thermal drift. This results in more stable imaging and less destruction of the biological samples.

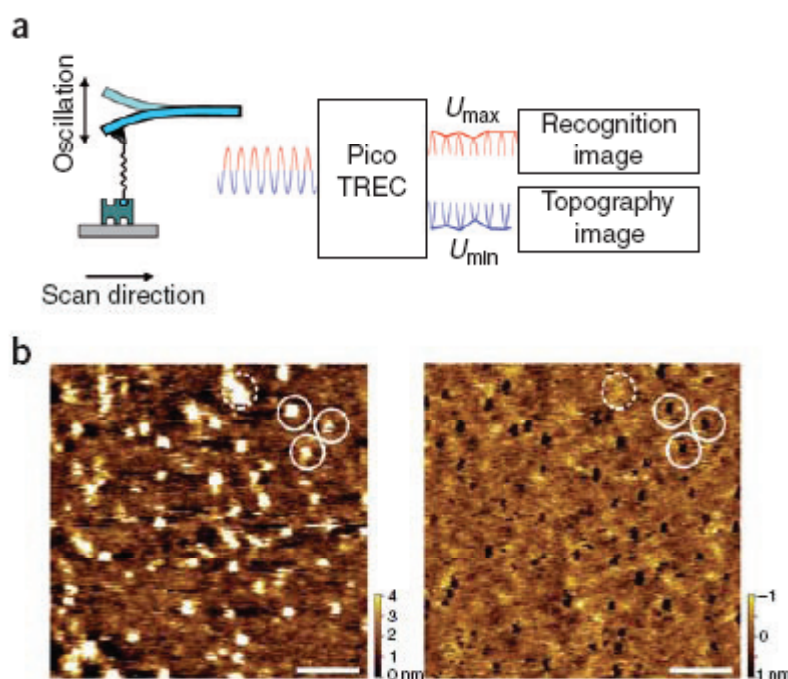


**Figure 4: Simultaneous topography and recognition imaging (TREC).**(a) The cantilever oscillation signal is split into minima  $U_{min}$  and maxima  $U_{max}$ . (b) Singly distributed avidin molecules imaged with a biotin-tethered tip. The bright dots 2 to 3 nm in height and 15 to 20 nm in diameter visible in the topography image (left, solid circles) are single avidin molecules, and the black dots of the recognition image (right) arise from a decrease of the oscillation maxima that result from the physical avidin-biotin connection during recognition. Some topographical features lack specific interaction (dashed circle). Scan size was 500 nm. Scale bars, 100 nm. (Adapted from Ebner et al 2005)

Thus AFM has several advantages over the other imaging techniques like scanning electron microscope (SEM) or confocal fluorescent microscopy. Unlike the electron microscope which provides a two-dimensional projection or a two-dimensional image of a sample, the AFM provides a true three-dimensional surface profile. Additionally, samples



viewed by AFM do not require any special treatments (such as metal/carbon coatings) that would irreversibly change or damage the sample. While an electron microscope needs an expensive vacuum environment for proper operation, most AFM modes can work perfectly well in ambient air or even a liquid environment. This makes it possible to study biological macromolecules and even living organisms. In principle, AFM can provide higher resolution than SEM. High resolution AFM is comparable in resolution to Scanning Tunneling Microscopy and Transmission Electron Microscopy. AFM offers an elegant technique to study the ligand-receptor kinetics and mapping the single molecular recognition sites and topography of the cells in physiological conditions.

#### **1.4 Latex beads system as a tool to study the cross-talk and landscape of receptors on macrophages surface**

The method using inert latex beads as a model system to study phagocytosis was introduced by Wetzel and Korn more than 35 years ago (Wetzel and Korn, 1969) and was re-discovered and expanded by Griffiths and co-workers in the early 1990's (Desjardins et al., 1994a). The ability of latex bead phagosomes (LBP) to display most of the functions of phagosomes containing other particles, such as apoptotic cells or non-pathogenic bacteria, qualified it as a system suitable to analyse the phagocytic process. LBP display fission and fusion events with endosomes and lysosomes over long time periods (Desjardins et al., 1994b; Jahraus et al., 1998; Kjekken et al., 2004; Wetzel and Korn, 1969), bind and move along microtubules (Blocker et al., 1997), promote the assembly of actin filaments (Jahraus et al., 2001) and bind to them (Al Haddad et al., 2001) and become acidified (Defacque et al., 2002). Phagosomes containing nonpathogenic *Mycobacterium smegmatis*, but not those containing the pathogens *M. tuberculosis* and *M. avium*, have also been shown to assemble actin (Anes et al., 2003), confirming that LBPs are a good model for providing insights into the behavior of phagosomes containing non-pathogenic bacteria. Moreover, the use of latex beads provides other unique advantages for the study of receptor-dependent phagocytosis, which are of high importance for this study. In contrast to pathogens, which are internalised after multiple ligand interactions, latex beads can be coupled to single ligands and offers the opportunity for the analysis of single receptor recognition pathways that influence not only uptake and signalling but also phagosomal maturation events (Desjardins & Griffiths 2003). Additionally, latex beads are easily detectable by microscopy and can readily be labelled with fluorochromes, allowing studies by fluorescence microscopy. Latex beads are available in a wide range of sizes that can be

coupled to ligand of choice. Thus, latex beads system provide an opportunity to study the landscape of different receptors on cell surface involve in phagocytosis.

### **1.5 Aims of the study**

In this study I aimed to unravel the nano-landscape of two very widely studied receptors present on the macrophage surface i.e mannose receptors and Fc $\gamma$  receptors that are involved in the phagocytosis of majority of microbes in a opsonin-independent and opsonin-dependent manner. For this study I have used latex beads system and a combination of high-resolution atomic force microscope (AFM) topography imaging with single molecule force spectroscopy have been used as tools to investigate the landscape of macrophage receptors. The latex bead system offers the possibility to conjugate beads to single ligands in order to trigger defined receptor-mediated uptake. I used Fc fragment of IgG, mannan and avidin as coupling ligand. Similarly AFM tips can also be conjugated with our ligand of choice. The specific aims of this study are as follows:

1. To investigate the distribution and possible interaction/cross-talk of mannose and Fc $\gamma$  receptors on the mouse macrophage cell surface using latex beads.
2. To estimate the nearest inter-receptor distances between mannose receptor and Fc $\gamma$ RI.
3. To gain the detailed information on the local organization of Fc $\gamma$ Rs on mouse macrophage cell surface by using atomic force microscope (AFM)
4. To investigate the dynamics of Fc fragment of IgG with their cognitive receptors (Fc $\gamma$ Rs) on mouse macrophage surface single using molecular recognition force spectroscopy (MRFS)

# *Materials and methods*

## 2.1 Cultivation of J774A.1 macrophage cells and bacteria

### 2.1.1 Used material, reagents and instruments

- Phosphate-buffered saline (PBS): 80 g/l NaCl + 2 g/l KCl + 11.5 g/l Na<sub>2</sub>HPO<sub>4</sub> \*2H<sub>2</sub>O + 2 g/l KH<sub>2</sub>PO<sub>4</sub> (Merck, Germany)
- Fetal bovine serum (FBS), Lot. #55H (Biochrom KG, Germany)
- Culture medium of J774 macrophages: DMEM (4500 mg/l glucose) + 1 % 10 000 U/10 000 µg/ml Penicillin/Streptomycin + 1% 200 mM L-Glutamine + 1 % nonessential amino acids (Invitrogen, Germany)
- Middlebrook 7H9 medium, ADC and OADC nutrient broth (Difco, BD DiagnosticSystems, Germany)
- Trypsin-EDTA, Hygromycin B, Ampicillin (Invitrogen, Germany)
- sterile cell culture material, like pipettes, dishes and flasks, cell scraper, centrifuge tubes etc. (TPP, Switzerland)
- Cryotubes, LabTek cell culture chambers (Nalge, USA); sterile filters (Sarstedt, Germany); syringes, cannula (Braun, Germany)
- Flow Hood (BDK, Germany); Centrifuge ZK 380 (Hermle, Germany); Incubator BB16 (Heraeus, Germany) adjusted to 37 °C, 5 % CO<sub>2</sub>

### 2.1.2 Cultivation of macrophage cells

Unless otherwise stated, all experiments were carried out using the mouse macrophage-like cell line J774A.1 (ACC170) obtained from the German Resource Center of Biological Material (DSMZ, Germany). J774 cells express a variety of phagocytic receptors and are frequently used for studies on phagocytosis. To avoid the influence of changes in the internalisation characteristics of this cell line, J774 macrophages were only used up to passage 25. New passages were obtained from stocks that were frozen in FBS supplemented with 10 % DMSO kept in liquid nitrogen. Confluent cell layers were split using Trypsin-EDTA.

For AFM experiments cells were grown on 22 mm diameter glass slides until 50-70% confluence. The cells were then fixed either with 0.5 % glutaraldehyde (for force spectroscopy control test) or with 4 % paraformaldehyde (PFA) in Hank's balanced salt solution (HBSS) buffer at 37 °C for 1-2 hours (for force spectroscopy and TREC measurements). Furthermore, In order to smooth the cellular surface during the AFM

measurements, cells before fixation were osmotically swelled in hypotonic medium (i.e. cell culture medium diluted in proportion 1:2 with distilled water).

### 2.1.3 Cultivation of bacteria

Non-pathogenic *Mycobacterium smegmatis* mc2 155 harbouring a p19-(long-lived) EGFP plasmid (Anes et al. 2003) was grown in medium containing Middlebrook's 7H9 broth and 10 % ADC nutrient broth, supplemented with 0.5 % D-glucose and 0.05 % Tween-80 at 37 °C on a shaker at 220 rpm until exponential phase. In order to stabilize GFP expression, medium was supplemented with 50 µg/ml Hygromycin B and bacteria were subcultured every day in fresh medium for 7-10 days before used for experiments. Fresh cultures were made out of glycerol stocks (50 % glycerol, 50 % bacteria in 7H9 medium) kept at -80 °C. For culturing the bacteria on plates, agar was added to the Middlebrook's 7H9 medium with above mentioned supplements.

Isolations of mycobacteria from macrophages in competition experiments was carried out as described previously (Chakraborty et al. 1994) with slight modifications. Cultures were grown until exponential growth phase was reached ( $OD_{600nm} = 0.2$ ; corresponds to  $\sim 10^8$  cells/ml). Bacteria were washed twice in PBS and re-suspended in PBS to a final concentration of  $5 \times 10^9$  cells/ml. The suspension was treated for 2 min. in a waterbath sonicator at RT using four times 30 sec. pulses to disperse clumps. Subsequently, bacteria were passed through a 23-gauge needle to disrupt remaining bacterial clumps. Before infection, residual bacterial aggregates were removed by low speed centrifugation at 120 g for 2 min. The absence of bacterial clumps was finally verified by phase contrast microscopy. J774 macrophages were grown in cell culture dishes until they reached around 70-80 % confluency and washed with PBS before infection. Mycobacteria suspensions were resuspended in prewarmed internalisation medium and macrophages were infected at an  $OD_{600nm} = 0.01$ . For competition experiments a mixture of Fc beads (0.01%) and Mycobacteria was used. Uptake of bacteria ('pulse' time) was allowed for 30 min. at 37 °C under continuous wiping to increase internalisation efficiency. Non-internalised bacteria were removed by intensive washing of the cells with PBS followed by another half hour (or different time points) of incubation in cell culture medium at 37 °C and 5 % CO<sub>2</sub>. Subsequently, the medium was removed, cells were washed with PBS and harvested by detaching them from the dish with a cell scraper in ice-cold PBS. Cells were collected in 50 ml tubes and centrifuged with 800 rpm for 7 min. at 4 °C. Pellets were resuspended in ice-cold PBS and centrifuged with 1500 rpm for 5 min. at 4 °C. Cell

pellets were lysed with 25 guage syringe and lysates were prepared in sterile water. Serial dilution of lysate were prepared and plated on Middlebrook 7H9 medium containing agar. Bacterial colonies were counted after an incubation period of 4 days. For the microscopic studies, similar concentrations of beads and bacteria were used and cells were fixed as mentioned in cell fixation section.

## 2.2 Preparation and coupling of latex beads to ligands

### 2.2.1 Used material and reagents

#### Latex beads

- Blue-fluorescent carboxylate-modified microspheres containing 2 % solids of diameter 1 $\mu$ m (Cat. F8815; Invitrogen, Germany)
- Red-fluorescent carboxylate-modified microspheres containing 2 % solids of diameter 1 $\mu$ m (Cat. F8821; Invitrogen, Germany)
- Red-fluorescent carboxylate-modified microspheres containing 2 % solids of diameter 0.02 $\mu$ m (Cat. F8786; Invitrogen, Germany)
- Red-fluorescent carboxylate-modified microspheres containing 2 % solids of diameter 0.2  $\mu$ m (Cat. F8810; Invitrogen, Germany)
- Red-fluorescent carboxylate-modified microspheres containing 2 % solids of diameter 0.5 $\mu$ m (Cat. F8812; Invitrogen, Germany)
- Red-fluorescent carboxylate-modified microspheres containing 2 % solids of diameter 2 $\mu$ m (Cat. F8826; Invitrogen, Germany)

#### Ligands

- Avidin (Cat. A2666; Invitrogen, Germany)
- Fc fragment of mouse IgG (Cat. 31205; Pierce Biotechnology, USA)
- Mannan from *Saccharomyces cerevisiae* (Man; Cat. M7504; Sigma-Aldrich, USA)

#### Reagents

- MES buffer (Cat. M8250; Sigma-Aldrich): 500 mM stock solution in Aqua dest. diluted 100 mM and 50 mM solutions were adjusted to pH 6.7
- Stop buffer: 1 % Triton X-100 in 10 mM Trizma base (Sigma-Aldrich, USA); adjusted to pH 9.4

- Bicarbonate buffer: 50 mM Na<sub>2</sub>CO<sub>3</sub> + 50 mM NaHCO<sub>3</sub> (both from Sigma-Aldrich, USA); adjusted to pH 9.6
- modified Phosphate buffer (PBS): 50 mM Na<sub>3</sub>PO<sub>4</sub> \* 12 H<sub>2</sub>O + 0.9 % NaCl (both from Sigma-Aldrich, USA); adjusted to pH 7.4
- Activator of surface carboxyl groups: N-(3-Dimethylaminopropyl)-N'-ethylcarbodiimide hydrochloride (EDAC; Cat. E1769; Sigma-Aldrich, USA); 10 mg/ml stock solution in Aqua dest., prepared freshly
- Cross-linker: Concanavalin A from *Canavalia ensiformis* (ConA; Cat. C2010;Sigma-Aldrich, USA)
- Bovine serum albumin (BSA), IgM (M5909) and sodium azide (all from Sigma-Aldrich, USA)

### 2.2.2 Coupling of latex beads to avidin

Latex beads were vortexed and sonicated in an ultrasonic waterbath for 2 min. 4 ml of bead suspension were mixed with 5 mg avidin diluted in 2 ml 50 mM MES. Suspension was filled to a final volume of 10 ml with 100 mM MES and mixed on a vertical tube rotator for 15 min. at RT. Subsequently, 0.14 ml EDAC stock solution was added to bead suspension and mixed on a vertical tube rotator for 1 hr. at RT. Another 0.14 ml EDAC were added and mixed for 1 hr. Afterwards, 2 ml stop buffer were added to the suspension, which was centrifuged in conical Eppis with 6.000 g for 5 min. at 4 °C. Pellets were resuspended in stop buffer and centrifuged again followed by three washes in PBS. Coupled latex beads were resuspended and combined in PBS containing 0.03 % FSG and suspension was adjusted to 1 % solids by measuring OD<sub>600nm</sub> using a photospectrometer.

### 2.2.3 Coupling of latex beads to IgG Fc fragment

Latex beads were vortexed and sonicated in an ultrasonic waterbath for 2 min. 5 ml of bead suspension were mixed with 0.5 mg mouse IgG Fc fragment. The following steps were carried out identical to the protocol of coupling beads to avidin. Latex bead suspensions coupled to the whole IgG molecule tend to aggregate easily and therefore caused problems during uptake of single beads. Alternatively, coupling to the Fc fragment was carried out, which did not cause much aggregation.

## 2.2.4 Coupling of latex beads to mannan

Latex beads were vortexed and sonicated in an ultrasonic waterbath for 2 min. 5 ml of bead suspension were mixed with 0.5 mg ConA and filled to a final volume of 10 ml with 100 mM MES. Suspension was mixed on a vertical tube rotator for 15 min. at RT. Subsequently, 0.14 ml EDAC stock solution was added to bead suspension and mixed on a vertical tube rotator for 1 hr. at RT. Another 0.14 ml EDAC were added and mixed for 1 hr. Afterwards, suspension was centrifuged in conical Eppis with 6.000 g for 5 min. at 4 °C, pellets were resuspended in PBS and centrifuged again followed by another two washes in PBS. Pellets were resuspended in 7.5 ml PBS and 2 mg mannan were added. Suspension was mixed on a vertical tube rotator for 15 min. at RT. Afterwards, 2 ml stop buffer were added to the suspension, which was centrifuged in conical Eppis again. Pellets were resuspended in stop buffer and centrifuged again followed by another spin down in stop buffer. Coupled latex beads were washed three times in PBS, resuspended in PBS containing 0.03 % FSG. and suspension was adjusted to 1 % solids by measuring OD<sub>600nm</sub> using a photospectrometer. All coupled 1 % latex bead suspensions were stored at 4 °C after adding 3 mM sodium azide.

## 2.3 Confocal Microscopy

### 2.3.1. Fixation and labelling of cells

#### Reagents and instruments

- 4 % paraformaldehyde, 4 % sucrose in PBS, pH 7.4 (Sigma-Aldrich, Germany)
- 50 mM NH<sub>4</sub>Cl (Merck, Germany) in PBS
- 0.2% Triton X-100 (Roth, Germany) in PBS
- 0.1% Saponin (Cat. # 47036, Fluka, Germany) in PBS
- 1% Gelatin 'gold' (Sigma-Aldrich, USA) in PBS
- 0.2% Gelatin 'gold' in PBS
- ProLong gold mounting medium (Invitrogen, Germany)
- Glass slides and coverslips (Menzel GmbH, Germany)
- Rhodamine phalloidin and FITC phalloidin (Sigma-Aldrich, Germany)



Cells were fixed in PBS containing 4 % paraformaldehyde and 4 % sucrose (pH 7.4; Sigma-Aldrich, USA) for 20 min. at RT followed by quenching in PBS containing 50 mM NH<sub>4</sub>Cl (Merck, Germany) for 10 min. at RT. Permeabilisation, when required, was achieved by treatment with 0.2 % Triton X-100 (Roth, Germany) in PBS for 5 min. at RT. After blocking of unspecific binding sites with PBS containing 1 % white gelatin 'gold' (Sigma-Aldrich, USA) for 60 min., samples were incubated with primary antibody (see table 2) diluted in blocking solution for 60 min. at RT, followed by three washes with PBS containing 0.2 % gelatin. Secondary antibodies (see table 2) were applied for 45 min. at RT, again followed by three washes. If necessary, samples were stained with markers for actin for 20 min. at RT. Coverslips were washed in PBS containing 0.2 % gelatin, PBS alone, in Aqua dest. and were mounted on glass slides (Menzel GmbH, Germany) using ProLong gold mounting medium (Invitrogen, Germany). Fluorescence labelling and counting of Mycobacteria were performed as described (Anes et al. 2003; Kühnel et al. 2006).

### **2.3.2 Procedure for analyzing phagocytic uptake rates**

Uptake of latex beads coupled to different ligands diluted at a ratio of 1:100 in internalisation medium (corresponding to 0.01 % solids) or 0.02% and 0.005% were fed to the cells and was then allowed to incubate for 30 min. After incubation, cells were fixed and F-actin was labelled by FITC-phalloidin for 30 min. In all samples, 30-50 cells were analysed by confocal microscopy to determine total number of beads attached and internalised. For the competition experiments, a mixture of 1 $\mu$ m Fc beads and 1 $\mu$ m mannan beads was used in a ratio of 1:1 or in different ratios. For the preincubation experiments, cells were fed with different beads and incubated for 30 minutes on ice so as to freeze the phagocytic activity. For the specificity of the receptor ligand interaction, soluble ligands (mannan, Fc fragment and Avidin) were used. Cells were preincubated with soluble ligands. The concentration of soluble ligand ranges from 0.01mg/ml to 0.5mg/ml. For counting samples containing fluorescent latex beads, 30 z-stacks of each field were recorded and internalised beads could be distinguished by the help of F-actin staining using the cross-section view of the confocal software. All images from fixed cells were acquired using a confocal laser scanning microscope (TSC SP2 AOBS, Leica microsystems, Germany), if not stated otherwise in the text. For uptake experiments, at least two independent experiments were analysed and averaged.

For experiments with the kinase inhibitors, SRTK-specific inhibitor PP2 (Merck, Calbiochem, Germany), the Syk kinase inhibitor piceatannol (Merck, Calbiochem, Germany), the PI3-kinase inhibitor wortmannin (Merck, Calbiochem, Germany) and general kinase inhibitor Genistein (Merck, Calbiochem, Germany) were used. Cells were preincubated for 30 min at 37°C with 1 ml PBS containing the specific inhibitor at the indicated concentrations or PBS alone. Following incubation, the cells were washed twice with PBS and beads added as described above to assay for phagocytosis.

### 2.3.3 Immunofluorescence

For immunostaining of J774.A1 cells with surface receptors FcγRI or mannose receptors, cells were fixed using 1% PFA and 4% sucrose in PBS, pH 7.4 for 20 min, quenched with 50mM NH<sub>4</sub>Cl for 10 min and incubated further with 1 % gelatin 'gold' in PBS to reduce the non-specific binding for one hour. Cells were subsequently incubated with rat anti-FcγRI (R&D systems, USA) for 1 hour followed by washing with PBS containing 0.2% gelatin and then incubated with Cy3-conjugated anti-rat IgG (Invitrogen, Germany) for 30 minutes. The distribution of FcγRI or mannose receptor was visualized using confocal laser scanning microscope (TSC SP2 AOBS, Leica microsystems, Germany).

### 2.3.4 Phagocytic assay using Fc-coated latex beads for AFM studies

Fluorescent carboxylated latex beads (Invitrogen, Germany) of 1 μm diameter were conjugated with Fc fragment of mouse IgG (Thermo Fisher Scientific, USA) and avidin (Invitrogen, Germany) as described by manufacturer. J774.A1 cells were incubated with serum-free DMEM containing 0.01 % of avidin or Fc-coated latex beads (OD<sub>600</sub>=1.6) for 30 min. Cells were washed twice with PBS and then fixed with 1 % PFA and 4 % sucrose in PBS, pH 7.4 for 20 min followed by quenching in PBS containing 50 mM NH<sub>4</sub>Cl for 10 min, both at room temperature. Cells were permeabilized with 0.2 % Triton X-100 in PBS for 5 min. After blocking of non-specific binding sites with PBS containing 1 % gelatin 'gold' (Sigma-Aldrich, USA) for 1 h, cells were labeled for F-actin by FITC-conjugated phalloidin (Sigma-Aldrich, USA). Labeling of F-actin was performed in order to determine the cell periphery. Number of beads attached or/and internalized by macrophages was controlled by using confocal laser-scanning microscope (TCS SP2, Leica microsystems, Germany).

**Table 2.** List of markers and antibodies used for immunofluorescence and immunoelectron microscopy labelling (IF and IM)

Antibody against	Antigen	Produced in	Working concentration	Obtained from (reference)
Mannose receptor	Mouse CD206	Rabbit	1:150	Santa Cruz Biotech. USA
Fc $\gamma$ RI	Mouse CD64	Rat	1:150	R&D Systems, USA
Anti-rabbit Alexa-488	Rabbit IgG	Goat	1:300	Invitrogen, Germany
Anti-Rat Alexa-647	Rat IgG	Goat	1:300	Invitrogen, Germany
Anti-rat 15nm gold conjugate	Rat IgG	Goat	1:10	Abcam, Germany
Anti-rat 30nm gold conjugate	Rabbit IgG	Goat	1:10	Abcam, Germany
<b>MARKERS</b>			-	
FITC phalloidin (F-actin label)	-----		1:500	Sigma Aldrich, USA
TRITC-phalloidin (F-actin label)	-----		1:500	Sigma Aldrich, USA

### 2.3.5 Confocal microscopy for uptake rates and colocalization

Uptake rates and co-localization imaging of fixed macrophages were performed by confocal fluorescence microscopy using a TCS SP2 laser-scanning microscope (Leica, Germany) equipped with a 405 nm diode laser, an argon-krypton laser with lines at 458,

476, 488, 514 nm and helium-neon lasers with 543, 594 and 633 nm lines. The system also contained acousto-optical tuneable filters (AOTF), an acousto-optical beam splitter (AOBS) and four prism spectrophotometer detectors that permitted simultaneous excitation and detection of multiple fluorochromes. Three-dimensional scans of usually 50 z-stacks were recorded and analysed by the help of the cross-sectioning option of Leica confocal software. Staining of cellular F-actin allowed to distinguish between outside or only attached latex beads and fully internalised beads forming latex bead phagosomes. All images from fixed cells stained for co-localization of different receptors were acquired using same confocal laser scanning microscope (TSC SP2 AOBS, Leica, Wetzlar, Germany), if not stated otherwise in the text. For the quantification of co-localization images were processed with Imaris software (V6.0-6.3, Bitplane, Zurich, Switzerland).

## **2.4 Atomic force microscopy**

### **2.4.1 Functionalization of tip with Fc fragment via PEG-linker**

Both molecular recognition force spectroscopy (MRFS) and TREC measurements require the AFM tip to be transformed into a biospecific molecular sensor by attaching a ligand onto the tip. One of the most elegant ways is to anchor a few ligands onto the AFM tip via a long, flexible tether, such as poly(ethylene glycol) (PEG) chains (Hinterdorfer et al., 1996). Such spacer molecule (here PEG linker) enhances the mobility of the ligand, thus increasing its chance to bind specifically to the cognitive receptor on sample surface.

AFM tips ( $\text{Si}_3\text{N}_4$ ) were firstly extensively washed in chloroform and ethanol, dried with nitrogen and subsequently amino ( $-\text{NH}_2$ ) groups were produced on the tip surface by using gas phase silanization with 3-aminopropyltriethoxysilane (APTES) (Ebner et al., 2005;Hinterdorfer et al., 1996). Next, heterobifunctional NHS-PEG-Aldehyde chains were attached with one end to the amino groups on the tip by amide bond formation, for which, PEG linkers possesses an activated carboxy ( $-\text{COOH}$ ) group in the form of an N-hydroxysuccinimide ester (NHS ester). Finally, a ligand molecule, Fc fragment of mouse IgG (Thermo Fisher Scientific, USA) was coupled to another free functional group (i.e. aldehyde residue) of PEG linker(Bonanni et al., 2005).

### 2.4.2 Molecular recognition force spectroscopy

For the evaluation of forces between Fc-coated tip (see functionalization procedure above) and FcγRs on macrophage surface in the absence and presence of Fc molecules, standard AFM force spectroscopy was applied. After a ligand-functionalized tip contacts the cell surface, a specific bond between Fc and FcγR can be formed and when the tip is pulled away from the macrophage surface, this bond will be ruptured (unbinding event) (Figure 3b). The amount by which the pulling cantilever bends before the bond ruptures is measured and unbinding force,  $F$ , is calculated using the Hook's law as  $F=k\cdot\Delta x$  where  $k$  is the spring constant of the AFM cantilever and  $\Delta x$  is deflection from tip. Such approach-retraction cycles (or force-distance cycles) were performed using Fc-coated cantilevers (rectangular cantilever, Veeco Instruments) with nominal spring constant of 20 pN/nm in the working buffer (PBS or HBSS, 1.8 mM  $\text{Ca}^{2+}$ ) at room temperature. The sweep-amplitude of the force-distance cycle was 600-800 nm at 1 Hz sweep rate. More than 1000 force-distance cycles were collected for each location on the surface of cells and up to 4-5 locations (different cells) for each condition (i.e. initial and blocking conditions). Usually one experiment was repeated three times and one typical experiment for each condition is shown in this study. Spring constants of cantilevers were determined using the thermal noise method (Oikhova et al., 2004) and analysis of interaction forces was performed using MATLAB Version 7. To present the final force distributions empirical distribution density functions (or probability density functions (pdf)) were constructed as in (Baumgartner et al., 2000).

### 2.4.3 Topographical and recognition imaging (TREC)

Both AFM topographical and recognition images were acquired in MAC (magnetic alternating current) mode (Han et al., 1997; Raab et al., 1999) using a PicoPlus AFM (Agilent Technologies, Chandler, USA) with magnetically coated tips having a nominal spring constant of 100 pN/nm with a quality factor  $Q$  of  $\sim 1$  in liquid. All images were taken in Hank's balanced salt solution (HBSS) containing 1.8 mM  $\text{Ca}^{2+}$  at room temperature. The TREC data were obtained by scanning  $\sim 2 \times 2 \mu\text{m}^2$  area of the cell surface with a lateral scan speed of  $\sim 3.0 \mu\text{m}/\text{sec}$  at 256 or 512 data points per line using a commercially available PicoTREC box (Agilent Technologies, Chandler, USA). In order to block the specific interactions between Fc-functionalized tip and macrophage surface, free Fc molecules in excess (final concentration was  $\sim 0.8 \text{ mg/ml}$ ) were gently injected into the fluid cell of the AFM during scanning.

Topographical images were collected as either 512 x 512 or 256 x 256 matrixes. The AFM raw data (height image) were used as initial data, which were then analyzed with MATLAB Version 7.1 (MathWorks Inc., Natick, NA). The further line-wise flattening, plane fitting and contrast enhancement were performed as in (Kienberger et al., 2006).

The operating principle of TREC can be briefly described as following. The functionalized tip with a ligand molecule via a PEG linker is oscillated close to its resonance frequency ( $\sim 10$  kHz). The set-point amplitude is adjusted to a value close to the free amplitude. When such a ligand-coated tip binds to its receptor on the sample surface, the PEG linker will be stretched during upward movement of the cantilever, provoking the reduction of the oscillation amplitude (i.e. recognition signal), as a result of specific recognition during the lateral scan. TREC exploits the lower part of the oscillation (called as half-amplitude feedback) to drive a feedback loop for obtaining the topography image, whereas the upper part of the oscillation is used for the generation of the corresponding recognition image. Furthermore, the use of cantilevers with low  $Q$  factor ( $\sim 1$  in liquid) in the combination with a proper chosen driving frequency and amplitude regime enables that both types of information are unrelated (Preiner et al., 2009).

## **2.5 Electron microscopy**

### **2.5.1 Scanning Electron Microscopy**

Scanning electron microscopy (SEM) was used to visualize membrane ruffles on macrophages. Cells were grown on glass coverslips and then fixed as mentioned previously. Additionally cells were washed with increasing concentrations of ethanol (up to 100%), vacuum dried and coated with carbon. Cells were imaged with the DSM 960 SEM (Zeiss, West Germany) at an acceleration voltage of 10 kV.

### **2.5.2 Transmission electron microscopy**

TEM was used to define co-localization and nearest neighbor distance between mannose receptor and Fc $\gamma$ RI. Images were taken with Zeiss (West Germany) EM 912 at an acceleration voltage of 100kV. The following procedure was used to fix and label the cells-

Cells were grown overnight on Formvar (Sigma aldrich) coated slides. Next day wash the cells two times with PBS. Add 100  $\mu$ l 2% PFA in PB to each slide. Incubate 20 min at RT. Wash three times with PBS. Block with 100  $\mu$ l blocking agent (1% gelatin, 5% FCS in PBS) for 60 min. Add 50  $\mu$ l primary Ab in blocking buffer. Incubate for 30 min. Wash three times with PBS. Fix with 100  $\mu$ l 1% PFA in PBS for 15 min. Wash three times with PBS. Block with 100  $\mu$ l blocking agent for 30 min. Wash three times with PBS. Add 100  $\mu$ l 15 nm or 30 nm gold conjugated secondary Ab in blocking buffer. Incubate for 1 hr. Wash twice with PBS. Wash once with PBS. Leave samples in PBS for 5 min. Fix with 100  $\mu$ l 1% PFA in PBS for 15 min at RT. Wash three times with PBS. Incubate 1 min with 30% EtOH. Incubate 1 min with 50% EtOH (store samples at 4°C). Incubate 1 min with 70% EtOH. Incubate 1 min with 96% EtOH. Incubate 1 min with 100% EtOH. Substitute EtOH by liquid CO<sub>2</sub> .Critical point dry samples. Carbon sputtering is optional step.

### 2.5.3 Analysis and derivation of the equation

An expression for the distribution of nearest neighbor distances is easily obtained for the random distribution of particles that is expected in the absence of any interactions as described form (Anderson et al., 2003) . Consider the two-dimensional case of P particles distributed at random in an area S surrounding an origin. The particle density  $\rho$  is P/S. The probability of any one of the particles being outside an areas s within S is given by  $(1-s/S)$  and the probability of all the particles being outside an area s is given by  $(1-s/S)^P$ . If  $s/S$  is small this last expression may be replaced by  $(\exp(-s/S))^P$  or  $\exp(-sp)$ . The probability of finding a particle in an infinitesimal area element  $2\pi r.dr$  at distance r from the origin is given by  $\rho 2\pi r.dr$  and the probability that no particles lie within r is  $\exp(-\pi r^2 \rho)$ . The combined probability, which corresponds to the probability of finding the particle nearest the origin at a distance between r and r+dr, is given by the product  $\exp(-\pi r^2 \rho) \rho 2\pi r.dr$ . For N systems the number dN with nearest neighbor distance r to r+dr is

$$dN = N \exp(-\pi r^2 \rho) \rho 2\pi r.dr$$

The number n with distances less than r is given by integration, and it becomes

$$n/N = 1 - \exp(-\pi r^2 \rho)$$

This gives the fraction n/N corresponding to position in an ordered list of samples with increasing nearest neighbor distance r. The above equation may be rearranged to yield a linear relationship  $-\ln(1 - n/N) = \pi r^2 \rho$ . A plot of  $-\ln(1 - n/N)$  versus  $r^2$  gives a straight line

passing through the origin at  $-\ln(1 - n/N) = 0$ ,  $r^2 = 0$  and having a slope equal to  $\pi\rho$ . For the distance measurements between mannose receptor and Fc $\gamma$ RI the nearest neighbor distances from gold particles marking the mannose receptor and to the gold particles marking Fc $\gamma$ RI were measured using Image J software and plotted  $-\ln(1 - n/N)$  against the  $r^2$ .



# Results

### 3.1 Determination of the nano-landscape of Fc $\gamma$ R<sub>s</sub> by Atomic force microscopy

Determining the distribution of specific binding sites on biological samples with high spatial accuracy (in the order of several nm) is an important challenge in many fields of biological science. Combination of high-resolution atomic force microscope (AFM) topography imaging with single molecule force spectroscopy provides a unique possibility for the detection of specific molecular recognition events. The identification and localization of specific receptor binding sites on complex heterogeneous biosurfaces such as cells and membranes are of particular interest in this context. In this work I used the recently developed AFM technique, simultaneous topography and recognition imaging (TREC), in order to unravel the nano-landscape of Fc receptors on the macrophage cell surface. This application is centred on pathogen recognition, which is one of major types of macrophage functions. The most studied phagocytic receptors include the Fc receptors (FcR) that bind to the Fc portion of immunoglobulins. Firstly, we aimed to gain detailed information on the organization of different Fc $\gamma$ R<sub>s</sub> (Fc receptors for IgG) on mouse macrophage cell surface. The corresponding recognition maps were obtained with magnetically coated AFM tips, which were functionalized with Fc fragment of mouse IgG molecules via long and flexible Poly ethylene glycol (PEG) linker. In addition, single molecule force spectroscopy was applied to quantify molecular interactions of complexes of ligands (Fc domain of IgG) with their cognitive receptors on the cell surface i.e. Fc $\gamma$ R<sub>s</sub>.

#### 3.1.1 Binding activity of Fc $\gamma$ R<sub>s</sub> on macrophage surface

To study the interaction between Fc $\gamma$ R<sub>s</sub> and their ligand, Fc fragment of IgG, cultured J774A.1 macrophages as professional phagocytes were used. Fc $\gamma$ R-dependent phagocytosis of these cells is very efficient. After 30 min of incubation more than 95% of Fc-coated latex beads were internalized (figure 5). The engulfment of Fc-coated beads to compare with that of non-specific targets such as avidin-coated latex beads was at least 6 fold higher. Under same conditions only 15% avidin-coated beads were internalized.

On the other hand, a very mobile and dynamic cell surface of J774A.1 macrophages makes the AFM investigations complicated. Evidently, the possible engulfment upon interaction of Fc-coated AFM tip with Fc $\gamma$ R<sub>s</sub> can have negative effect on specific ligand-receptor AFM measurements. Therefore, in order to “freeze” the phagocytic process, cell surface dynamics and receptors mobility, and to elucidate proper binding properties and spatial resolution of interaction between Fc-coated tip and Fc $\gamma$ R, a suitable cell fixation procedure

was elaborated. The macrophages were fixed at different conditions (see materials and methods) and force spectroscopy measurements were conducted with Fc-coated tip on J774.A1 cells, which were either gently fixed with glutaraldehyde (GD) or

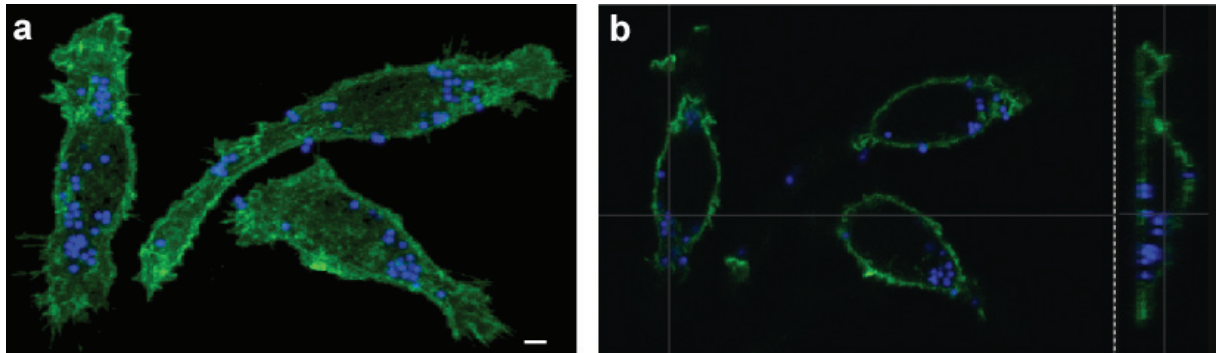


**Figure 5.** Engulfment of Fc coated latex beads by J774.A1 cells confirmed by confocal laser scanning microscope. Cells were incubated with  $1\mu\text{m}$  Fc fragment coated latex beads (blue) in internalization medium for 30 minutes. Thereafter cells were fixed and stained for F-actin (green) (a). The efficiency of engulfment of Fc-coated latex beads was determined by 3D cross section analysis; almost all beads (95%) were found inside the cell (b). (Bar =  $5\mu\text{m}$ ).

paraformaldehyde (PFA). The binding probabilities (probability to record an unbinding event in force-distance cycles) (figure 6b) from several experiments were quantified. When the cells were fixed with PFA (1% and 4%), high binding probability of  $\sim 30\%$  was observed (Figure 6c). However, the use of GD (0.2% and 0.5%) led to the reduced level of binding (8-10%). These results illustrate that binding capacity of Fc $\gamma$ R<sub>s</sub> is still very high after cell fixation with PFA. Moreover, the interaction between Fc-fragment bound to the AFM tip and Fc $\gamma$ R<sub>s</sub> on the cell surface after PFA fixation was found to be very specific. When free Fc fragments were present in solution, the binding probability drastically decreased to the level of  $\sim 5-7\%$  (Figure 6c). By construction an empirical probability density function (pdf) of the unbinding forces (Figure 6d), the maximum of the distribution was found to be  $25 \pm 4$  pN.

Since receptor-ligand interactions are dependent on the dynamics of the experiment ((Hinterdorfer and Dufrene, 2006), the unbinding forces  $f$  was measured as a function of the loading rate  $r$ . The loading rate is defined as the force increase over time during pulling the receptor-ligand complex and can be calculated by the effective spring constant of the system (cantilever and bound molecules) multiplied by the pulling velocity. It can be varied by changing the spring constant of the cantilever or by changing the retraction

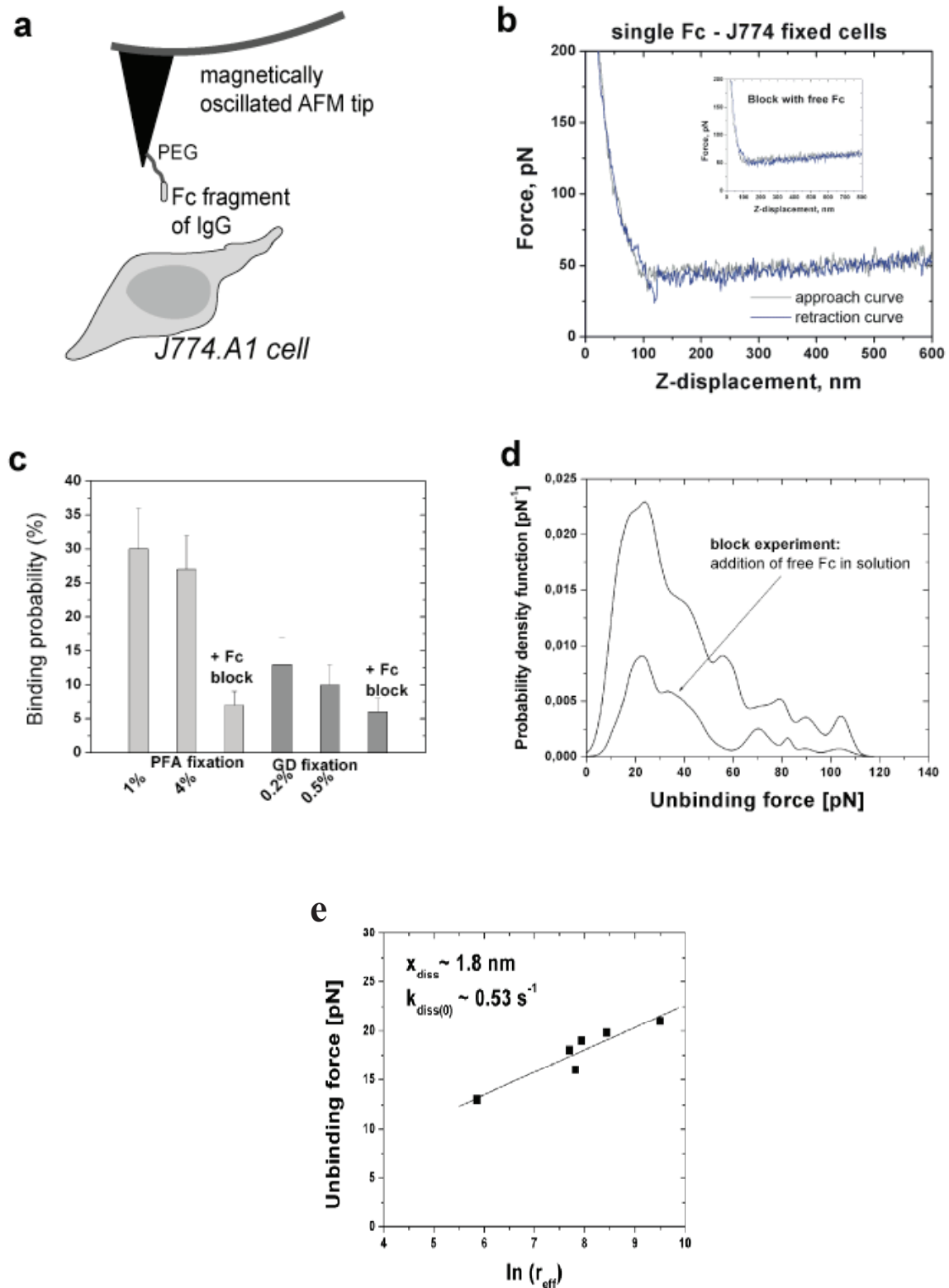


**Figure 6.** Force spectroscopy of Fc-coated AFM tip on fixed J774.A1 cells. a) Schematic of recognition imaging to sense and visualize Fc $\gamma$ Rs on macrophage surface. b) The force-distance cycle on macrophage with Fc-coated tip represents specific unbinding in the retrace. (Inset) Specific interaction is blocked with free Fc in solution (cell surface block). c) Binding probabilities of Fc-coated tip on cell surface fixed either with paraformaldehyde (PFA, *light grey*) or with glutaraldehyde (GD, *dark grey*), and with free Fc fragments

in solution (block) in the case of fixation procedure with 4% PFA and 0,5% GD, respectively. d) Probability density function (pdf) of specific molecular forces giving the distribution of unbinding forces in the absence and in the presence of Fc molecules. Areas are scaled to the corresponding binding probabilities. e). Dependence of unbinding force  $f$  on loading rate  $r$ . Using equation (described in text) the separation of the energetic barrier to the equilibrium position,  $x=1.8\text{nm}$  and the dissociation constant at zero force  $k_{off} = 0.53 \text{ s}^{-1}$  was determined

speed. According to theory a linear rise of the unbinding force with respect to a logarithmically increasing loading rate is characteristic for a single-energy barrier in the thermally activated regime. The unbinding force is related to the loading rate as:

$f = (k_B T/x) \ln(r \cdot x / k_B T \cdot k_{off})$  where  $x$  is the separation of the energetic barrier to the equilibrium position,  $k_{off}$  is the dissociation constant at zero force and  $k_B T$  is the thermal energy.  $f$  is the most probable unbinding force and  $r$  is the loading rate. A linear increase of the most probable unbinding force was found against the loading rate as shown in figure 6e. for the Fc-Fc $\gamma$ R interaction. From the relationship mentioned above, the separation of the energetic barrier from the equilibrium  $x$  and the  $k_{off}$  were calculated, resulting in  $x = 01.8\text{nm}$  and  $k_{off} = 0.53 \text{ s}^{-1}$ .

Finally, in order to show the interaction between Fc and Fc $\gamma$ Rs after PFA fixation comparable with that without cell fixation, the control experiments with native living cells were carried out. The binding assays with Fc-coated beads were performed on native living cells, which were kept at 0 °C to fully inhibit uptake but not the binding activity of Fc $\gamma$ Rs. I found that the number of Fc-coated beads interacted with living cells at 0 °C was just 20-30% higher in comparison to that of interacted with PFA fixed cells (figure 7). Furthermore, the interaction between Fc-coated beads and PFA fixed cells was very specific, since it was almost fully inhibited by pre-incubation the cells with soluble Fc fragment. Thus, these results confirmed once again that macrophage Fc $\gamma$ Rs after PFA fixation still have a high ligand binding activity. In addition, such gentle fixation method is likely prevent unexpected osmotic and temperature changes in fixative solution. As a result, the cell volume as well the cell membrane structures are mostly preserved that makes possible further AFM investigations at a subcellular (and even at single molecule) level.

### 3.1.2 Topographical landscape of J774.A1 cells

J774.A1 cells grown to subconfluent monolayers were fixed and the corresponding AFM topography images (figure 8a) illustrate a characteristic whirl-like morphology typical for macrophages that was also obtained with fluorescence microscope (figure 5, 7

and 8b). The macrophages are found to be highly extended ( $\sim 40\text{-}50\ \mu\text{m}$  in length, with  $\sim 10\text{-}15\ \mu\text{m}$  in width in the central part), and the heights of rest cells vary from  $\sim 500\ \text{nm}$  at the periphery to  $\sim 2\text{-}3\ \mu\text{m}$  on the nucleus (figure 7 and 8a).

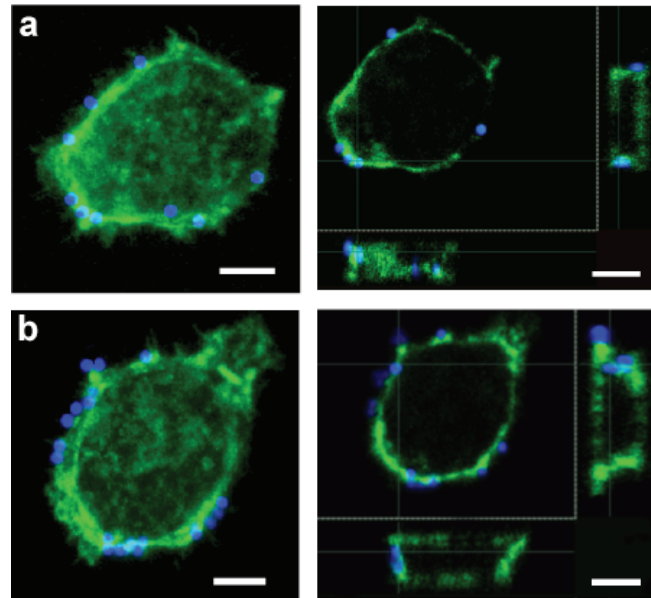


**Figure 7.** Binding assays of Fc-coated latex beads onto either living (a) or fixed (b) J774.A1 cell surface. a) The cells were firstly incubated with  $0.2\ \mu\text{M}$  Fc coated latex beads (blue) in internalization medium for 30 min at  $4^{\circ}\text{C}$  (i.e. phagocytosis process abolished). Thereafter cells were fixed with 1% PFA and stained for F-actin (green). b) J774 cells were initially fixed using 1% PFA and then incubated with Fc-coated latex beads. Direct binding of beads onto the surface was confirmed by 3D cross section analysis (right panels) of the images. Bars in all images are  $5\ \mu\text{m}$ .

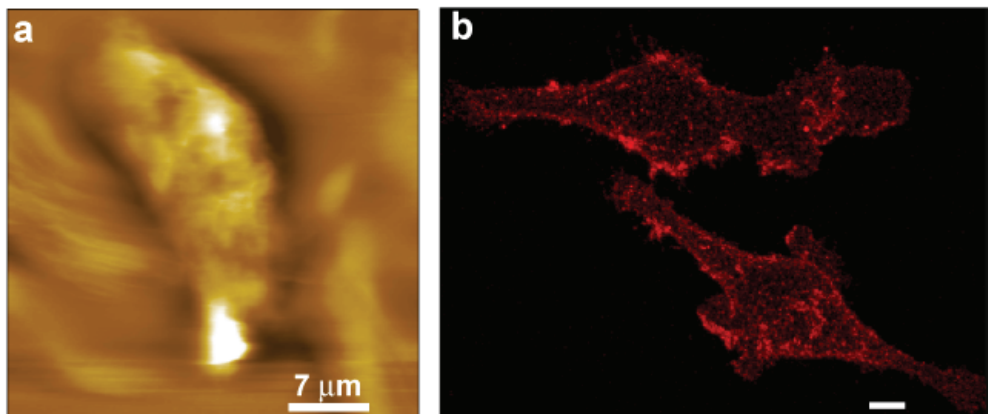


**Figure 8.** Morphology of whole J774.A1 cell (a) and overall distribution of  $\text{Fc}\gamma\text{RI}$  on cell surface (b). For immunochemical experiments cells were fixed and stained for  $\text{Fc}\gamma\text{RI}$  (red) using monoclonal antibody. Colour scale (from dark brown to white) in a) is  $0 - 1.5\ \mu\text{m}$ , bar in b) is  $5\ \mu\text{m}$ .

In most cases, due to the elevated macrophage heights comparable to the AFM scanner z-range, it was not possible to perform proper topographical images (without artifacts) of whole cell. Indeed, fluorescence image of whole cell stained for F-actin (figure 9a) as well the partial cell scanning images (central part of cell) (figure 9b) illustrated the complex nature of the cell surface representing large number of ruffles with the sizes of about 300-400 nm. At high magnification images (figure 9c) one could see the complex like “granular sponge” filamentous network with wide range of forms. Moreover, the local roughness on smaller areas of  $\sim 2 \times 2 \mu\text{m}^2$  was observed as relatively elevated (80-100 nm) that could bring undesirable artifacts in the recognition imaging such as so called cross-talk between topography and recognition (Ahmad et al., 2010; Preiner et al., 2009). In order to smooth the cellular surface, cells before fixation were osmotically swelled in hypotonic medium (i.e. cell culture medium diluted in proportion 1:2 with distilled water) as illustrated in figure 9d. Topographical AFM images of swelled cells showed the augmented cell heights (figure 9e). However, the cellular surface represented the complex organization of sheets with the size of 1-3  $\mu\text{m}$ , which can be characterized by “rose-flower” formation (figure 9e).

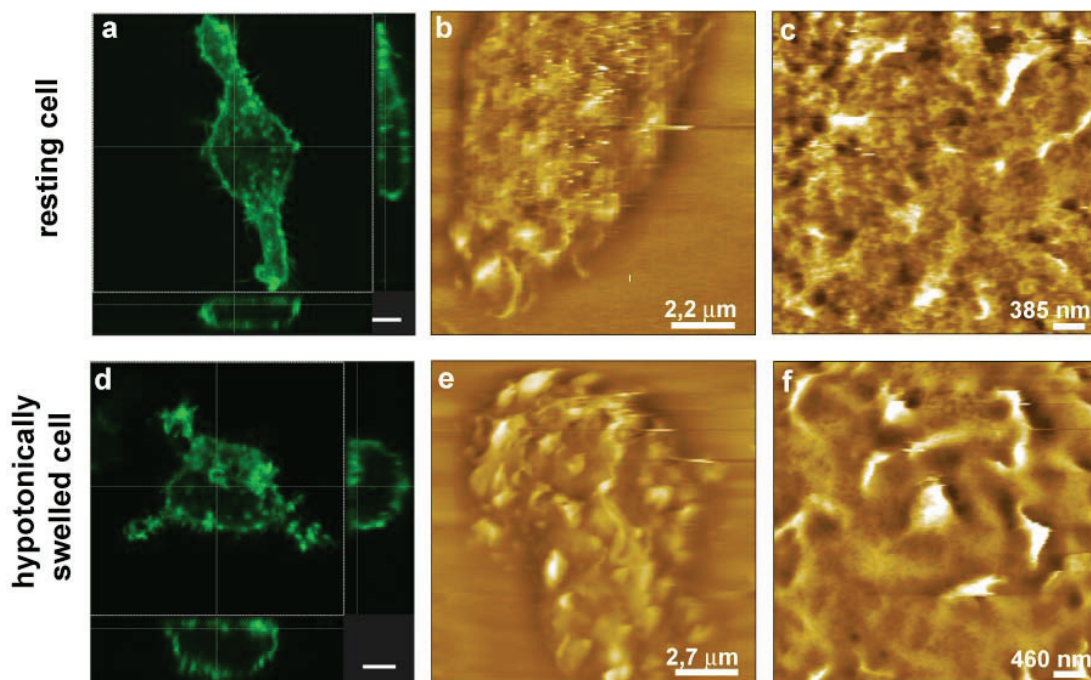


**Figure 9. Fluorescence and AFM topographical images of resting (a, b, c) and osmotically swelled (d, e, f) J774.A1 cells.** a-c) Fluorescence (a) and AFM images (b, c) of normal fixed cells. d-f) Fluorescence (d) and AFM images (e, f) of swelled cells. The osmotic swelling was achieved by the incubation of cells in hypotonic media for 30 minutes. Cells were further fixed with PFA. For fluorescence images (a, d) cells were additionally stained for F-actin (green). Cross-sections of 3D images indicate the heights of cells. Bars in fluorescence images are 5  $\mu\text{m}$ . Colour scales (dark brown to white) in b) is 0 – 400 nm, c) 0 – 140 nm, e) 0 – 650 nm and f) 0 – 100 nm, respectively.

Furthermore, the local roughness on such sheets was successfully reduced to 30-40 nm (figure 9f, 10a). One could presume that the changed cell morphology might induce the reorganization of cell receptors. The local organization of Fc $\gamma$ R on resting and osmotically swelled macrophages is discussed in the next paragraph.

### 3.1.3 Nano-mapping of Fc $\gamma$ Rs using TREC

The subcellular localization of major high affinity Fc $\gamma$ R, Fc $\gamma$ RI, was achieved by immunofluorescence staining (figure 8b), which is a widely spread technique to visualize receptor binding sites on cell

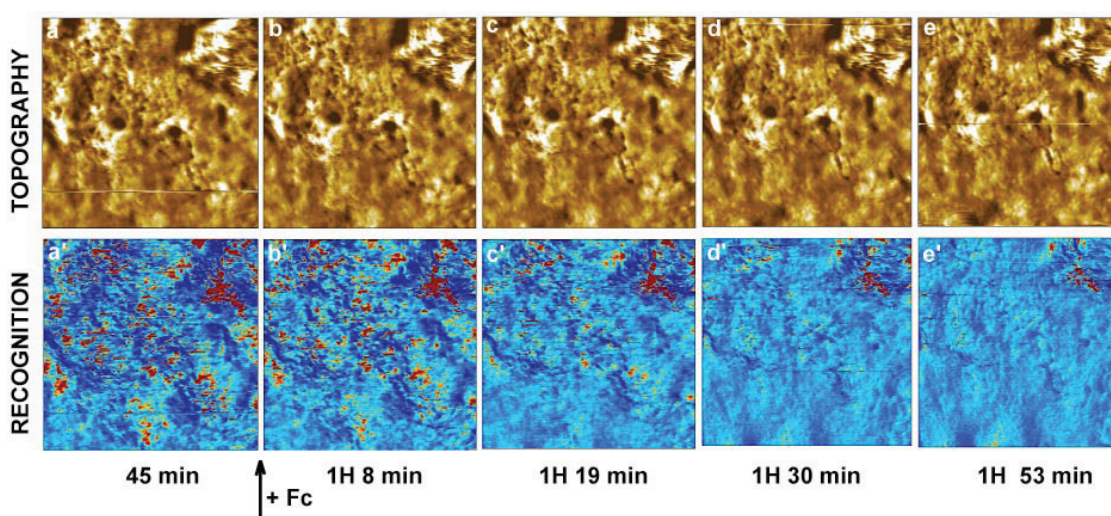


**Figure 10. Nano-mapping of Fc $\gamma$ R on macrophage cell surface with Fc-functionalized tip.** a – e) Topographical images simultaneously recorded with recognition maps (a' – e'), respectively. a' – e') Recognition images of Fc $\gamma$ R micro-domains representing an amplitude reduction due to a specific binding between Fc fragment on the AFM tip and Fc $\gamma$ R on the cell surface. b' – e') Subsequent disappearance of the recognition clusters in the presence of free Fc molecules in solution. Without Fc fragments, no changes were detected during the same time of observation. Furthermore, during cell surface blocking with free Fc fragments, topographical images (b - e) remain unchanged, indicating that the blocking does not affect membrane topography.

surfaces. It is clearly seen that Fc $\gamma$ RI has a tendency to form microdomains or clusters, which were almost homogeneously distributed on the whole J774.A1 cellular surface. However, in these light microscopy studies no information about topography could be obtained and the observed lateral resolution is not better than 200 nm. Therefore, TREC has been exploited here in order to locally identify binding sites of Fc $\gamma$ R on gently fixed macrophages. Measurements were started with the scanning of whole cell surface with subsequent zooming into small areas  $\sim 2 \times 2 \mu\text{m}^2$ . The oscillation amplitude was adjusted to be less than the extended PEG-linker to provide the proper recognition image with high



efficiencies and repeatability (>90%) (Ahmad et al., 2010; Chtcheglova et al., 2007; Preiner et al., 2009; Stroh et al., 2004). Correspondingly, the recognition map represents an amplitude reduction due to specific binding between Fc fragments on the tip and Fc $\gamma$ R<sub>s</sub> on the cell surface (dark spots in figure 10a'). These recognition spots (amplitude reduction up to 2 nm) are distributed patchily and reveal microdomains with dimensions (linear size) from ~ 5 nm up to ~ 300 nm. During several subsequent rescans recognition maps of Fc $\gamma$ R<sub>s</sub> remain unchanged. To confirm the specificity of these measurements, Fc fragments at high concentration (~ 0.8 mg/ml) were very slowly injected in the fluid cell while scanning the cell surface. Figure 10 demonstrate considerable changes in the recognition maps (low panels) (e.g. subsequent disappearance of dark spots with imaging time). Nevertheless, the surface blocking of Fc $\gamma$ R<sub>s</sub> does not affect the cell topography (high panels in figure 10).

The location of receptor binding sites can be properly identified on the topographical images of cells or membrane fragments with high lateral resolution and high efficiency (Chtcheglova et al., 2007). Figure 11 illustrates the superimpositions of the recognition maps onto the corresponding topographical images for normal resting and osmotically swelled cells. Repeated measurements reveal that the size of Fc $\gamma$ R<sub>s</sub> microdomains ranges from ~ 4 to as much as 300 nm, but with different spot size distributions (Figure 11 low panels). Taking account the size of Ig-like domain of Fc $\gamma$ R (diameter of 3-4 nm or 6.3 nm<sup>2</sup> ligand binding surface area (Maxwell et al., 1999) and the free orientation of PEG-chain during specific binding (e.g. binding can happen even before/after the binding site position) (Chtcheglova et al., 2007; Raab et al., 1999), the spots with linear sizes of ~ 4-12 nm (1-3 pixels, 1 pixel ~ 4 nm) were classified as single Fc $\gamma$ R<sub>s</sub>. The recognition spots are rather homogeneously distributed on the cellular surface and most of them are located on the high features of cell surface (figure 11).

For instance, on the resting (e.g. not stressed) cell recognition map (figure 11a) consist of ~ 5 % of relatively large clusters with sizes > 200 nm, ~ 40 % of micro-domains with sizes of ~ 60-150 nm (mean  $\pm$  SD, 57  $\pm$  50, n=339 (statistics from figure 11a), surrounding by high number (~ 55 %) of smaller domains (7-30 nm). By contrast, on swelled cells (figure 11b, c) huge clusters (linear size > 200 nm) are practically not observed and significant increase in the number of single events (~ 50 %) and spots with size of ~ 25 nm (~ 27 %) (mean  $\pm$  SD, 25  $\pm$  20, n=374 (statistics from figure 11c) is clear seen. Consequently, due to the considerable increase of whole macrophage surface area

caused by the osmotic swelling of cell, Fc $\gamma$ R<sub>s</sub> have tendency to reorganize in single receptors or in smaller domains containing from 4 to 16 receptors.

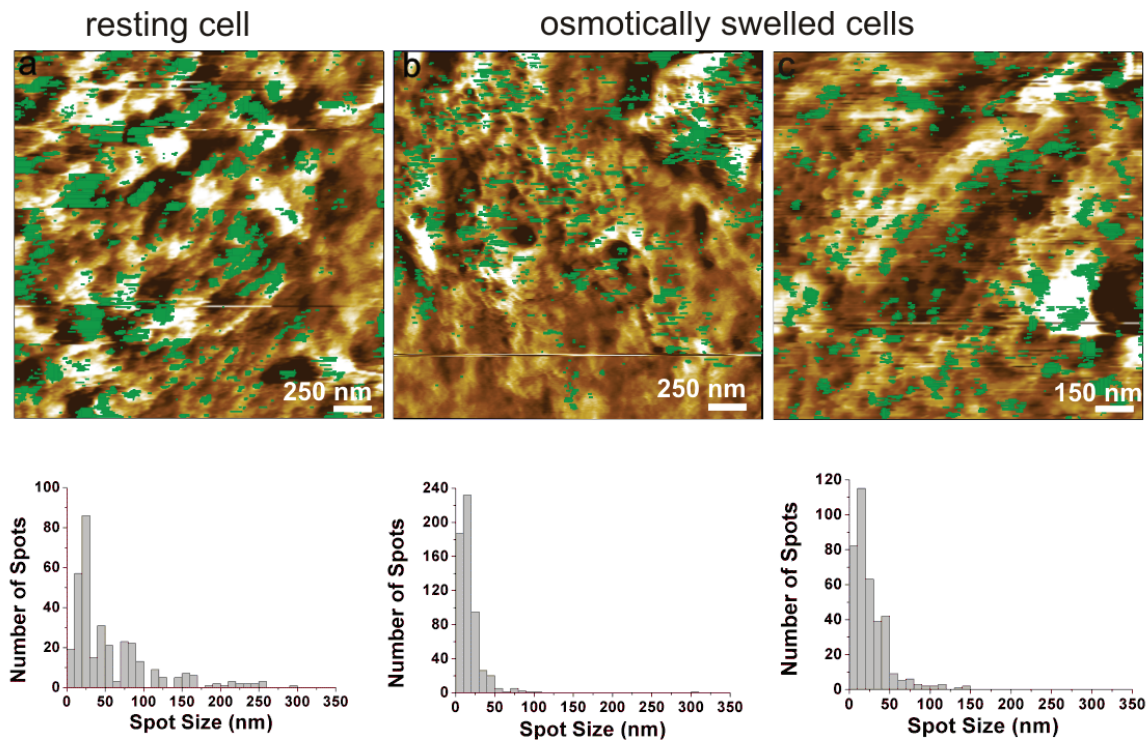


**Figure 11.** Overlays of recognition maps of Fc $\gamma$ R<sub>s</sub> (in green) onto the corresponding topography images of either resting cell (a) or osmotically swelled cells (b, c). Lower panels represent the size distributions of micro-domains detected in the recognition images. Colour scales (dark brown to white) in a) is 0-90 nm, b) 0-35 nm and in c) 0-50 nm, respectively.

### 3.2 Immunofluorescent and immune-electron microscopic studies of mannose receptor and Fc $\gamma$ receptors on the macrophages:

I next investigated the distribution of the MRs and Fc $\gamma$ R<sub>s</sub> on macrophages by performing immunofluorescence and confocal microscopy. For this cells were stained with anti MR and anti Fc $\gamma$ RI antibodies. As expected I found that MR colocalize with Fc $\gamma$ R to a great extent, but Fc $\gamma$ R do not colocalize to the same extent. Mannose receptors have shown tendency to colocalize with Fc gamma receptors at all the parts of the cell, e.g. cell surface or cell periphery (figure 12a). I further quantified the colocalization of the MR and Fc $\gamma$ R<sub>s</sub> using imaris software in terms of voxels. For the quantification of colocalization, analysis was done for the whole cell, periphery and surface separately where the voxels of the two channels were compared. It was observed that 50% of the MR on the periphery of the cell co-localizes with Fc $\gamma$ RI, on cell surface 60% and on the whole cell it was found to be 55%. (figure 12 b). This data suggested that MR are homogeneously distributed throughout the cell and their distribution is mainly colocalized with Fc $\gamma$ RI. On the other hand, Fc $\gamma$ RI

showed only 20% of colocalization with the MR. (figure 12b). The immunofluorescence data clearly indicated that number of Fc $\gamma$ RI on the macrophage cell surface is far more than MR and MR are mainly surrounded by the Fc $\gamma$ RI.

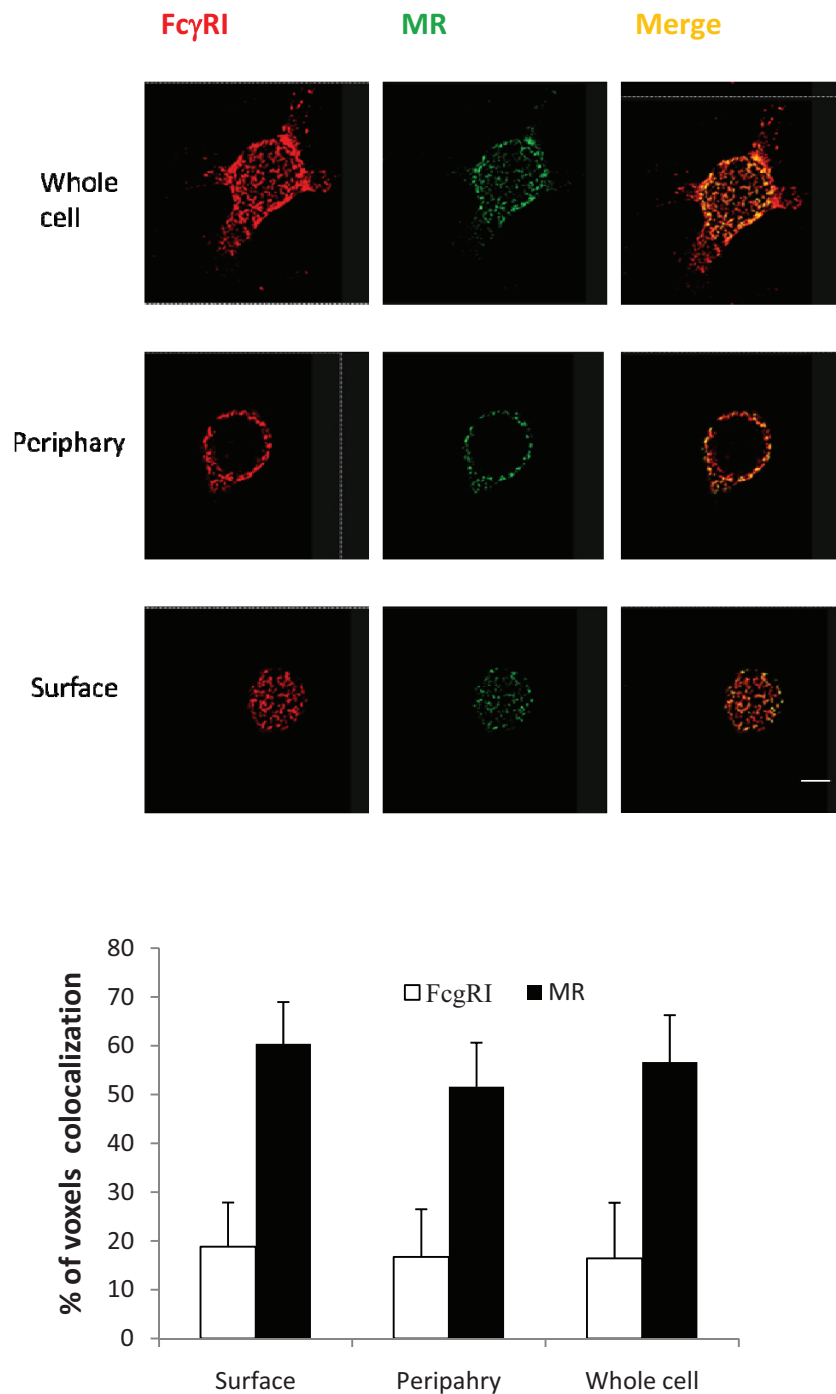


**Figure 12.** Immuno-fluorescent staining of macrophages with anti MR and anti-Fc $\gamma$ RI. a) Both types of receptors are evenly distributed throughout the cell but Fc $\gamma$ RI are more than mannose receptors. Bar = 5 $\mu$ m b) Quantification of voxels colocalization at all places on the cell is shown. Mannose receptors are mainly colocalized with Fc $\gamma$ RI in terms of voxels. Data shown is average of three independent experiments.

I next determine the inter-receptor nearest neighbor distance analysis between MR and FcγR using transmission electron microscope. Macrophages were fixed and stained as described in materials and methods.

A scanning electron micrograph of the J774A.1 macrophages has been shown in figure 13a and a portion of macrophages doubly labeled with anti MR and anti FcγRI antibodies is shown in figure 13b. FcγRI were labeled with 15nm gold conjugated secondary antibody and MR were labeled with 30nm gold conjugated secondary antibody. For distance measurements ImageJ software was used. A total of 275 measurements were analysed on 55 different cells. I found that MR and FcR are located close enough to suggest a possible interaction between them. Average distance between the MR and FcγRI was found to be 413 nm and nearly 80% of the events have shown distance less than 500nm between MR and FcγRI. The distribution curve in figure 14a has shown the maximum number of events showing inter receptor distance to be in between 300nm and 400nm. I then analysed

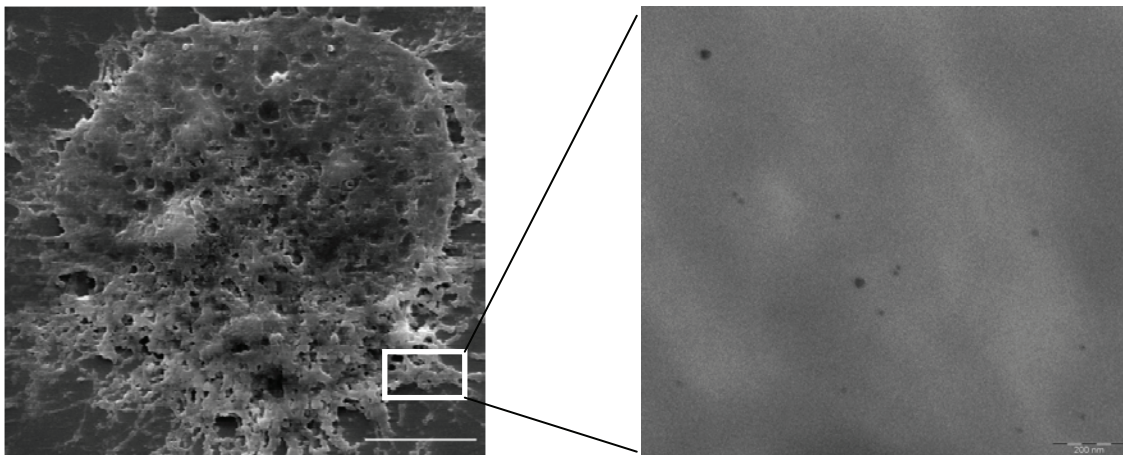
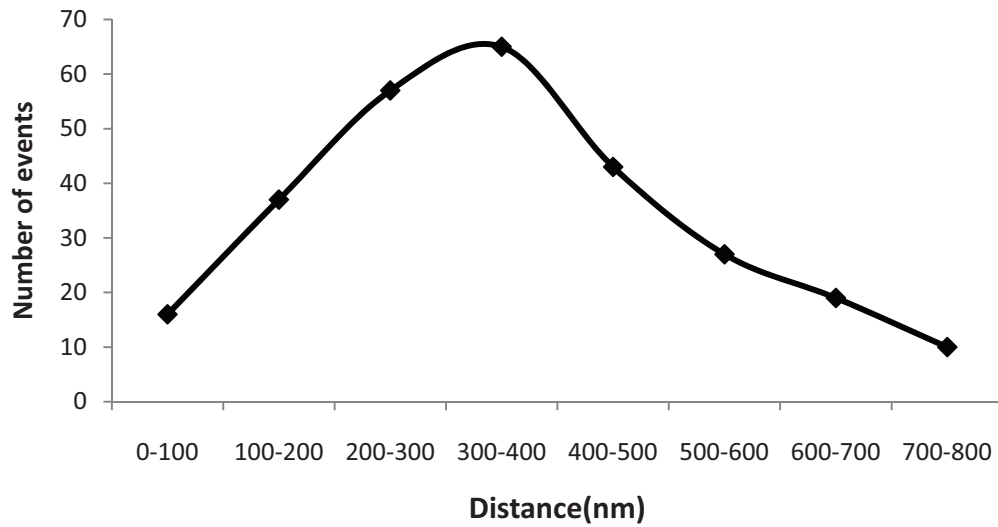


**Figure 13 a).** Scanning electron micrograph of J774 macrophage displaying a ruffled membrane. Bar= 4  $\mu\text{m}$  **b).** A portion of a macrophages cell section that was doubly labeled with anti-mannose receptor (anti-MR) and with anti-FcγRI antibodies. Gold particles were 30nm (anti-MR) and 15nm (anti- FcγRI) in diameter. Bar=200 nm. Gold particles are close enough to one another to suggest interaction between two receptors.

nearest neighbor distances between MR and FcγRI by plotting  $r^2$  against  $-\ln(1-n/N)$ . the data fits in a straight line (figure 14b) which is consistent with theory (see materials and methods for details).

a).



b).

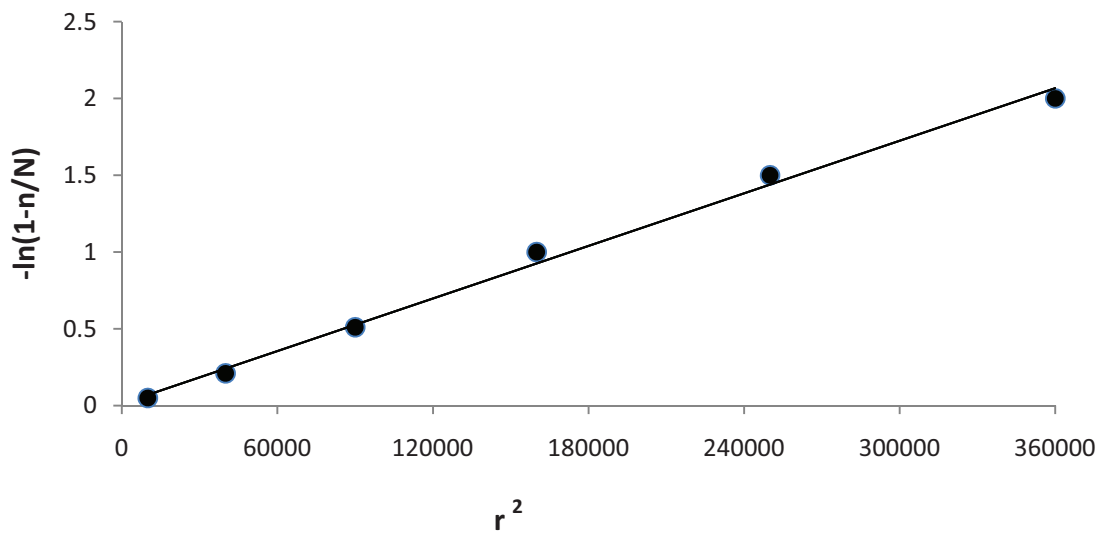


**Figure 14.** Nearest distance distribution curves. **a)** Cells were double labeled with anti-MR and anti- Fc $\gamma$ RI using 30nm and 15 nm gold colloidal particles. Distances between the receptors were measured and a distribution graph is plotted showing average distance between the MR and Fc $\gamma$ RI nearly 413 nm and more of the events have shown distance less than 500nm between MR and Fc $\gamma$ RI. **b)** Plots of data from double labeling experiments with anti-MR and anti-Fc $\gamma$ RI antibodies. Plot of the negative log of (1- fraction) in the ordered list of measurements against the square of the distance between gold particles marking mannose receptor and the nearest gold particle marking the Fc $\gamma$ RI, from the experiment in Fig.13. Data shown is average of three independent experiments.

### **3.3 Investigation of binding and internalization of latex beads coupled to different ligands in mouse macrophages**

Ligand-receptor interactions are an essential part of phagocytosis not only during internalisation but also for the intracellular fate of phagocytosed particle. The uptake of pathogens and other particles like cell debris in macrophages is associated with many early intracellular signalling events and the contribution and number of involved receptors varies according to the ligand of interaction involved. Depending on the characteristics of the ligand on the surface, target-specific receptors are triggered and mediate receptor-dependent phagocytosis. Pathogenic mycobacteria, like *M. tuberculosis*, are believed to be recognised and internalised in nonopsonic pathways predominantly by mannose receptors, whereas opsonised particles, like erythrocytes, are taken up by immunoglobulin-dependent Fc receptors. The surface of latex beads can be coupled to a variety of ligands to get internalized by phagocytes in receptor-specific pathways. Carboxylated microspheres offer the possibility to interact with different proteins and carbohydrates, which form covalent bounds with the surface of the bead. To enter cells in different receptor-dependent pathways, latex beads were coupled to Fc fragment of mouse immunoglobulin G, and mannan from *Saccharomyces cerevisiae*. These coupling agents triggered specific uptake via receptor classes which are mainly involved in the recognition of these ligands: IgG via Fc $\gamma$  (an opsonic receptor class), whereas the recognition of mannan predominantly via the mannose receptor belong to non-opsonic receptor class. As it was already mentioned in the introduction in more detail, particle recognition and uptake are not results of single receptor molecules, but are based on the cooperation of specific receptor classes, which interact and identify pattern on the particle surface. In comparison to these receptor-specific internalisation processes beads coupled to avidin were used for comparison. Avidin is believed to be taken up in nonspecific receptor pathways by the help of different receptor classes, e.g. by the involvement of scavenger receptors. The coupling of latex bead surfaces was carried out following protocols described in materials and methods and J774 macrophages were fed with the same or different amount of the different coated beads depending upon the objective of the experiment.

#### **3.3.1. Determination of the rate of phagocytic particle binding and internalization using differently coated latex beads**

Covalently coated latex beads with different ligands were used to initiate the phagocytosis event. In this study I have used Fc fragment of mouse IgG, mannan and

avidin as ligand. Unless otherwise stated latex beads coated with Fc fragment of mouse IgG should be referred to as Fc-beads, mannan coated latex beads as mannan-beads and avidin coated latex beads as avidin-beads. The specific signaling events initiated by different ligand-receptor interaction at the macrophage surface during particle recognition are responsible for different phagocytic efficiency. This is well established that Fc-beads are recognized by Fc $\gamma$  receptors, mannan beads by mannose receptors (Hoffmann et al., 2010) and avidin-beads are recognized by non-specific receptors and therefore avidin-beads were used as a control in the study.

Firstly I estimated the concentration dependence of macrophages towards binding and internalization of Fc beads and mannan beads at a 30 minutes time point. I have found that the rate of particle binding and internalization depends upon the number of phagocytic particles available to the macrophages (figure 15a) I observed that both the type of ligands induced a linear increase of uptake over concentration of beads but the rates of uptake were significantly different for both of the ligands used. Mannan beads show higher rate of internalization than Fc beads (figure 15a) These results showed that J774A.1 macrophages are highly efficient phagocytes and therefore important cells to study the receptors distribution on its surface. I chose the 0.01% concentration of beads to perform further studies as at this concentration macrophages were not fully saturated. In order to confirm the different ligand-receptor specificity, the competition experiments were performed where cells were first pre-incubated with the ligands in soluble form for 30 min followed by a co-incubation of ligand coated beads together with the soluble ligands. I found that a given soluble ligand efficiently competed for binding of the cognate ligand coated bead. This resulted in a nearly 50% decrease of the corresponding bead uptake to less than compare to control conditions for IgG Fc, mannan, and for avidin (figure 15c). The specificity of the ligand-receptor interaction was further confirmed by cross competition experiments where macrophages were co-incubated with beads together with another ligand than the one present on the bead surface, phagocytic uptake rates were not significantly affected (figure 15b) Furthermore, I checked the effect of different concentrations of soluble mannan and soluble Fc on the binding of mannan and Fc beads. It was again found that soluble Fc and soluble mannan do not inhibit the phagocytosis of mannan beads and Fc beads respectively (figure 15c). This proves that all the studied ligands bound to the latex beads interacted specifically to their expected receptors.

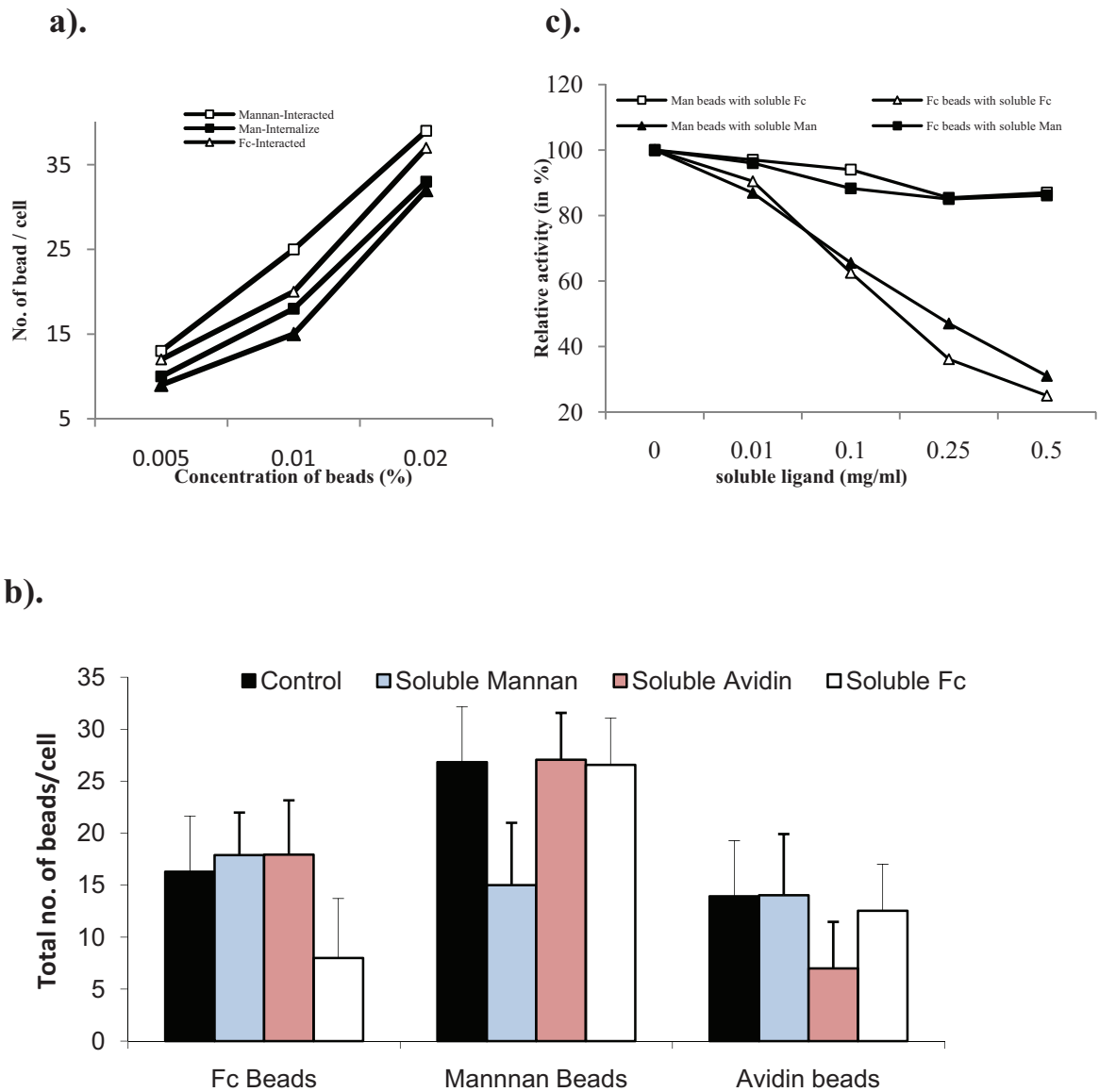


**Figure 15. (a)** Binding and internalization of 1  $\mu\text{m}$  Fc and mannan beads depends upon the concentration over a time point of 30 min. Three different concentrations (0.01 % corresponds to an OD of 1.6) of Fc and mannan beads were used to feed the cells and 30 cells were analysed. Both, the binding and internalization of the Fc and mannan beads depends upon the concentration and increase linearly with the increase in concentration of beads used. **b & c).** The specificity of the ligand-receptor interaction. Cells were preincubated with an increase in concentration of soluble ligand for 30 min followed by a co-incubation of ligand coated beads. Soluble Fc, mannan and avidin specifically inhibited the binding and uptake of corresponding coated latex beads by 50% but not the other beads (**b**). Similarly, incubation of the cells with an increase in soluble Fc or mannan concentration further decrease the Fc and mannan beads uptake. (**c**)



### 3.3.2 Binding and internalization analysis of Fc beads and mannan beads simultaneously used in a mixture

During microbial contact many parallel signaling pathways are simultaneously activated that together define the phagocyte response and regulate internalization. Phagocytosis is a complex system where many different receptors recognize microbes and their subsequent recognition and internalization is mediated by either a single type of a phagocytic receptor or through cooperation of multiple receptors. My results with different microscopic techniques had suggested to have an interacting role of mannose receptors and Fc  $\gamma$  receptors. Therefore, I used our latex beads system to check this phenomenon. Macrophages were incubated with a mixture of Fc beads and mannan beads in a ratio of 1:1. In control experiments the cells were incubated with the similar number of Fc beads and mannan beads alone. The numbers of beads used for all the sets of experiments were kept at a constant concentration which corresponds to 0.01% of individual beads in incubation

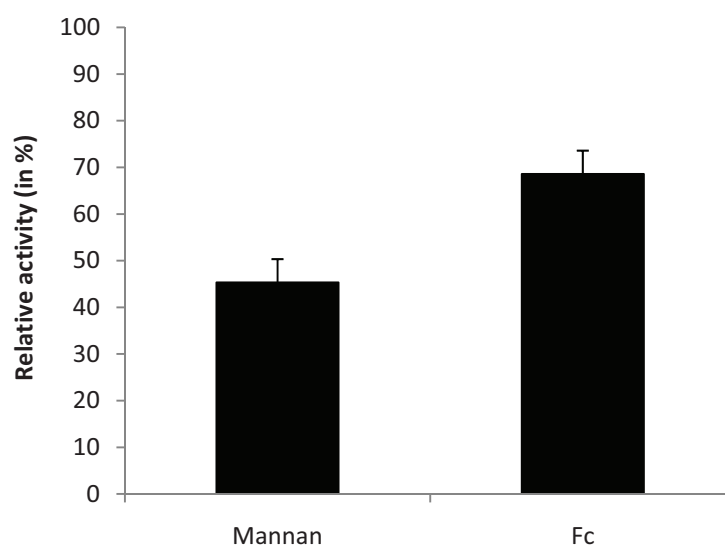


**Figure 16.** Inhibition of phagocytic activity of mannan coated beads by Fc beads. Macrophages were fed with a mixture of Fc and mannan beads of 1 $\mu$ m size and incubated for 30 min. at least 30 cells were selected for each experiment and analyzed for the binding and internalization. Fc beads have shown to inhibit the internalization of mannan beads predominantly. The phagocytic activity was decreased to 50 % in presence of Fc beads.

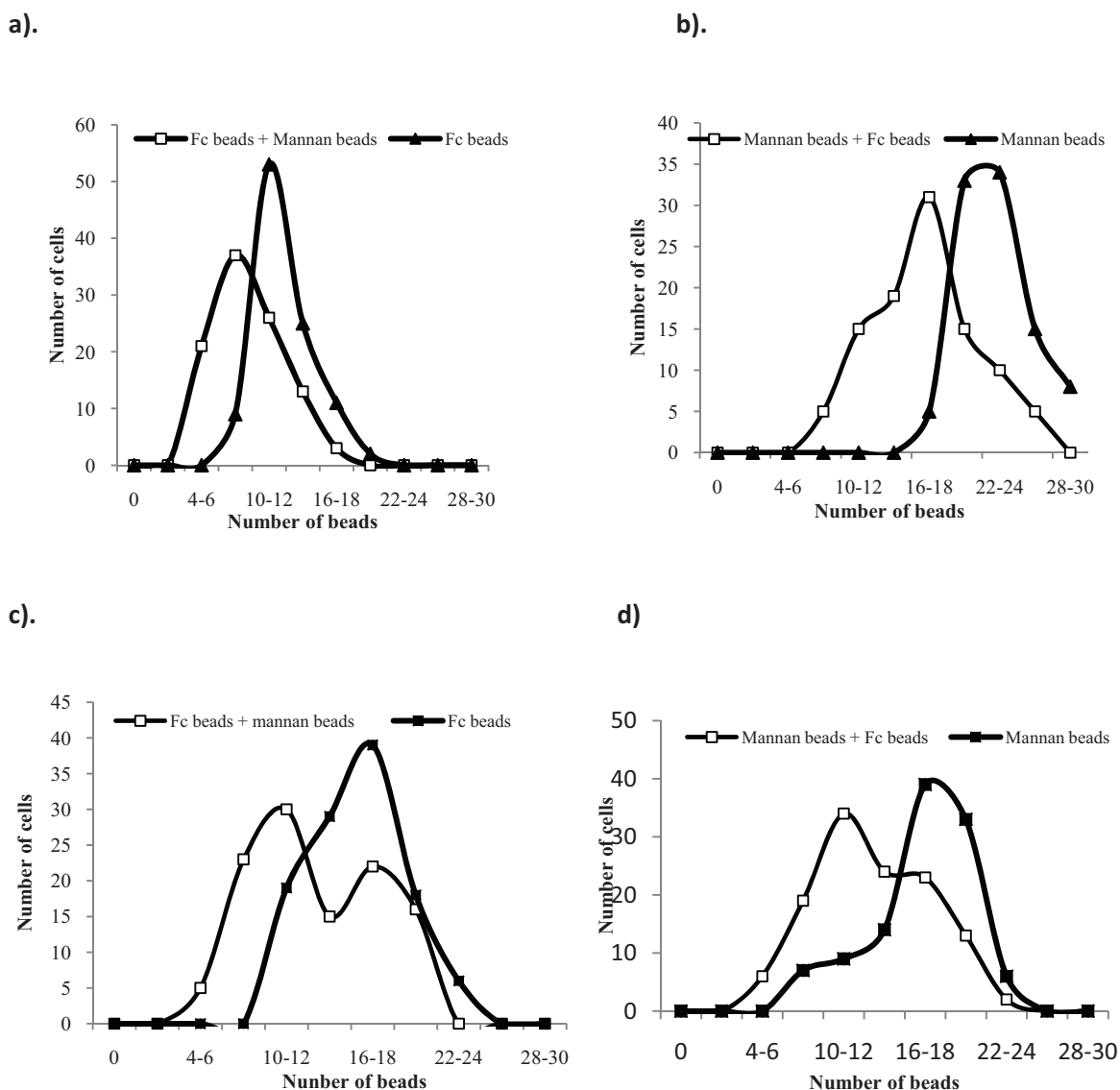


**Figure 17.** Mannan and Fc fragment of IgG coated latex bead interferes with each other for binding to the cell surface receptors and subsequently for the internalization. Macrophages were incubated with a mixture of 1 $\mu$ m latex beads coupled with mannan and Fc fragment of IgG. A total of 100 cells were selected randomly and analysed. **a).** Binding of Fc coated beads to the cell surface receptors in presence of mannan coated beads was slightly reduced to 15%. **b).** Binding of mannan coated beads to the cell surface receptors in presence of Fc coated beads was also reduced to 30% only. **c).** Internalization of mannan coated beads in presence of Fc coated beads was significantly reduced and it corresponds to 50% inhibition as compare to control. **d).** Internalization of Fc coated beads was also Interfered by mannan coated beads. In this case inhibition was only 30%.

medium. A total of 100 cells were selected randomly and analysed for bound and internalized beads. I found that mannan and Fc beads compete for binding and internalization with each other. Binding of mannan beads to the cell surface receptors in presence of Fc beads was reduced by 30% but binding of Fc coated beads to the cell surface receptors in presence of mannan beads was also reduced by 15% only (figure 17c

and 17d). Internalization of mannan beads in presence of Fc beads was significantly reduced and it corresponds to 50% inhibition as compare to control (figure 16 and 17b). However, internalization of Fc beads was also interfered by mannan beads. In this case inhibition was only 30% (figure 16 and 17a). The distribution of number of beads attached or internalized per cell in mixtures and individual beads is shown in (figure 17c and 17d). These findings suggested that Fc beads dominate over the mannan beads for the attachment and internalization.

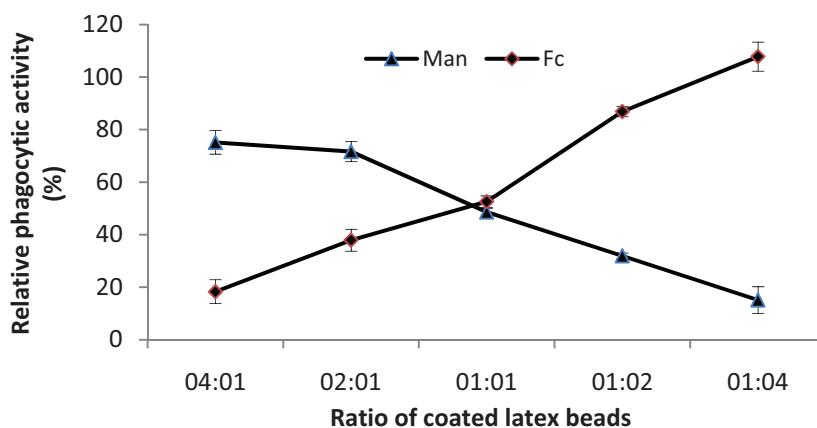
### **3.3.3 Use of mixed beads in different ratios and beads of smaller size to find out the distance between MR and FcγRs**

In order to check our hypothesis of competition of binding sites, I performed two different experiments 1). Mixture of beads composed in various ratios of Fc beads and mannan beads. In the first experiment I have prepared the mixtures where ratios of mannan beads and Fc beads were kept at 4:1, 2:1 and 1:1. I used these mixtures to feed the cells and total number of attached and internalized beads were counted. I found that even a smaller number of Fc beads were able to reduce the mannan beads uptake. When the mixture has mannan beads 4 times more than Fc beads, their attachment and internalization was reduced to 70% but the similar effect was not shown by mannan beads on Fc beads. (figure 18a) As the number of Fc beads increased in the mixture, the phagocytic ability of cells towards mannan beads reduced significantly and this reduction was linear. These results suggested once again that there is a competition for the binding sites of MR and FcγR and that the number of MR present on the surface of cell are far less than FcγRs. Since the beads used in this experiment was of the size 1 μm, therefore it was assumed that MR and FcγRs are at least as close as 1 μm.

2). In the second experiment I used different size Fc beads ranging from 20nm to 2 μm in the mixture of mannan beads of 1 μm size. I further checked the effect of other size Fc beads (ranging from 20nm to 2 μm) on the binding of mannan beads of 1 μm size on cell surface. It was found that preincubation of the cells with 0.5 μm Fc beads reduced the binding of mannan beads to nearly 50% but the similar effect was not found for the Fc beads. Preincubation of the cells with 0.5 μm mannan beads could not significantly reduce the binding of the Fc beads (figure 18b). Similar observation was found with the use of smaller size of Fc beads (20nm, 100 nm and 200 nm) as they could block the binding of mannan beads but to a lesser extent i.e. lesser than 25%. On the other hand, smaller sized mannan beads did not block the binding of Fc beads to a significant level. (figure 18b). Furthermore, pre-incubation with 2 μm Fc beads inhibited the binding of mannan beads

down to nearly 15 % only but the pre-incubation with 2  $\mu\text{m}$  mannan beads did not inhibit the binding of Fc beads to this level. Taken together these results confirmed that mannose receptors and Fc receptors are present at a close proximity and mannose receptors are mainly surrounded by Fc receptors.

a).



b).

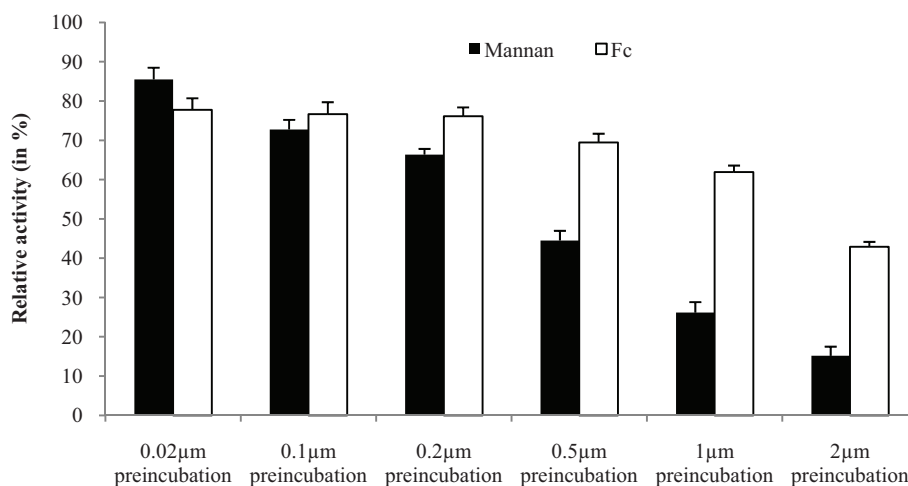


**Figure 18.** Phagocytic activity of mixture of beads in different ratios and beads of smaller size. a). Macrophages were incubated with a mixture of 1  $\mu\text{m}$  latex beads coupled with mannan and Fc fragment of IgG in different ratios. A total of 30 cells were selected randomly and analysed for the binding and internalization. Fc beads even in smaller concentration can inhibit the phagocytosis of mannan beads. b). Preincubation with different size of Fc beads inhibit the binding of mannan beads preferentially. Data shown is an average of three independent experiments.

### 3.4 Interaction between *Mycobacterium smegmatis* and J774 macrophages in presence of 1 $\mu\text{m}$ Fc beads

As a proof of concept I took advantage of the well established ability of J774 macrophages to kill non-pathogenic *Mycobacterium smegmatis* which has been extensively

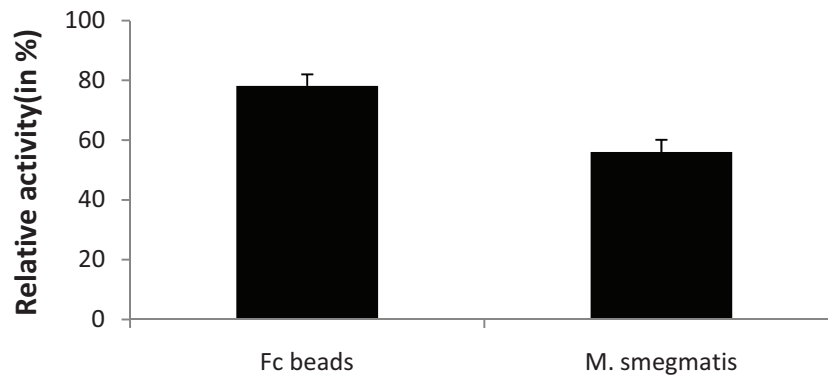


**Figure 19.** Competition of *M. smegmatis* and 1  $\mu\text{m}$  Fc beads. Bacterial cultures in exponential growth phase were pelleted, washed twice in sterile PBS and resuspended in PBS to a final  $\text{OD}_{600\text{nm}} = 0.10$ . Macrophages were then infected with bacteria or a mixture of bacteria and Fc fragment of mouse IgG coated beads and incubated for 30 min at  $37^\circ\text{C}$ . Fc beads and *M. smegmatis* show competition for internalization as total number of bacteria were decreased when used in mixture. Internalization of *M. smegmatis* in presence of Fc coated beads was significantly reduced and it corresponds to nearly 50% inhibition as compare to control, on the other hand internalization of Fc coated beads in presence of *M. smegmatis* was not reduce and it corresponds to only 20% inhibition as compare to control. Shown are the average of three experiments.

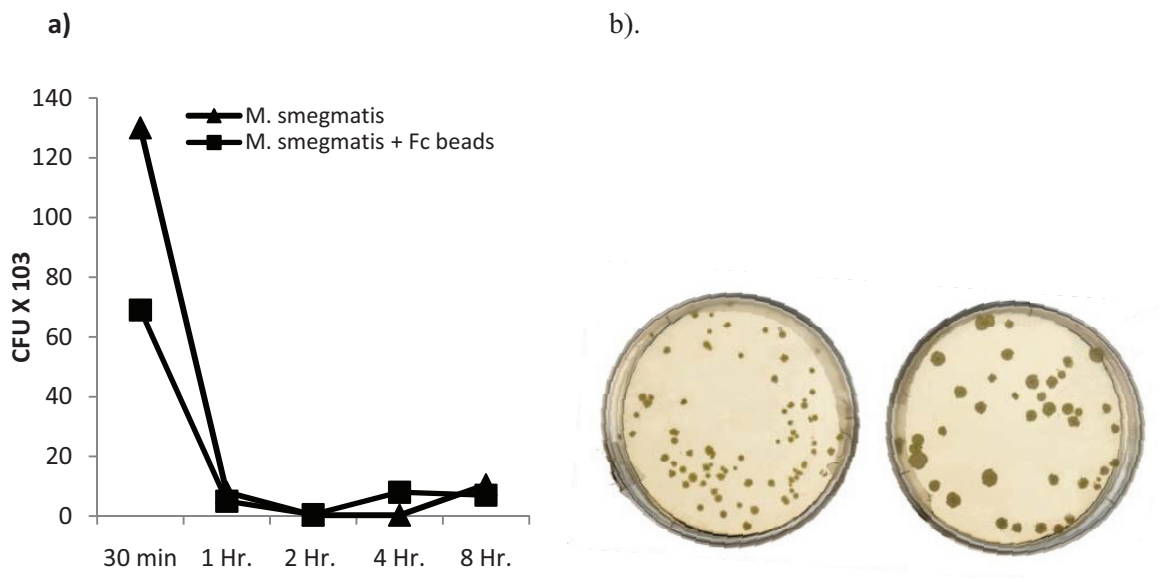


**Figure 20.** Intacellular fate of *M. smegmatis* in macrophage cells in presence of Fc fragment of IgG coated beads. Macrophages were infected with *M. smegmatis* alone or with a mixture of bacteria and Fc fragment of mouse IgG coated beads and incubated for 30 min at  $37^\circ\text{C}$ . cells were then washed with PBS extensively and allowed to grow further for various time points. After each time point cells were lysed using 23-gauge needle and bacteria were recovered in Middlebrook's 7H10 medium at  $37^\circ\text{C}$ . **a).** More no. of colonies were found when bacteria were infected the macrophages alone and comparison was drawn as colony forming unit (cfu). It shows 50% reduction in uptake of bacteria in presence of Fc fragment of IgG coated beads. **b).** A picture showing different pattern of bacterial growth with or without Fc fragment of IgG coated beads. Shown are the average of five independent experiments.

studied model organism for tuberculosis. The internalization of *M. smegmatis* was reported through the interaction of Toll like receptors but TLRs are not sufficient to internalize the bacteria alone and works as a co-receptors for the receptors like mannose receptor (Astarie-Dequeker et al., 1999). I examined the effect of Fc beads on the internalization of *M. smegmatis* when used in mixture. The specificity of *M. smegmatis* towards MR was first confirmed with the preincubation of the cells with soluble mannan. When used in mixture, cell shown lesser number of bacteria internalized In control experiments macrophages were incubated with the similar concentration of Fc beads and bacteria alone. *M. smegmatis* showed competition for internalization with Fc beads as total number of beads or bacteria were decreased when used in mixture. Internalization of *M. smegmatis* in presence of Fc coated beads was significantly reduced and it corresponds to nearly 40% inhibition as compare to control, on the other hand internalization of Fc coated beads in presence of *M. smegmatis* was also reduced and it corresponds to almost 20% inhibition as compare to control (figure 19). In order to confirm these results intracellular fate of *M. smegmatis* in macrophage cells in presence of Fc beads was determined. Macrophages were infected with *M. smegmatis* alone or with a mixture of bacteria and Fc beads and incubated for 30min at 37°C. Cells were then washed with PBS extensively and allowed to grow further for various time points. After each time point cells were lysed and bacteria were recovered and plated on More no. of colonies were found when bacteria were infected the macrophages alone and comparison was drawn as colony forming unit (cfu) . It shows 50% reduction in uptake of bacteria in presence of Fc fragment of IgG coated beads (figure 20a ) after 30 minutes time point. However, at and after 1 hour time point *M. smegmatis* shown similar behaviour inside the macrophages i.e. killing efficiency of the macrophages were found to be similar. (figure 20a) A picture showing different pattern of bacterial growth with or without Fc fragment of IgG coated beads has been shown in figure 20b). These results have confirmed the biological relevance of the competition between MR and FcγRI on mouse macrophages. Taken together, our results have revealed the distribution of the MR and FcγRI on the macrophage cell surface and suggested a possible interaction of MR and FcγRI on macrophages that is relevant biologically.

### **3.5 Effect of kinase inhibitors on Fc and mannose receptor mediated phagocytosis**

Protein and lipid kinases are the known mediators of the FcγR-signaling events. Inhibitors of these kinases have been shown to block phosphorylation of several proteins involved in FcγR-signaling in monocytes and macrophages. However the role of these

kinase is not reported in case of MR mediated phagocytic signaling. Therefore, I further dissect the molecular requirements that mediate the Fc $\gamma$ R and mannose receptor mediated phagocytosis and could be possible reason for the inhibition of Fc $\gamma$ R signaling with the help of three well known inhibitors of protein kinases I investigated the effect of Genistein, which specifically inhibits tyrosine-dependent protein kinases, the Src related tyrosine kinases (SRTK) specific inhibitor PP2, the Syk kinase specific inhibitor piceatammol and the PI3K inhibitor wortmannin for the binding and internalization of the Fc and mannan beads by macrophages. I compared the requirement for three kinases generally associated with efficient Fc $\gamma$ R-signaling: Src related tyrosine kinases (SRTKs), Syk kinase and phosphatidylinositol 3 kinases (PI3K). A broad concentration range of genistein, PP2, piceatammol and wortmannin has been used in order to find out the optimal concentration of the inhibitor to be used.

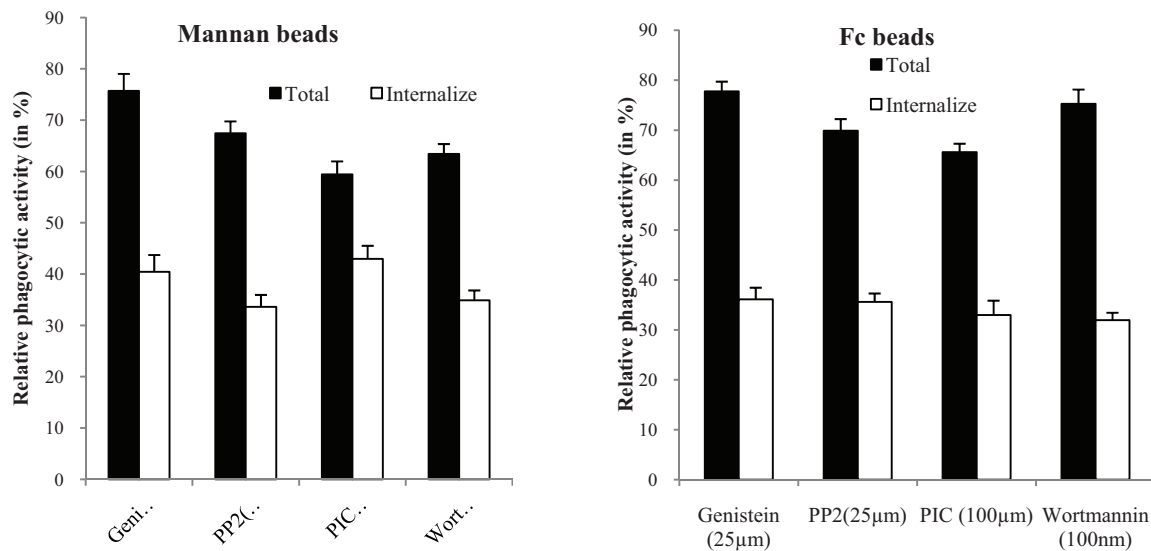


**Figure.21** Effect of different kinase inhibitors on Fc and mannan coated beads binding and uptake. Macrophages were incubated with different kinase inhibitors prior to co-incubation with mixture of Fc and mannan beads for 30 min (see materials and methods) to analyse the binding and internalization of Fc beads and mannan beads. All the kinase inhibitors have shown significant decrease in binding and internalization of both the types of beads. Average of three independent experiments.

Pre-treatment of all the inhibitors used in the study have shown inhibition of mannose and Fc $\gamma$ R phagocytosis in a dose dependent manner (data not shown), suggesting that protein kinases are required for the effective signaling in both Fc $\gamma$ R and mannose receptor mediated signaling. Genistein at a concentration of 25 $\mu$ M caused a significant decrease in attachment and internalization of Fc beads and mannan beads. Reduction in attachment was found to be 20 % less than control but the internalization of Fc beads and mannan

beads reduced significantly (nearly 50%) as compare to control (figure 21a and 21 b). I found the similar effects of the other kinase inhibitors used. Preincubation with PP2 (25 $\mu$ M), piceatannol (100 $\mu$ M) and wortmannin (100nm) have shown a reduction in attachment of Fc and mannan beads by nearly 20% but the internalization was reduced to nearly 40% as compare to control (figure 21a and 21b.)

Once I confirmed the role of different kinases in Fc beads and mannan beads mediated phagocytosis, I checked the all of above mentioned inhibitors in case of phagocytosis of mixed beads. In this set of experiment, the attachment and internalization of mixed beads was compared to the control single type of beads As expected, the attachment of mannan beads was reduced to 70% and internalization was reduced to less than 40% but the attachment and internalization of Fc beads were not significantly reduced (Fig 22).

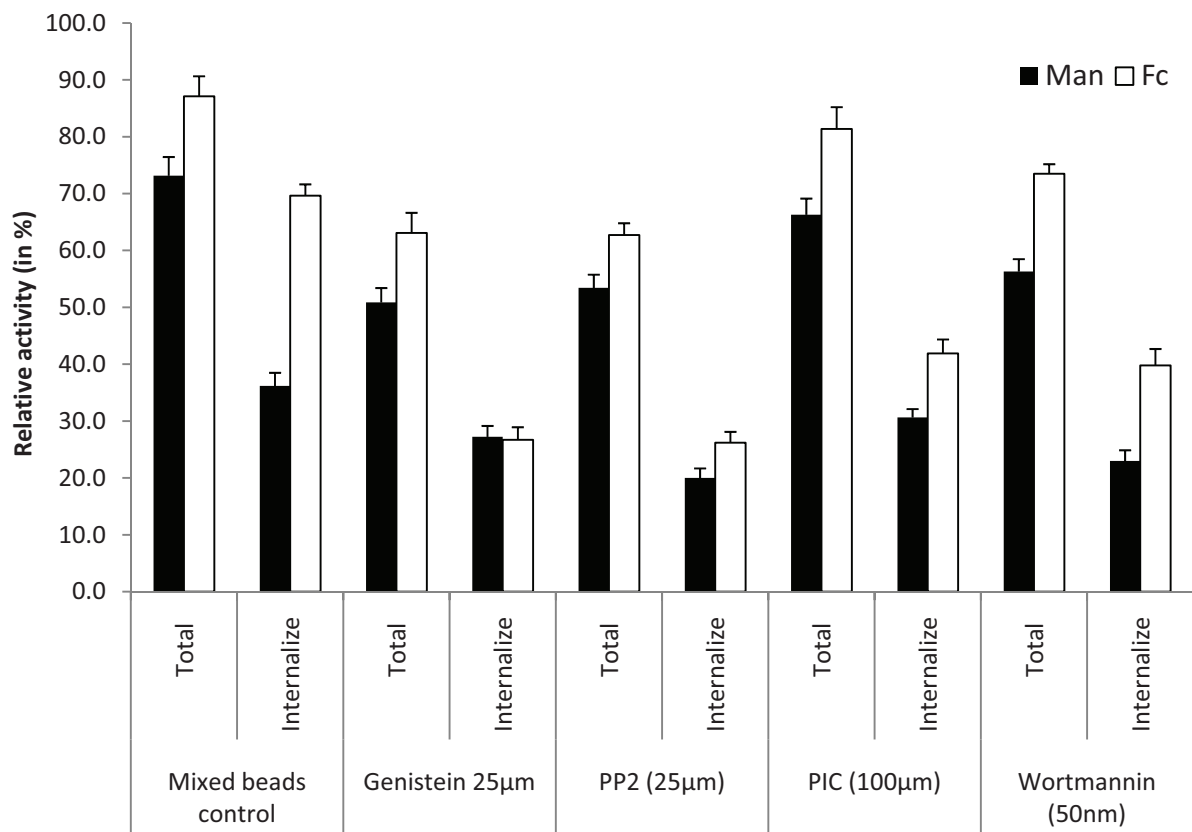


**Figure22.** Effect of different kinase inhibitors on Fc and mannan coated beads binding and uptake in mixture. Macrophages were incubated with different kinase inhibitors prior to co-incubation with mixture of Fc and mannan beads for 30 min (see materials and methods) to analyse the binding and internalization of Fc beads and mannan beads in mixture. All the kinase inhibitors did not show a significant decrease in internalization of both the types of beads in mixture. Average of three independent experiments.



I then checked the effect of all the above mentioned kinase inhibitors in the phagocytosis of mixed beads. I found that kinase inhibitors could not further reduce the internalization of mixed beads. The reduction in attachment of mannan beads and Fc beads in mixture was nearly 50% and 70% to that of control but the internalization of both types of beads was just 30% of control and that reduction was almost similar to that of mixed beads in control. (figure 22). These results suggested that the competition of the beads is mainly because of the number of binding sites available to the different ligand coated beads. I hypothesized that the reason for the reduction in internalization of mannan beads is upstream of the attachment and the Fc receptors dominate over the MR for the binding sites. Taken together my results suggested a possible cross-talk between the MR and Fc $\gamma$  receptors due to their spatial arrangements.

# *Discussion*

#### **4.1 FcγRs are homogeneously distributed on macrophage surface as nano-domains of various size**

Molecular recognition between receptors and their cognate ligands plays important role during the phagocytosis. These are the highly specific events where ligands on the surface of microbes interact with their cognate receptors on the phagocyte cell surface. Thus these interactions are very important during immune response and initiation of infection and many other cellular functions. Furthermore, there is a vast body of available literature on the structure and function of receptor-ligand complexes, yet information about the molecular dynamics within the complexes during the association and dissociation process is usually lacking. Moreover, until recently, mapping the spatial distribution of individual binding sites on cellular surfaces was not accessible because of a lack of appropriate imaging techniques. Consequently, there is clearly a need to develop and exploit single molecule tools for sensing and mapping molecular recognition interactions on biosurfaces. Owing to its capacity to allow observation and manipulation of biosurfaces under physiological conditions, the AFM has revolutionized the way in which researchers now explore biological structures at the single molecule level (Binnig et al., 1986;Hinterdorfer et al., 1996). Although AFM imaging provides three dimensional views of specimens with unprecedented resolution and with minimal sample preparation (Engel and Muller, 2000) , AFM force spectroscopy allows measurement of piconewton( $10^{-12}$  N) forces associated with single molecules (Clausen-Schaumann et al., 2000) thereby providing fundamental insights into the molecular basis of biological phenomena and properties like molecular recognition (Florin et al., 1994a;Hinterdorfer et al., 1996), protein folding and unfolding, DNA mechanics and cell adhesion (Benoit et al., 2000;Hinterdorfer et al., 1996;Oberhauser et al., 1998;Rief et al., 1999).

Fluorescence microscopy is an important tool for localizing receptor/ligand recognition in in vitro systems and in living cells. However, due to its limited resolution, the recognition sites cannot be resolved on the nm scale nor can they be correlated to topography features. The atomic force microscope can resolve nm-sized details very well and yields the greatest structural details on biological samples such as proteins, nucleotides, membranes, and cells in their native, aqueous environment (Binnig et al., 1986;Hinterdorfer et al., 1996). In addition, due to its force detection sensitivity, it has opened the possibility of measuring interand intramolecular forces of biomolecules on the single molecule level (Florin et al., 1994b;Hinterdorfer et al., 1996;Oberhauser et al., 1998;Rief et al., 1999). These

capabilities lead to the development of the method described in this study, which enables us to investigate the interaction of a single ligand molecule with its cognate receptor while simultaneously recording a high resolution topography image. Single molecular interaction forces are typically studied in force spectroscopy experiments (Yuan et al., 2000; Baumgartner et al., 2000). An AFM tip carrying ligands is brought in contact with a surface that contains the respective cognate receptors, so that a receptor/ligand bond is formed. This bond is subsequently broken at a characteristic measurable unbinding force by retracting the tip from the surface. In a first attempt of localizing antigenic sites via force spectroscopy, force-distance cycles using tips that were functionalized with antibodies were performed during linear lateral scans on a surface to which the cognate receptor, human serum albumin (HSA), was covalently attached (Hinterdorfer et al., 1996). Binding probabilities were determined in dependence on the lateral position, resulting in binding profiles for single HSA molecules that showed a maximum, which allowed to determine lateral positions of antigenic sites with 1.5-nm accuracy. I have used force spectroscopy and dynamic recognition imaging (TREC) on gently fixed macrophage surfaces to sense and thus to determine the local organization of FcγRs at single molecule level. When using single-molecule AFM force spectroscopy and TREC imaging on cellular surface, immobilization of cells while preserving their viability and integrity is a challenge. For animal cells chemical fixation using cross linking agents such as glutaraldehyde can be used but this approach is not suitable for single molecule recognition studies (Le Grimellec et al., 2002) although this approach works well for topographic imaging. I showed by binding assays with Fc-coated beads and as well by force measurements with Fc-coated tip that the activity of binding sites of FcγRs practically remain intact by using paraformaldehyde as fixative agent. Paraformaldehyde proved to be better fixative than widely used chemical fixative glutaraldehyde. The paraformaldehyde fixing method is so gentle that it leaves the binding sites on the cell intact and therefore Fc beads can bind to the cell even after fixation. Another key issue was that the macrophage surface is so uneven and dynamic that it could produce artifacts while scanning the cell surface with AFM tip. This problem was solved by incubating the cells in a hypotonic medium prior to fixation which makes the cell surface smoother. Molecular recognition force spectroscopy with Fc fragment modified tips provides a powerful tool for exploring the molecular bases of receptor-ligand interactions. The interaction forces between Fc fragment and the Fc receptors on a single-molecule basis were determined and found to be

in the range of 25pN. In addition the dynamics of the receptor-ligand interaction by varying the loading rate was also determined.

Simultaneous topography and RECOgnition (TREC) imaging is a newly developed AFM technique to image the topography and recognition of receptor binding sites on cell surface in physiological conditions. TREC allows to determine the distribution of receptors on cell surface with a resolution of 5 nm. (Chtcheglova et al., 2007). In TREC, the functionalized tip is oscillated close to its resonance frequency and scanned across the cell surface. TREC has been successfully used to map the binding sites on a number of surfaces such as organic semiconductor surfaces or on more complex and heterogeneous biosurfaces such as cell membranes (Chtcheglova et al., 2007;Preiner et al., 2009). In the present study I have used the TREC to unravel the nano-landscape of one of the most important phagocytic receptors, the Fc $\gamma$ Rs. The recognition images presented here illustrate rather uniformly distributed microdomains of different sizes reached in Fc $\gamma$ Rs, single Fc $\gamma$ Rs are also detectable. Thus, the surface of normal macrophage represents a map of relatively large Fc $\gamma$ R clusters (widths > 200 nm) surrounding by smaller microdomains with typical size of ~ 60 nm and single receptors. Such compact cluster organization of Fc $\gamma$ Rs would favors rapid recognition of huge phagocytes and thus their effective internalization. It is important to remark that using Fc-coated AFM tips in this study we could not distinguish between different types of mouse Fc $\gamma$ Rs on J774.A1 macrophage surface neither with force spectroscopy nor TREC. However, since Fc $\gamma$ RI characterized by much higher affinity to Fc (Ravetch and Kinet, 1991) and mostly abundant on macrophage surface (our immunofluorescence observations) than Fc $\gamma$ RII or Fc $\gamma$ RIII, we can speculate that the observed recognition maps most likely contain Fc $\gamma$ RI. In order to elucidate this hypothesis, further AFM measurements with tips carrying monoclonal antibodies specific to Fc $\gamma$ RI and Fc $\gamma$ RII will be performed. Another question can be addressed how the principal effect of cell activation (e.g. activation of Fc $\gamma$ Rs) will cause the reorganization of these receptors. Taking together, further analysis of the local composition of Fc $\gamma$ Rs on the macrophage membrane is expected to reveal new insights into the function of different Fc $\gamma$ Rs in the initial stages of phagocytosis. The benefits of utilizing this AFM-based approach are twofold. First, the investigations are noninvasive and performed directly in aqueous solution without any cell pretreatment, thus preserving the native organization and conformation of the surface molecules. Second, the piconewton force sensitivity of the atomic force microscope permits a functional analysis of individual adhesins. In the future,

this type of nanoscale cell imaging study may be of biomedical relevance by serving to facilitate the development of new drugs capable of blocking ligand-receptor interactions.

#### **4.2 Latex beads system offers a powerful tool to study the receptors distribution on the cell surface**

Phagocytosis is a complex process that requires coordinated activation of signaling leads to events like actin remodeling, membrane trafficking, particle engulfment, microbial killing and production of inflammatory mediators that direct the adaptive response. Macrophages are important phagocytes that express a broad spectrum of receptors that participate in particle recognition and internalization. It is widely accepted fact that initial receptor-ligand interaction leads to subsequent signaling pathways which are highly receptor-ligand interaction specific. Since macrophages have a variety of receptors on their surface which are involve in recognition of several microbes and microbes also has several ligands, therefore it is thought that there is an extensive cross talk between different phagocytic signaling pathways. In addition, the fate of phagocytosed particle is also depend on the receptor-ligand interaction involved. And this phenomenon is recently reported by several studies on pathogens, such as *Mycobacterium tuberculosis* (Clemens and Horwitz, 1995) and *Toxoplasma gondii* (Mordue and Sibley, 1997), where recognition events at the phagocyte surface modulate phagosomal fate. When a macrophage ingests a pathogen, the pathogen becomes trapped in a phagosome, which then fuses with a lysosome. Within the phagolysosome, enzymes and toxic peroxides digest the pathogen. However, some bacteria, such as *Mycobacterium tuberculosis*, have become resistant to these methods of digestion which depends on the receptors involved.

For this study I decided to explore the possible interaction and distribution of FcγRs (as an opsonic receptor) and MRs (as a non-opsonic receptors) on macrophage cell surface. I have used latex beads system as a tool to investigate the nano-landscape of the receptors on the macrophage surface. Latex beads is a versatile model system, allows the scientists over the last 15 years to study the detailed analysis of a variety of functions during phagocytosis *in vitro* and in cells and led to the development of several *in vitro* assays using isolated phagosomes for detailed proteomics and lipidomics analyses and the characterization of various phagosome functions in living macrophages (Desjardins and Griffiths, 2003;Griffiths and Mayorga, 2007). *In vitro* assays were applied to monitor microtubule binding and motility, actin assembly and binding as well as fusion events with different

endocytic compartments (Desjardins and Griffiths, 2003). Furthermore, the *in vitro* actin assembly assay has opened up a system to analyse pathogen-induced signalling networks regulating defined and complex membrane functions (Anes et al., 2003; Kalamidas et al., 2006). However, a limiting factor in our understanding until now is that crucial receptors that internalise beads or pathogens are either unknown or too many to be analysed in detail.

By using coated latex beads of various size, this study and the approaches it introduces provide a platform for understanding interactions between phagocytic particles having defined ligands with specific receptors on macrophages and open ways to determine how different receptor-ligand interactions are modulated during phagocytosis in a single cell. Although it is important to address phagocytic processes and signalling events at cellular and tissue levels, it seems likely that detailed mechanisms will ultimately emerge from the use of *in vitro* systems where all components are under the control of the investigator. Taking advantage of the use of ligand coated latex beads to study the receptor-ligand interaction during phagocytosis previous work in our lab has shown that latex beads coupled with different ligands, trigger the specific uptake via different receptors. (Hoffmann et al., 2010). Thus, coating of latex beads with the Fc fragment of mouse IgG (Fc beads) induced Fc $\gamma$  receptor-mediated uptake, whereas coating of latex beads with mannan (mannan beads) induced an internalization predominantly via the mannose receptor. These specific internalization routes were compared to the non-selective uptake of latex beads coupled to avidin (avidin beads). By using defined type of coated latex beads it was shown that the choice of a particular ligand on the bead and following initial receptor- ligand interaction had a significant influence on the whole phagocytic process, including phagocytic uptake efficiency, phagosomal fusion with lysosomes, macrophage gene expression and the protein composition of the phagosomes (Hoffmann et al., 2010). Therefore it was suggested that there exist a specific receptor-ligand 'signature' during the whole process of phagocytosis. In the present study I have used latex beads conjugated to specific ligands as a powerful tool to analyze the response of a phagocyte such as macrophages when two differently coated beads with a single ligand are applied simultaneously to these cells. The ligand coated latex bead system offers an elegant approach to unravel the nano-landscape of different receptors present on the macrophage surface involved in phagocytosis. Another advantage of latex beads is that they are commercially available in different size ranging from 20 nm to 2  $\mu$ m and different fluorescence. Therefore, two types of differently coated latex beads i.e. mannan coated and Fc fragment of IgG coated latex beads of different size can be applied simultaneously to

the cells and distribution of their cognate receptors can be mapped. These ligands were chosen because of their specific interaction with Fc $\gamma$  receptors (Fc $\gamma$  receptors) and mannose receptors (MR) specifically mediates two major types of phagocytosis i.e. opsonic and non-opsonic respectively (Aderem and Underhill, 1999; Anderson et al., 1990; Blander, 2007; Cox and Greenberg, 2001; Taylor et al., 2005). Irrespective of the ligand macrophages can bind and internalize the beads in a morphologically indistinguishable manner. However, although macrophages were incubated with same numbers of beads, the ones coated with mannan were internalized at faster rates and in higher numbers compared to beads coated with Fc fragment (Hoffmann et al., 2010; Kruskal et al., 1992).

In order to work with two types of beads at optimal non-saturated conditions we determined first the phagocytic activity of the cells in the presence of different concentrations of single type of beads. We found that J774A.1 macrophages showed a linear increase of the phagocytic activity of both the types of beads with increase in the concentration of beads from 0.005% to 0.02% in internalization medium. Therefore for further experiments a concentration of 0.01% of both the types of beads in internalization medium was used. In order to prove that all the studied ligands bound to the latex beads interacted specifically to their expected receptors the competition experiments were performed. I found that a given soluble ligand efficiently competed for binding of the cognate ligand coated bead. This resulted in a nearly 50% decrease of the corresponding bead uptake to less than compare to control conditions for IgG Fc, mannan, and for avidin. The specificity of the ligand-receptor interaction was further confirmed by cross competition experiments where macrophages were co-incubated with beads together with another ligand than the one present on the bead surface, phagocytic uptake rates were not significantly affected. In addition, I found that soluble Fc and soluble mannan do not inhibit the phagocytosis of mannan beads and Fc beads respectively. These findings have proved the robustness of latex beads system to study the receptors nano-landscape on the macrophages surface. In the next experiments I have used a mixture of mannan and Fc beads in a ratio of 1:1 where the concentration of a single beads in a mixture is kept at 0.01% so as to compare it with the control. It was found that there is a competition between Fc beads and mannan beads for phagocytosis by macrophages. The competition between the beads leads to a greater decrease in attachment and internalization of the mannan beads in presence of Fc beads. On the other hand mannan beads did not exert an inhibitory effect on Fc beads binding and internalization. In previous studies it has shown that binding of IgG opsonized particles to cell surface Fc $\gamma$ R is an active stage of



phagocytosis (Sobota et al., 2005). Binding of particles, rather than internalization, triggers phosphorylation of Fc $\gamma$ R and most of the accompanied proteins (Strzelecka-Kiliszek et al., 2002). It is well documented that binding of particles is achieved by progressive interaction of Fc $\gamma$ Rs with IgG coated particles in a so called Zipper mode. Simultaneously clusters of engaged Fc $\gamma$ Rs are apparently formed at the bound particle. Thus particle binding and the clustering of Fc $\gamma$ Rs is a prerequisite for the receptor phosphorylation and initiation of phagocytic signals (Ravetch and Kinetic, 1991; Cox and Greenberg, 2001). However, the lack of defined cytoplasmic signaling motif in mannose receptors makes it difficult to understand how signaling occurs following particle binding. Our results also supports the fact that particle binding is an active stage of phagocytosis and It was hypothesised that this competition is at very early step of phagocytosis i.e. during the initial receptor-ligand interaction at the time of particle binding. The effect of competition was significant during the binding of the beads. The binding of mannan beads in presence of Fc beads reduced significantly by 30%. However, the vice versa was not true. Conclusion of these experiments was that the competition was at very early stage of phagocytosis and beads compete for their respective binding sites i.e. their cognate receptors. To my knowledge at least two previous studies have shown the involvement of mannose receptor during the Fc $\gamma$ R mediated phagocytosis (Murai et al., 1995; Murai et al., 1996) where mannose receptors were contributing in stimulation of protein tyrosine phosphorylation for Fc $\gamma$ R mediated phagocytosis by the activation of the cells with preincubation of  $\alpha$ 2-macroglobulin which binds to the mannose receptors through their terminal mannose residues. Therefore, it was interesting to find the fact that there is a competition between mannan and Fc beads when used in a mixture and cells were incubated with this mixture.

I used mixture of Fc and mannan beads in different ratios to check the effect and results were in support of the proposed hypothesis. It was found that even a smaller number of Fc beads could inhibit the phagocytosis of mannan beads by macrophages. In a mixture where concentration of Fc beads was kept 4 times lesser than mannan, inhibitory effect of Fc beads on mannan beads phagocytosis was observed. The overall deficiency in mannan beads phagocytosis was found to be nearly 25% as compare to control. This effect was linearly increased as the concentration of Fc beads increased in the mixture. On the other hand, similar effect of mannan beads on Fc beads was not observed. The smallest concentration at which Fc beads have shown inhibition of mannan beads phagocytosis was 0.002% of beads in mixture. However, mannan beads did not show any inhibition of Fc

beads on this concentration. These findings were in support of the suggestion that the competition is due to receptor-ligand interaction on surface of macrophages.

In another set of experiments, cells were preincubated with different sized Fc beads ranging from 20 nm to 2  $\mu$ m and then mannan beads of size 1  $\mu$ m were applied to the cell. The binding of mannan beads was reduced significantly with 0.5  $\mu$ m, 1  $\mu$ m and 2  $\mu$ m Fc beads pre-incubation. Moreover, pre-incubation with smaller Fc beads could also reduce the binding of Fc beads. On the other hand, pre-incubation with mannan beads did not bring about any significant reduction in Fc beads binding. These findings were again in accordance with the hypothesis that there is competition of binding sites between mannan and Fc beads. At this point of the study it can be postulated that number of mannose receptors are much less than Fc receptors and also that mannose receptors are distributed in such a way that they are mainly surrounded by Fc receptors which is in agreement with the other studies where numbers of Fc $\gamma$  receptors and mannose receptors have been described (Murai et al., 1996; Murai et al., 1995; Ravetch and Kinetic, 1991; Fiani et al., 1998). The number of mannose receptors present on the J774A1 macrophages is reported to be nearly  $10^4$  (Fiani et al., 1998) and the Fc $\gamma$  receptors are reported much more than that nearly  $10^5$  (Unkeless and Eisen, 1975; Unkeless, 1977). In addition, this was also clear that both the type of receptor-ligand interaction induces signaling pathways which are independent of each other and there is no competition for the machinery required for the signaling. However, the Fc $\gamma$ R mediated phagocytic signaling pathway is very well described but the mannose receptor mediated phagocytic signaling still need to be unraveled. These findings led us to study the distribution of the two types of receptors in more detail using confocal laser scanning microscopy and immune-electron microscopy.

#### **4.3 Mannose receptors are present in lesser number than Fc $\gamma$ Rs and majority of them are located very near to Fc $\gamma$ RI**

Contribution of MR in Fc $\gamma$ R mediated phagocytosis has been described. Although interaction between MR and Fc $\gamma$ R has not been extensively reported. Very recently it was shown that MR interacts with Fc $\gamma$ Rs and this interaction is critical for the development of crescentic glomerulonephritis in mice (Chavele et al., 2010). Another point is that MR are available in far less numbers as compare to Fc $\gamma$ Rs on the macrophage cell surface. My results of immunofluorescence studies with MR and Fc $\gamma$ RI are also in support of these findings. The distribution of the MR on the macrophage cell was found to be 5 times less

than Fc $\gamma$ RI. This was also in agreement with the fact that MR are present in the cytoplasm as well from where they keep recycling to the cell surface. This phenomenon is not true for the Fc $\gamma$ Rs. The colocalization of the MR with Fc $\gamma$ RI in terms of voxels at the different places on the cell i.e. cell surface, cell periphery or the whole cell was found to be nearly 60% but only 20% of the total Fc $\gamma$ RI were colocalized with MR in terms of total voxels compared. This finding was again pointing towards the fact that MR are present in a lesser number than Fc $\gamma$ Rs on macrophage cell surface. Finally these results were confirmed by the immune-electron microscopy where the co-localization and the nearest neighbor distance analysis between the two receptors i.e. Fc $\gamma$ RI and MR was quantified on the immunolabeled electron micrographs. This method has been proved for identifying colocalization and nearest neighbor distance between the interaction proteins on the surface of chloroplasts (Anderson et al., 2003). This method was found to be equally applicable and provide evidence in support of my results that were achieved by immunofluorescence that Fc $\gamma$ RI and MR are located very close to each other for their possible interaction. Nearest neighbor analysis as described here is a robust method for identifying protein species that are located close to one another in situ. Where there are great disparities in the concentrations of the two species, it is important to measure distances from the species present, it is important to measure distances from the species present at lower concentration to the species present at higher concentration. Unlike the methods for nearest neighbor data analysis derived by Gathercole et al. (2000) and by Philimonenko et al. (2000), this method does not require density measurements. Co-localization of stromal enzymes is evident in the thylakoid-containing chloroplast. Like the analysis of Cullen et al. (1998) this method should be applicable to membrane-bound species. It should also be satisfactory when labeling levels are low and/or where not all of the proteins interact with one another. The methods of Gathercole et al. (2000), Philimonenko et al. (2000), and Cullen et al. (1998) give information about the actual size of the complex. My data clearly indicate that the MR and Fc $\gamma$ RI are located close to one another on the macrophage surface. The average distance between the two receptors was found to be 413 nm which is in agreement with the findings with different sized latex beads where it was found that 0.5 $\mu$ m Fc beads could inhibit the binding of mannan beads. Since there are more number of Fc $\gamma$ RI are present than MR, therefore the binding of Fc beads in presence of mannan beads was not significantly reduced.

#### **4.4 Fc beads inhibit the phagocytosis of *Mycobacterium smegmatis***

The biological relevance of this phenomenon of inhibition of MR mediated phagocytosis due to Fc $\gamma$ Rs was studied using non-pathogenic *M. smegmatis* which is recognized by the macrophages through MR (Astarie-Dequeker et al., 1999). MR has been reported to recognize glycosylated molecules with terminal mannose, fucose or N-acetylglucosamine moieties and efficiently internalize and phagocytose several pathogens such as *Candida albicans*, *Leishmania donovani*, *Mycobacterium tuberculosis* strains H37Rv and Erdman. In macrophages the role of MR is coupled to bactericidal functions such as secretion of lysosomal enzymes, production of cytokines and O<sub>2</sub><sup>-</sup> (Underhill and Ozinsky, 2002). Thus MR is very important receptor present on the macrophage surface. In the present study I therefore undertaken to examine the effect on the phagocytosis of widely studied non-pathogenic *Mycobacterium smegmatis* in the presence of Fc beads. The objective of this part of the study was to determine whether the phenomenon of competition between the Fc beads and mannan beads is comparable with the model microorganism like *M. smegmatis* which is recognized by the MR on the macrophages. First I have done the microscopic studies and the internalization of *M. smegmatis* was quantified. It was found that the internalization as well as binding of *M. smegmatis* in presence of Fc beads was reduced to nearly 40%. Furthermore these findings were confirmed by culturing the bacteria recovered after the lysis of the cells and plated onto the appropriate culture medium. Once again the results obtained were in agreement that the binding and internalization of the *M. smegmatis* was reduced to 50% in presence of Fc beads. Taken together all our results indicate the possible interaction of Fc $\gamma$ Rs and MR on the macrophage surface due to their distribution pattern.

#### **4.5 Kinases are required for the initial steps of mannose receptor mediated phagocytosis of latex beads**

Cross-linking of the Fc $\gamma$ R ligand-binding extracellular domain causes tyrosine phosphorylation of the cytoplasmic ITAM domain by the Src family kinases (Garcia-Garcia and Rosales, 2002). Phosphorylated ITAMs then serve as docking sites for the SH2-containing signaling molecules like Syk tyrosine kinase. Syk activation subsequently leads to activation of signaling cascades that involve various molecules like protein kinase C (PKC), phospholipase A2 (PLA2), phosphatidyl inositol 3-kinase (PI3K), extracellular

signal-regulated kinase (ERK) etc (Aderem and Underhill, 1999; Anderson et al., 1990). On the other hand very little is known about the mannose receptor mediated phagocytosis and only PI3K has been shown to involve in mannose receptor mediated phagocytosis (Lee et al., 2007). In case of Fc $\gamma$ R, my findings with the kinase inhibitors are in agreement with the well established model of Fc $\gamma$ R mediated phagocytic signaling where characterization of the molecular associations of Syk protein tyrosine kinase with downstream partners showed a direct interaction between Syk and PI3K (Sanchez-Mejorada and Rosales, 1998; Kwiatkowska and Sobota, 1999). However, in case of mannose receptor, the role of SRTKs and Syk kinase are not well established yet because of lack of signaling motif in the cytoplasmic tail of the mannose receptor. But PI3K is known to play role in mannose receptor mediated phagocytosis. For the first time we have shown the possible involvement of SRTKs and Syk kinase in MR mediated phagocytosis. However, further detailed studies are required in order to confirm these findings and to resolve the molecular mechanisms which are responsible for the MR mediated phagocytosis. Since MR have been reported to involve in recognition of several microbes including *Mycobacterium tuberculosis* therefore our findings will open up new directions for studying mechanisms. *Mycobacterium* spp. are responsible for several pathologies like tuberculosis, leprosy etc. The bacterium can infect the macrophages where they can survive and multiply (Ehlers and Daffe, 1998). The mechanism behind this is poorly understood and elucidation of mechanisms involved in the interaction between macrophages and mycobacteria could help to develop new pharmacological strategies to prevent macrophage infection. Also phagocytosis is a complex process where many receptors recognize microbes and receptors-microbe interaction induce different signaling pathways. Since the microbial surfaces are highly complex therefore this is very likely that several receptors induce signaling simultaneously in response to microbe. Our findings have suggested the role of interaction between opsonic and non-opsonic receptors i.e. MR and Fc $\gamma$ RI. During the phagocytosis of key microbes like *M. smegmatis*. We have shown that MR and Fc $\gamma$ RI are located close enough to compete with each other for the recognition and internalization of *M. smegmatis*. Taken together, further analysis of the local composition of Fc $\gamma$ Rs and MRs on the macrophage membrane is expected to reveal new insights into the function of different receptors in the initial stages of phagocytosis.

# References

- Aderem, A., and D.M.Underhill. 1999. Mechanisms of phagocytosis in macrophages. *Annu. Rev. Immunol.* 17:593-623.
- Agarwal, A., P.Salem, and K.C.Robbins. 1993. Involvement of p72syk, a protein-tyrosine kinase, in Fc gamma receptor signaling. *J. Biol. Chem.* 268:15900-15905.
- Al Haddad, A., M.A.Shonn, B.Redlich, A.Blocker, J.K.Burkhardt, H.Yu, J.A.Hammer, III, D.G.Weiss, W.Steffen, G.Griffiths, and S.A.Kuznetsov. 2001. Myosin Va bound to phagosomes binds to F-actin and delays microtubule-dependent motility. *Mol. Biol. Cell* 12:2742-2755.
- Allen, L.A., and A.Aderem. 1996. Molecular definition of distinct cytoskeletal structures involved in complement- and Fc receptor-mediated phagocytosis in macrophages. *J. Exp. Med.* 184:627-637.
- Allison, A.C., P.Davies, and S.De Petris. 1971. Role of contractile microfilaments in macrophage movement and endocytosis. *Nat. New Biol.* 232:153-155.
- Aman, M.J., T.D.Lamkin, H.Okada, T.Kurosaki, and K.S.Ravichandran. 1998. The inositol phosphatase SHIP inhibits Akt/PKB activation in B cells. *J. Biol. Chem.* 273:33922-33928.
- Amigorena, S., C.Bonnerot, J.R.Drake, D.Choquet, W.Hunziker, J.G.Guillet, P.Webster, C.Sautes, I.Mellman, and W.H.Fridman. 1992. Cytoplasmic domain heterogeneity and functions of IgG Fc receptors in B lymphocytes. *Science* 256:1808-1812.
- Anderson, C.L., and G.N.Abraham. 1980. Characterization of the Fc receptor for IgG on a human macrophage cell line, U937. *J. Immunol.* 125:2735-2741.
- Anderson, C.L., L.Shen, D.M.Eicher, M.D.Wewers, and J.K.Gill. 1990. Phagocytosis mediated by three distinct Fc gamma receptor classes on human leukocytes. *J. Exp. Med.* 171:1333-1345.
- Anderson, J.B., A.A.Carol, V.K.Brown, and L.E.Anderson. 2003. A quantitative method for assessing co-localization in immunolabeled thin section electron micrographs. *J. Struct. Biol.* 143:95-106.
- Anes, E., M.P.Kuhnel, E.Bos, J.Moniz-Pereira, A.Habermann, and G.Griffiths. 2003. Selected lipids activate phagosome actin assembly and maturation resulting in killing of pathogenic mycobacteria. *Nat. Cell Biol.* 5:793-802.
- Ashkin, A., K.Schutze, J.M.Dziedzic, U.Euteneuer, and M.Schliwa. 1990. Force generation of organelle transport measured in vivo by an infrared laser trap. *Nature* 348:346-348.
- Astarie-Dequeker, C., E.N.N'Diaye, C.Le, V, M.G.Rittig, J.Prandi, and I.Maridonneau-Parini. 1999. The mannose receptor mediates uptake of pathogenic and nonpathogenic mycobacteria and bypasses bactericidal responses in human macrophages. *Infect. Immun.* 67:469-477.
- Astarie-Dequeker, C., E.N.N'Diaye, C.Le, V, M.G.Rittig, J.Prandi, and I.Maridonneau-Parini. 1999. The mannose receptor mediates uptake of pathogenic and nonpathogenic mycobacteria and bypasses bactericidal responses in human macrophages. *Infect. Immun.* 67:469-477.
- Avrameas, A., D.McIlroy, A.Hosmalin, B.Autran, P.Debre, M.Monsigny, A.C.Roche, and P.Midoux. 1996. Expression of a mannose/fucose membrane lectin on human dendritic cells. *Eur. J. Immunol.* 26:394-400.
- Baumgartner, W., P.Hinterdorfer, and H.Schindler. 2000. Data analysis of interaction forces measured with the atomic force microscope. *Ultramicroscopy* 82:85-95.
- Benoit, M., D.Gabriel, G.Gerisch, and H.E.Gaub. 2000. Discrete interactions in cell adhesion measured by single-molecule force spectroscopy. *Nat. Cell Biol.* 2:313-317.
- Binnig, G., C.F.Quate, and C.Gerber. 1986. Atomic force microscope. *Phys. Rev. Lett.* 56:930-933.

- Blander, J.M. 2007. Signalling and phagocytosis in the orchestration of host defence. *Cell Microbiol.* 9:290-299.
- Blocker, A., F.F. Severin, J.K. Burkhardt, J.B. Bingham, H. Yu, J.C. Olivo, T.A. Schroer, A.A. Hyman, and G. Griffiths. 1997. Molecular requirements for bi-directional movement of phagosomes along microtubules. *J. Cell Biol.* 137:113-129.
- Bolland, S., and J.V. Ravetch. 1999. Inhibitory pathways triggered by ITIM-containing receptors. *Adv. Immunol.* 72:149-177.
- Bolland, S., R.N. Pearse, T. Kurosaki, and J.V. Ravetch. 1998. SHIP modulates immune receptor responses by regulating membrane association of Btk. *Immunity.* 8:509-516.
- Bonanni, B., A.S. Kamruzzahan, A.R. Bizzarri, C. Rankl, H.J. Gruber, P. Hinterdorfer, and S. Cannistraro. 2005. Single molecule recognition between cytochrome C 551 and gold-immobilized azurin by force spectroscopy. *Biophys. J.* 89:2783-2791.
- Bonilla, F.A., R.M. Fujita, V.I. Pivniouk, A.C. Chan, and R.S. Geha. 2000. Adapter proteins SLP-76 and BLNK both are expressed by murine macrophages and are linked to signaling via Fc $\gamma$  receptors I and II/III. *Proc. Natl. Acad. Sci. U. S. A.* 97:1725-1730.
- Boskovic, J., J.N. Arnold, R. Stilion, S. Gordon, R.B. Sim, A. Rivera-Calzada, D. Wienke, C.M. Isacke, L. Martinez-Pomares, and O. Llorca. 2006. Structural model for the mannose receptor family uncovered by electron microscopy of Endo180 and the mannose receptor. *J. Biol. Chem.* 281:8780-8787.
- Brown, G.D., and S. Gordon. 2001. Immune recognition. A new receptor for beta-glucans. *Nature* 413:36-37.
- Chakraborty, P., D. Ghosh, and M.K. Basu. 2001. Modulation of macrophage mannose receptor affects the uptake of virulent and avirulent *Leishmania donovani* promastigotes. *J. Parasitol.* 87:1023-1027.
- Chavele, K.M., L. Martinez-Pomares, J. Domin, S. Pemberton, S.M. Haslam, A. Dell, H.T. Cook, C.D. Pusey, S. Gordon, and A.D. Salama. 2010. Mannose receptor interacts with Fc receptors and is critical for the development of crescentic glomerulonephritis in mice. *J. Clin. Invest* 120:1469-1478.
- Chitchevlova, L.A., J. Waschke, L. Wildling, D. Drenckhahn, and P. Hinterdorfer. 2007. Nano-scale dynamic recognition imaging on vascular endothelial cells. *Biophys. J.* 93:L11-L13.
- Clausen-Schaumann, H., M. Seitz, R. Krautbauer, and H.E. Gaub. 2000. Force spectroscopy with single bio-molecules. *Curr. Opin. Chem. Biol.* 4:524-530.
- Clausen-Schaumann, H., M. Seitz, R. Krautbauer, and H.E. Gaub. 2000. Force spectroscopy with single bio-molecules. *Curr. Opin. Chem. Biol.* 4:524-530.
- Clemens, D.L., and M.A. Horwitz. 1995. Characterization of the *Mycobacterium tuberculosis* phagosome and evidence that phagosomal maturation is inhibited. *J. Exp. Med.* 181:257-270.
- Cone, J.C., Y. Lu, J.M. Trevillyan, J.M. Bjorndahl, and C.A. Phillips. 1993. Association of the p56lck protein tyrosine kinase with the Fc  $\gamma$  RIIIA/CD16 complex in human natural killer cells. *Eur. J. Immunol.* 23:2488-2497.
- Cox, D., and S. Greenberg. 2001. Phagocytic signaling strategies: Fc( $\gamma$ )receptor-mediated phagocytosis as a model system. *Semin. Immunol.* 13:339-345.



- Crowley, M.T., P.S.Costello, C.J.Fitzer-Attas, M.Turner, F.Meng, C.Lowell, V.L.Tybulewicz, and A.L.DeFranco. 1997. A critical role for Syk in signal transduction and phagocytosis mediated by Fc $\gamma$  receptors on macrophages. *J. Exp. Med.* 186:1027-1039.
- Czop, J.K., and J.Kay. 1991. Isolation and characterization of beta-glucan receptors on human mononuclear phagocytes. *J. Exp. Med.* 173:1511-1520.
- Daeron, M. 1997b. Fc receptor biology. *Annu. Rev. Immunol.* 15:203-234.
- Daeron, M., S.Latour, O.Malbec, E.Espinosa, P.Pina, S.Pasmans, and W.H.Fridman. 1995. The same tyrosine-based inhibition motif, in the intracytoplasmic domain of Fc  $\gamma$  RIIb, regulates negatively BCR-, TCR-, and FcR-dependent cell activation. *Immunity.* 3:635-646.
- Defacque, H., E.Bos, B.Garvalov, C.Barret, C.Roy, P.Mangeat, H.W.Shin, V.Rybin, and G.Griffiths. 2002. Phosphoinositides regulate membrane-dependent actin assembly by latex bead phagosomes. *Mol. Biol. Cell* 13:1190-1202.
- Desjardins, M., and G.Griffiths. 2003. Phagocytosis: latex leads the way. *Curr. Opin. Cell Biol.* 15:498-503.
- Desjardins, M., J.E.Celis, G.van Meer, H.Dieplinger, A.Jahraus, G.Griffiths, and L.A.Huber. 1994a. Molecular characterization of phagosomes. *J. Biol. Chem.* 269:32194-32200.
- Devitt, A., O.D.Moffatt, C.Raykundalia, J.D.Capra, D.L.Simmons, and C.D.Gregory. 1998. Human CD14 mediates recognition and phagocytosis of apoptotic cells. *Nature* 392:505-509.
- Dupres, V., C.Verbelen, and Y.F.Dufrene. 2007a. Probing molecular recognition sites on biosurfaces using AFM. *Biomaterials* 28:2393-2402.
- East, L., and C.M.Isacke. 2002. The mannose receptor family. *Biochim. Biophys. Acta* 1572:364-386.
- Ebner, A., F.Kienberger, G.Kada, C.M.Stroh, M.Geretschlager, A.S.Kamruzzahan, L.Wildling, W.T.Johnson, B.Ashcroft, J.Nelson, S.M.Lindsay, H.J.Gruber, and P.Hinterdorfer. 2005. Localization of single avidin-biotin interactions using simultaneous topography and molecular recognition imaging. *Chemphyschem.* 6:897-900.
- Ehlers, M.R., and M.Daffe. 1998. Interactions between *Mycobacterium tuberculosis* and host cells: are mycobacterial sugars the key? *Trends Microbiol.* 6:328-335.
- Engel, A., and D.J.Muller. 2000. Observing single biomolecules at work with the atomic force microscope. *Nat. Struct. Biol.* 7:715-718.
- Engering, A., I.Lefkovits, and J.Pieters. 1997. Analysis of subcellular organelles involved in major histocompatibility complex (MHC) class II-restricted antigen presentation by electrophoresis. *Electrophoresis* 18:2523-2530.
- Ezekowitz, R.A., D.J.Williams, H.Kozziel, M.Y.Armstrong, A.Warner, F.F.Richards, and R.M.Rose. 1991. Uptake of *Pneumocystis carinii* mediated by the macrophage mannose receptor. *Nature* 351:155-158.
- Ezekowitz, R.A., K.Sastry, P.Bailly, and A.Warner. 1990. Molecular characterization of the human macrophage mannose receptor: demonstration of multiple carbohydrate recognition-like domains and phagocytosis of yeasts in Cos-1 cells. *J. Exp. Med.* 172:1785-1794.
- Falasca, M., S.K.Logan, V.P.Lehto, G.Baccante, M.A.Lemmon, and J.Schlessinger. 1998. Activation of phospholipase C  $\gamma$  by PI 3-kinase-induced PH domain-mediated membrane targeting. *EMBO J.* 17:414-422.

- Ferguson, K.M., M.A.Lemmon, J.Schlessinger, and P.B.Sigler. 1995. Structure of the high affinity complex of inositol trisphosphate with a phospholipase C pleckstrin homology domain. *Cell* 83:1037-1046.
- Fiani, M.L., J.Beitz, D.Turvy, J.S.Blum, and P.D.Stahl. 1998. Regulation of mannose receptor synthesis and turnover in mouse J774 macrophages. *J. Leukoc. Biol.* 64:85-91.
- Fisher, T.E., P.E.Marszalek, and J.M.Fernandez. 2000. Stretching single molecules into novel conformations using the atomic force microscope. *Nat. Struct. Biol.* 7:719-724.
- Florin, E.L., V.T.Moy, and H.E.Gaub. 1994a. Adhesion forces between individual ligand-receptor pairs. *Science* 264:415-417.
- Fries, L.F., R.P.Hall, T.J.Lawley, G.R.Crabtree, and M.M.Frank. 1982. Monocyte receptors for the Fc portion of IgG studies with monomeric human IgG1: normal in vitro expression of Fc gamma receptors in HLA-B8/Drw3 subjects with defective Fc gamma-mediated in vivo clearance. *J. Immunol.* 129:1041-1049.
- Garcia-Garcia, E., and C.Rosales. 2002. Signal transduction during Fc receptor-mediated phagocytosis. *J. Leukoc. Biol.* 72:1092-1108.
- Ghazizadeh, S., J.B.Bolen, and H.B.Fleit. 1994. Physical and functional association of Src-related protein tyrosine kinases with Fc gamma RII in monocytic THP-1 cells. *J. Biol. Chem.* 269:8878-8884.
- Griffiths, G., and L.Mayorga. 2007. Phagosome proteomes open the way to a better understanding of phagosome function. *Genome Biol.* 8:207.
- Gumbiner, B.M. 2005. Regulation of cadherin-mediated adhesion in morphogenesis. *Nat. Rev. Mol. Cell Biol.* 6:622-634.
- Guyre, P.M., P.M.Morganelli, and R.Miller. 1983a. Recombinant immune interferon increases immunoglobulin G Fc receptors on cultured human mononuclear phagocytes. *J. Clin. Invest* 72:393-397.
- Han, W., S.M.Lindsay, M.Dlakic, and R.E.Harrington. 1997. Kinked DNA. *Nature* 386:563.
- Harris, N., M.Super, M.Rits, G.Chang, and R.A.Ezekowitz. 1992. Characterization of the murine macrophage mannose receptor: demonstration that the downregulation of receptor expression mediated by interferon-gamma occurs at the level of transcription. *Blood* 80:2363-2373.
- Heinz, W.F., and J.H.Hoh. 1999. Spatially resolved force spectroscopy of biological surfaces using the atomic force microscope. *Trends Biotechnol.* 17:143-150.
- Hinterdorfer, P., and Y.F.Dufrene. 2006. Detection and localization of single molecular recognition events using atomic force microscopy. *Nat. Methods* 3:347-355.
- Hinterdorfer, P., and Y.F.Dufrene. 2006b. Detection and localization of single molecular recognition events using atomic force microscopy. *Nat. Methods* 3:347-355.
- Hinterdorfer, P., W.Baumgartner, H.J.Gruber, K.Schilcher, and H.Schindler. 1996. Detection and localization of individual antibody-antigen recognition events by atomic force microscopy. *Proc. Natl. Acad. Sci. U. S. A* 93:3477-3481.
- Hodge, S., G.Hodge, H.Jersmann, G.Matthews, J.Ahern, M.Holmes, and P.N.Reynolds. 2008. Azithromycin improves macrophage phagocytic function and expression of mannose receptor in chronic obstructive pulmonary disease. *Am. J. Respir. Crit Care Med.* 178:139-148.

- Hodge, S., G.Hodge, R.Scicchitano, P.N.Reynolds, and M.Holmes. 2003. Alveolar macrophages from subjects with chronic obstructive pulmonary disease are deficient in their ability to phagocytose apoptotic airway epithelial cells. *Immunol. Cell Biol.* 81:289-296.
- Hoffmann, E., S.Marion, B.B.Mishra, M.John, R.Kratzke, S.F.Ahmad, D.Holzer, P.K.Anand, D.G.Weiss, G.Griffiths, and S.A.Kuznetsov. 2010. Initial receptor-ligand interactions modulate gene expression and phagosomal properties during both early and late stages of phagocytosis. *Eur. J. Cell Biol.* 89:693-704.
- Horber, J.K., and M.J.Miles. 2003. Scanning probe evolution in biology. *Science* 302:1002-1005.
- Hulett, M.D., and P.M.Hogarth. 1994a. Molecular basis of Fc receptor function. *Adv. Immunol.* 57:1-127.
- Indik, Z.K., J.G.Park, S.Hunter, and A.D.Schreiber. 1995. The molecular dissection of Fc gamma receptor mediated phagocytosis. *Blood* 86:4389-4399.
- Jahraus, A., M.Egeberg, B.Hinner, A.Habermann, E.Sackman, A.Pralle, H.Faulstich, V.Rybin, H.Defacque, and G.Griffiths. 2001. ATP-dependent membrane assembly of F-actin facilitates membrane fusion. *Mol. Biol. Cell* 12:155-170.
- Jahraus, A., T.E.Tjelle, T.Berg, A.Habermann, B.Storrie, O.Ullrich, and G.Griffiths. 1998. In vitro fusion of phagosomes with different endocytic organelles from J774 macrophages. *J. Biol. Chem.* 273:30379-30390.
- Janeway, C.A., Jr., and R.Medzhitov. 2002. Innate immune recognition. *Annu. Rev. Immunol.* 20:197-216.
- Kalamidas, S.A., M.P.Kuehnel, P.Peyron, V.Rybin, S.Rauch, O.B.Kotoulas, M.Houslay, B.A.Hemmings, M.G.Gutierrez, E.Anes, and G.Griffiths. 2006. cAMP synthesis and degradation by phagosomes regulate actin assembly and fusion events: consequences for mycobacteria. *J. Cell Sci.* 119:3686-3694.
- Kang, P.B., A.K.Azad, J.B.Torrelles, T.M.Kaufman, A.Beharka, E.Tibesar, L.E.DesJardin, and L.S.Schlesinger. 2005. The human macrophage mannose receptor directs Mycobacterium tuberculosis lipoarabinomannan-mediated phagosome biogenesis. *J. Exp. Med.* 202:987-999.
- Kawakami, Y., L.Yao, W.Han, and T.Kawakami. 1996. Tec family protein-tyrosine kinases and pleckstrin homology domains in mast cells. *Immunol. Lett.* 54:113-117.
- Kienberger, F., V.P.Pastushenko, G.Kada, T.Puntheeranurak, L.Chtcheglova, C.Riethmueller, C.Rankl, A.Ebner, and P.Hinterdorfer. 2006. Improving the contrast of topographical AFM images by a simple averaging filter. *Ultramicroscopy* 106:822-828.
- Kjeken, R., M.Egeberg, A.Habermann, M.Kuehnel, P.Peyron, M.Floetenmeyer, P.Walther, A.Jahraus, H.Defacque, S.A.Kuznetsov, and G.Griffiths. 2004. Fusion between phagosomes, early and late endosomes: a role for actin in fusion between late, but not early endocytic organelles. *Mol. Biol. Cell* 15:345-358.
- Krieger, M., and J.Herz. 1994. Structures and functions of multiligand lipoprotein receptors: macrophage scavenger receptors and LDL receptor-related protein (LRP). *Annu. Rev. Biochem.* 63:601-637.
- Kruskal, B.A., K.Sastry, A.B.Warner, C.E.Mathieu, and R.A.Ezekowitz. 1992. Phagocytic chimeric receptors require both transmembrane and cytoplasmic domains from the mannose receptor. *J. Exp. Med.* 176:1673-1680.

- Kurlander, R.J., and J.Batker. 1982. The binding of human immunoglobulin G1 monomer and small, covalently cross-linked polymers of immunoglobulin G1 to human peripheral blood monocytes and polymorphonuclear leukocytes. *J. Clin. Invest* 69:1-8.
- Kurosaki, T. 1999. Genetic analysis of B cell antigen receptor signaling. *Annu. Rev. Immunol.* 17:555-592.
- Kwiatkowska, K., and A.Sobota. 1999. Signaling pathways in phagocytosis. *Bioessays* 21:422-431.
- Lanier, L.L. 1998. NK cell receptors. *Annu. Rev. Immunol.* 16:359-393.
- Largent, B.L., K.M.Walton, C.A.Hoppe, Y.C.Lee, and R.L.Schnaar. 1984. Carbohydrate-specific adhesion of alveolar macrophages to mannose-derivatized surfaces. *J. Biol. Chem.* 259:1764-1769.
- Le Grimellec, C., M.C.Giocondi, M.Lenoir, M.Vater, G.Sposito, and R.Pujol. 2002. High-resolution three-dimensional imaging of the lateral plasma membrane of cochlear outer hair cells by atomic force microscopy. *J. Comp Neurol.* 451:62-69.
- Leckband, D.E., J.N.Israelachvili, F.J.Schmitt, and W.Knoll. 1992. Long-range attraction and molecular rearrangements in receptor-ligand interactions. *Science* 255:1419-1421.
- Lee, J.S., W.M.Nauseef, A.Moeenrezakhanlou, L.M.Sly, S.Noubir, K.G.Leidal, J.M.Schlomann, G.Krystal, and N.E.Reiner. 2007. Monocyte p110alpha phosphatidylinositol 3-kinase regulates phagocytosis, the phagocyte oxidase, and cytokine production. *J. Leukoc. Biol.* 81:1548-1561.
- LeNeveu, D.M., R.P.Rand, and V.A.Parsegian. 1976. Measurement of forces between lecithin bilayers. *Nature* 259:601-603.
- Lew, D.B., E.Songu-Mize, S.E.Pontow, P.D.Stahl, and M.C.Rattazzi. 1994. A mannose receptor mediates mannosyl-rich glycoprotein-induced mitogenesis in bovine airway smooth muscle cells. *J. Clin. Invest* 94:1855-1863.
- Linehan, S.A., L.Martinez-Pomares, P.D.Stahl, and S.Gordon. 1999. Mannose receptor and its putative ligands in normal murine lymphoid and nonlymphoid organs: In situ expression of mannose receptor by selected macrophages, endothelial cells, perivascular microglia, and mesangial cells, but not dendritic cells. *J. Exp. Med.* 189:1961-1972.
- Liu, Q., T.Sasaki, I.Kozieradzki, A.Wakeham, A.Itie, D.J.Dumont, and J.M.Penninger. 1999. SHIP is a negative regulator of growth factor receptor-mediated PKB/Akt activation and myeloid cell survival. *Genes Dev.* 13:786-791.
- Long, E.O. 1999. Regulation of immune responses through inhibitory receptors. *Annu. Rev. Immunol.* 17:875-904.
- Looney, R.J., G.N.Abraham, and C.L.Anderson. 1986. Human monocytes and U937 cells bear two distinct Fc receptors for IgG. *J. Immunol.* 136:1641-1647.
- Maluish, A.E., W.J.Urba, D.L.Longo, W.R.Overton, D.Coggin, E.R.Crisp, R.Williams, S.A.Sherwin, K.Gordon, and R.G.Steis. 1988. The determination of an immunologically active dose of interferon-gamma in patients with melanoma. *J. Clin. Oncol.* 6:434-445.
- Marodi, L., H.M.Korchak, and R.B.Johnston, Jr. 1991. Mechanisms of host defense against *Candida* species. I. Phagocytosis by monocytes and monocyte-derived macrophages. *J. Immunol.* 146:2783-2789.
- Martinez-Pomares, L., D.M.Reid, G.D.Brown, P.R.Taylor, R.J.Stillion, S.A.Linehan, S.Zamze, S.Gordon, and S.Y.Wong. 2003. Analysis of mannose receptor regulation by IL-4, IL-10, and proteolytic processing using novel monoclonal antibodies. *J. Leukoc. Biol.* 73:604-613.

- Martinez-Pomares, L., J.A.Mahoney, R.Kaposzta, S.A.Linehan, P.D.Stahl, and S.Gordon. 1998. A functional soluble form of the murine mannose receptor is produced by macrophages in vitro and is present in mouse serum. *J. Biol. Chem.* 273:23376-23380.
- Maxwell, K.F., M.S.Powell, M.D.Hulett, P.A.Barton, I.F.McKenzie, T.P.Garrett, and P.M.Hogarth. 1999. Crystal structure of the human leukocyte Fc receptor, Fc gammaRIIa. *Nat. Struct. Biol.* 6:437-442.
- Merkel, R., P.Nassoy, A.Leung, K.Ritchie, and E.Evans. 1999. Energy landscapes of receptor-ligand bonds explored with dynamic force spectroscopy. *Nature* 397:50-53.
- Mordue, D.G., and L.D.Sibley. 1997. Intracellular fate of vacuoles containing *Toxoplasma gondii* is determined at the time of formation and depends on the mechanism of entry. *J. Immunol.* 159:4452-4459.
- Mrksich, M. 2002. What can surface chemistry do for cell biology? *Curr. Opin. Chem. Biol.* 6:794-797.
- Murai, M., Y.Aramaki, and S.Tsuchiya. 1995. Contribution of mannose receptor to signal transduction in Fc gamma receptor-mediated phagocytosis of mouse peritoneal macrophages induced by liposomes. *J. Leukoc. Biol.* 57:687-691.
- Murai, M., Y.Aramaki, and S.Tsuchiya. 1996. alpha 2-macroglobulin stimulation of protein tyrosine phosphorylation in macrophages via the mannose receptor for Fc gamma receptor-mediated phagocytosis activation. *Immunology* 89:436-441.
- Muta, T., T.Kurosaki, Z.Misulovin, M.Sanchez, M.C.Nussenzweig, and J.V.Ravetch. 1994. A 13-amino-acid motif in the cytoplasmic domain of Fc gamma RIIB modulates B-cell receptor signalling. *Nature* 368:70-73.
- Nimmerjahn, F., and J.V.Ravetch. 2006. Fc gamma receptors: old friends and new family members. *Immunity.* 24:19-28.
- Nimmerjahn, F., P.Bruhns, K.Horiuchi, and J.V.Ravetch. 2005. Fc gamma RIV: a novel FcR with distinct IgG subclass specificity. *Immunity.* 23:41-51.
- Oberhauser, A.F., P.E.Marszalek, H.P.Erickson, and J.M.Fernandez. 1998. The molecular elasticity of the extracellular matrix protein tenascin. *Nature* 393:181-185.
- Olkhova, E., M.C.Hutter, M.A.Lill, V.Helms, and H.Michel. 2004. Dynamic water networks in cytochrome C oxidase from *Paracoccus denitrificans* investigated by molecular dynamics simulations. *Biophys. J.* 86:1873-1889.
- Ono, M., S.Bolland, P.Tempst, and J.V.Ravetch. 1996. Role of the inositol phosphatase SHIP in negative regulation of the immune system by the receptor Fc(gamma)RIIB. *Nature* 383:263-266.
- O'Riordan, D.M., J.E.Standing, and A.H.Limper. 1995. Pneumocystis carinii glycoprotein A binds macrophage mannose receptors. *Infect. Immun.* 63:779-784.
- Pearse, R.N., T.Kawabe, S.Bolland, R.Guinamard, T.Kurosaki, and J.V.Ravetch. 1999. SHIP recruitment attenuates Fc gamma RIIB-induced B cell apoptosis. *Immunity.* 10:753-760.
- Perussia, B., E.T.Dayton, R.Lazarus, V.Fanning, and G.Trinchieri. 1983a. Immune interferon induces the receptor for monomeric IgG1 on human monocytic and myeloid cells. *J. Exp. Med.* 158:1092-1113.
- Preiner, J., N.S.Losilla, A.Ebner, P.Annibale, F.Biscarini, R.Garcia, and P.Hinterdorfer. 2009. Imaging and detection of single molecule recognition events on organic semiconductor surfaces. *Nano. Lett.* 9:571-575.

- Raab, A., W.Han, D.Badt, S.J.Smith-Gill, S.M.Lindsay, H.Schindler, and P.Hinterdorfer. 1999. Antibody recognition imaging by force microscopy. *Nat. Biotechnol.* 17:901-905.
- Rabinovitch, M. 1995a. Professional and non-professional phagocytes: an introduction. *Trends Cell Biol.* 5:85-87.
- Rabinovitch, M. 1995b. Professional and non-professional phagocytes: an introduction. *Trends Cell Biol.* 5:85-87.
- Ratner, B.D., and S.J.Bryant. 2004. Biomaterials: where we have been and where we are going. *Annu. Rev. Biomed. Eng.* 6:41-75.
- Ravetch, J.V. 1994. Fc receptors: rubor redux. *Cell* 78:553-560.
- Ravetch, J.V., and J.P.Kinet. 1991. Fc receptors. *Annu. Rev. Immunol.* 9:457-492.
- Rief, M., H.Clausen-Schaumann, and H.E.Gaub. 1999. Sequence-dependent mechanics of single DNA molecules. *Nat. Struct. Biol.* 6:346-349.
- Salcedo, T.W., T.Kurosaki, P.Kanakaraj, J.V.Ravetch, and B.Perussia. 1993. Physical and functional association of p56lck with Fc gamma RIIIA (CD16) in natural killer cells. *J. Exp. Med.* 177:1475-1480.
- Salim, K., M.J.Bottomley, E.Querfurth, M.J.Zvelebil, I.Gout, R.Scaife, R.L.Margolis, R.Gigg, C.I.Smith, P.C.Driscoll, M.D.Waterfield, and G.Panayotou. 1996. Distinct specificity in the recognition of phosphoinositides by the pleckstrin homology domains of dynamin and Bruton's tyrosine kinase. *EMBO J.* 15:6241-6250.
- Sallusto, F., M.Cella, C.Danieli, and A.Lanzavecchia. 1995. Dendritic cells use macropinocytosis and the mannose receptor to concentrate macromolecules in the major histocompatibility complex class II compartment: downregulation by cytokines and bacterial products. *J. Exp. Med.* 182:389-400.
- Sanchez-Mejorada, G., and C.Rosales. 1998. Signal transduction by immunoglobulin Fc receptors. *J. Leukoc. Biol.* 63:521-533.
- Scharenberg, A.M., O.El Hillal, D.A.Fruman, L.O.Beitz, Z.Li, S.Lin, I.Gout, L.C.Cantley, D.J.Rawlings, and J.P.Kinet. 1998. Phosphatidylinositol-3,4,5-trisphosphate (PtdIns-3,4,5-P3)/Tec kinase-dependent calcium signaling pathway: a target for SHIP-mediated inhibitory signals. *EMBO J.* 17:1961-1972.
- Schlesinger, L.S. 1993. Macrophage phagocytosis of virulent but not attenuated strains of *Mycobacterium tuberculosis* is mediated by mannose receptors in addition to complement receptors. *J. Immunol.* 150:2920-2930.
- Schulert, G.S., and L.A.Allen. 2006. Differential infection of mononuclear phagocytes by *Francisella tularensis*: role of the macrophage mannose receptor. *J. Leukoc. Biol.* 80:563-571.
- Shepherd, V.L., B.I.Tarnowski, and B.J.McLaughlin. 1991. Isolation and characterization of a mannose receptor from human pigment epithelium. *Invest Ophthalmol. Vis. Sci.* 32:1779-1784.
- Smith, S.B., L.Finzi, and C.Bustamante. 1992. Direct mechanical measurements of the elasticity of single DNA molecules by using magnetic beads. *Science* 258:1122-1126.
- Sobota, A., A.Strzelecka-Kiliszek, E.Gladkowska, K.Yoshida, K.Mrozinska, and K.Kwiatkowska. 2005. Binding of IgG-opsonized particles to Fc gamma R is an active stage of phagocytosis that involves receptor clustering and phosphorylation. *J. Immunol.* 175:4450-4457.

- Stein, M., and S.Gordon. 1991. Regulation of tumor necrosis factor (TNF) release by murine peritoneal macrophages: role of cell stimulation and specific phagocytic plasma membrane receptors. *Eur. J. Immunol.* 21:431-437.
- Stroh, C., H.Wang, R.Bash, B.Ashcroft, J.Nelson, H.Gruber, D.Lohr, S.M.Lindsay, and P.Hinterdorfer. 2004a. Single-molecule recognition imaging microscopy. *Proc. Natl. Acad. Sci. U. S. A* 101:12503-12507.
- Stroh, C.M., A.Ebner, M.Geretschlager, G.Freudenthaler, F.Kienberger, A.S.Kamruzzahan, S.J.Smith-Gill, H.J.Gruber, and P.Hinterdorfer. 2004b. Simultaneous topography and recognition imaging using force microscopy. *Biophys. J.* 87:1981-1990.
- Strzelecka-Kiliszek, A., K.Kwiatkowska, and A.Sobota. 2002. Lyn and Syk kinases are sequentially engaged in phagocytosis mediated by Fc gamma R. *J. Immunol.* 169:6787-6794.
- Sung, S.S., R.S.Nelson, and S.C.Silverstein. 1983. Yeast mannans inhibit binding and phagocytosis of zymosan by mouse peritoneal macrophages. *J. Cell Biol.* 96:160-166.
- Tamir, I., J.C.Stolpa, C.D.Helgason, K.Nakamura, P.Bruhns, M.Daeron, and J.C.Cambier. 2000. The RasGAP-binding protein p62dok is a mediator of inhibitory Fc gamma RIIB signals in B cells. *Immunity.* 12:347-358.
- Taylor, M.E., K.Bezouska, and K.Drickamer. 1992. Contribution to ligand binding by multiple carbohydrate-recognition domains in the macrophage mannose receptor. *J. Biol. Chem.* 267:1719-1726.
- Taylor, P.R., L.Martinez-Pomares, M.Stacey, H.H.Lin, G.D.Brown, and S.Gordon. 2005. Macrophage receptors and immune recognition. *Annu. Rev. Immunol.* 23:901-944.
- Titus, J.A., P.Perez, A.Kaubisch, M.A.Garrido, and D.M.Segal. 1987. Human K/natural killer cells targeted with hetero-cross-linked antibodies specifically lyse tumor cells in vitro and prevent tumor growth in vivo. *J. Immunol.* 139:3153-3158.
- Underhill, D.M., and A.Ozinsky. 2002. Phagocytosis of microbes: complexity in action. *Annu. Rev. Immunol.* 20:825-852.
- Unkeless, J.C. 1977. The presence of two Fc receptors on mouse macrophages: evidence from a variant cell line and differential trypsin sensitivity. *J. Exp. Med.* 145:931-945.
- Unkeless, J.C., and H.N.Eisen. 1975. Binding of monomeric immunoglobulins to Fc receptors of mouse macrophages. *J. Exp. Med.* 142:1520-1533.
- Unkeless, J.C., and J.Jin. 1997. Inhibitory receptors, ITIM sequences and phosphatases. *Curr. Opin. Immunol.* 9:338-343.
- Vivier, E., and M.Daeron. 1997. Immunoreceptor tyrosine-based inhibition motifs. *Immunol. Today* 18:286-291.
- Wang, D., J.Feng, R.Wen, J.C.Marine, M.Y.Sangster, E.Parganas, A.Hoffmeyer, C.W.Jackson, J.L.Cleveland, P.J.Murray, and J.N.Ihle. 2000. Phospholipase C gamma 2 is essential in the functions of B cell and several Fc receptors. *Immunity.* 13:25-35.
- Wehrle-Haller, B., and B.Imhof. 2002. The inner lives of focal adhesions. *Trends Cell Biol.* 12:382-389.
- Weinshank, R.L., A.D.Luster, and J.V.Ravetch. 1988. Function and regulation of a murine macrophage-specific IgG Fc receptor, Fc gamma R-alpha. *J. Exp. Med.* 167:1909-1925.
- Weiss, A., and D.R.Littman. 1994. Signal transduction by lymphocyte antigen receptors. *Cell* 76:263-274.

- Wetzel, M.G., and E.D.Korn. 1969b. Phagocytosis of latex beads by *Acanthamoeba castellanii* (Neff). 3. Isolation of the phagocytic vesicles and their membranes. *J. Cell Biol.* 43:90-104.
- Yamanashi, Y., T.Tamura, T.Kanamori, H.Yamane, H.Nariuchi, T.Yamamoto, and D.Baltimore. 2000. Role of the rasGAP-associated docking protein p62(dok) in negative regulation of B cell receptor-mediated signaling. *Genes Dev.* 14:11-16.
- Young, J.D., S.S.Ko, and Z.A.Cohn. 1984. The increase in intracellular free calcium associated with IgG gamma 2b/gamma 1 Fc receptor-ligand interactions: role in phagocytosis. *Proc. Natl. Acad. Sci. U. S. A* 81:5430-5434.
- Yuan, C., A.Chen, P.Kolb, and V.T.Moy. 2000. Energy landscape of streptavidin-biotin complexes measured by atomic force microscopy. *Biochemistry* 39:10219-10223.
- Zamze, S., L.Martinez-Pomares, H.Jones, P.R.Taylor, R.J.Stillion, S.Gordon, and S.Y.Wong. 2002. Recognition of bacterial capsular polysaccharides and lipopolysaccharides by the macrophage mannose receptor. *J. Biol. Chem.* 277:41613-41623.



## Acknowledgement

Most of this work has been done in the Light Microscopy Centre of the University of Rostock over the past three years. Parts of the study were carried out in collaboration with the Johannes Kepler University of Linz, Austria. The project was financially supported by the EU project IMMUNANOMAP (MRTN-CT-2006-0359476). Numerous people helped me during the whole duration of this study, whom I want to thank for their continuous support.

I owe my deepest gratitude to my graduate supervisor Dr. Sergei A. Kuznetsov for the opportunities I have had during my studies at Light Microscopy Centre of the University of Rostock for the last three years. Sergei has given me incredible freedom in deciding the direction of my research work. His enthusiasm for cell biology, expertise, kindness and most of all, his patience encouraged me to study and investigate. I am grateful to him for an experience that I will carry with me throughout my life.

My group head, Prof. Dr. Deiter G. Weiss, has been a valuable source of advice and direction with the success of the project. I am lucky to have worked with him and thankful to him for the advice and direction. I wish to acknowledge Prof. Dr. Qamar Rahman who has been guiding me for the last five years. I was encouraged to pursue my own interests in research and has given her strong recommendation to secure this position. I am also thankful to Prof. Dr. Peter Hinterdorfer for encouraging me and to provide me the space in his laboratory in JKU of Linz, Austria to work on atomic force microscope. I would like to extend my thanks to Dr. Lilia for her support and guidance during my stay at Linz.

I am highly indebted to Devang for guiding me during my PhD. He has been an asset for me with his valuable suggestions regarding research and life. Life would not be so easy in Rostock without Birgit. She has been a great help for me not only in the lab but also for taking care of my personal requirements. Thanks a lot Birgit!

It would be an understatement to say that I would not be the person I am today without my family. Ammi and Abbu have been the biggest influences in my life. It is an honor to be their son, and I hope that someday I will be able to earn a mere fraction of what they have done for me. I will extend my thanks to all my family members, Mummy-Daddy, Appi-Bhai, Yab-Muniya appi, Yam-Nida Appi, Shadab, Faisal, Yasir, Saif, Sheebu, Fasi, Injela, Talish and Maaz.

I am grateful to all people in the Department of Cell Biology in Rostock, especially Tarek, Ben, Eik, Heiko, Bärbel, Maren and Anne. I would like to thank my friends who have supported me during this journey. The years I spent in Rostock would not have been as wonderful without my Indian friends Vaishanvi & Payal, Rahul, Amit, Raymond, Prakash, Saijo, Leijo, Jiju, Vijay Bhaskar. Life would not have been the same without these during my stay in Rostock.

Special thanks for my beloved wife Sana who has been here for me. Dear thank you for your encouragement and support, for standing by my side in difficult situations, for giving me strength to work hard and makin life cheerful. Since being together, she has always given me everything I could have ever possibly wanted, and continue to do so to this very day.

## Curriculum vitae and list of publications

### Personal Information

---

Name	Syed Furquan Ahmad
Date and place of birth	16.03.1982, Lucknow, India

### Education

---

Oct 2007–present	PhD thesis in the lab of PD Dr. Sergei A Kuznetsov
Aug 2004–Jul 2006	Master of Science (Biotechnology), Nainital, India
Jul 2001-Jun2004	Bachelor of Science, Lucknow, India
Jul 1997-Mar 1999	Senior Secondary School, Lucknow, India

### Practical Experience

---

Oct 2007-present	Member of the group of Dr Seregei A. Kuznetsov, University of Rostock, Germany
Mar 2008 and May 2009	Research visits in the lab of Prof Peter Hinterdorfer, JKU Linz, Austria
Jan 2007 –Aug 2007	Junior research fellow at SGPGI, Lucknow, India
Mar 2006- July2006	Master dissertation “Micropropagation of Aloe and molecular, biochemical and antimicrobial activity of Aloe” at Kumaun University, Nainital, India
Jan 2006-Feb 2006	Master student training at CDRI, Lucknow, India

### Publications

---

1. **Ahmad S. F.**, Patel D., Weiss D. G., Kuznetsov S. A.; Influence of Fcγ receptor distribution on mannose receptor mediated phagocytosis in mouse macrophages (manuscript under preparation for *J. Cell Sci.*).
2. **Patel, D. M.**; Ahmad S. F.; Weiss D. G.; Gerke V.; Kuznetsov S. A. (2010) Influence of receptor signalling on annexin A1 recruitment during Fc and Mannose receptor mediated phagocytosis. (Under preparation for FEBS Letters)
3. Patel D., **Ahmad S. F.**, Gerke V., Weiss D. G., Kuznetsov S. A.; Annexin A1 is a new functional linker between actin filaments and phagosome during phagocytosis ; *J. Cell Sci.* 2010 (returned with minor revision).
4. **Ahmad S. F.**, Chtcheglova L. A., Mayer B., Kuznetsov S. A., Hinterdorfer P.; 2010. Nanosensing of Fcγ receptors on macrophages; *Anal. Bioanal. Chem.* (in Press)
5. Hoffman E., Marion S., Mishra B. B., John M., Kratzke R., **Ahmad S. F.**, Holzer D., Anand P. K., Weiss D. G., Griffiths G., Kuznetsov S. A.; 2010. Initial receptor-ligand interactions modulate gene expression and phagosomal properties during both early and late stages of phagocytosis; *Eur. J. Cell Biol.* 89(9):693-704

## Presentations

---

1. Patel D. M., **Ahmad S. F.** and Kuznetsov S. A.; Annexin A1 as a functional linker between actin systems and phagosomes in mouse macrophages; poster at EMBO meeting, 2009, Amsterdam, The Netherlands
2. Hoffmann E., Marion S., Mishra B. B., John M., Kratzke R., **Ahmad S. F.**, Holzer D., Anand P.K., Weiss D. G., Griffiths G. and Kuznetsov S. A., The phagocytic receptor modulates gene expression and phagosome function in mouse macrophage; poster at ELSO meeting, 2008, Nise, France
3. **Ahmad S. F.**, Chtcheglova L.A., Patel D., Wildling, L., Hinterdorfer P. and Kuznetsov S. A.; Mapping of macrophage receptors using latex bead system and atomic force microscopy, Poster at Advanced Microscopy Techniques for Immunoscopes, 2008, Barcelona, Spain
4. Patel D. M., **Ahmad S. F.** and Kuznetsov S. A.; Plasma membrane receptors define annexin-dependent interaction of mature phagosomes with F-actin; poster at Advanced Microscopy Techniques for Immunoscopes, 2008, Barcelona, Spain
5. Latex beads and Atomic Force Microscopy to map the nano-landscape of macrophage receptors, Oral presentation at Annual Phagosome Meeting, 2008, Titisee, Germany

**Selbststaendigkeitserklaerung**

Ich versichere hiermit an Eides statt, dass ich die vorliegende Arbeit selbststaendig angefertigt und ohne fremde Hilfe verfasst habe, keine außer den von mir angegebenen Hilfsmitteln und Quellen dazu verwendet habe und die den benutzten Werken inhaltlich und woertlichentnommenen Stellen als solche kenntlich gemacht habe.

**Rostock, 30.09.2010**

**Syed Furquan Ahmad**